
Spacetime Defects and Bouncing
Cosmology

Zur Erlangung des akademischen Grades eines
DOKTORS DER NATURWISSENSCHAFTEN

von der KIT-Fakultät für Physik
des Karlsruher Instituts für Technologie (KIT)

genehmigte

DISSERTATION

von

M.Sc. Ziliang Wang

aus China

Referent: Prof. Dr. Frans R. Klinkhamer (KIT)

Korreferent: Prof. Dr. Janos Polónyi (Université de Strasbourg)

Tag der mündlichen Prüfung: 30. Oktober 2020



This document is licensed under a Creative Commons Attribution-ShareAlike 4.0 International License (CC BY-SA 4.0):

<https://creativecommons.org/licenses/by-sa/4.0/deed.en>

Eidesstattliche Versicherung gemäß § 13 Absatz 2 Ziffer 3 der Promotionsordnung des Karlsruher Instituts für Technologie (KIT) für die KIT-Fakultät für Physik:

1. Bei der eingereichten Dissertation zu dem Thema

Spacetime Defects and Bouncing Cosmology

handelt es sich um meine eigenständig erbrachte Leistung.

2. Ich habe nur die angegebenen Quellen und Hilfsmittel benutzt und mich keiner unzulässigen Hilfe Dritter bedient. Insbesondere habe ich wörtlich oder sinngemäß aus anderen Werken übernommene Inhalte als solche kenntlich gemacht.
3. Die Arbeit oder Teile davon habe ich bislang nicht an einer Hochschule des In- oder Auslands als Bestandteil einer Prüfungs- oder Qualifikationsleistung vorgelegt.
4. Die Richtigkeit der vorstehenden Erklärungen bestätige ich.
5. Die Bedeutung der eidesstattlichen Versicherung und die strafrechtlichen Folgen einer unrichtigen oder unvollständigen eidesstattlichen Versicherung sind mir bekannt.

Ich versichere an Eides statt, dass ich nach bestem Wissen die reine Wahrheit erkläre und nichts verschwiegen habe.

Karlsruhe, den 14. Oktober 2020

.....
(Ziliang Wang)

To my grandmothers

Abstract

Up to this day, general relativity is widely accepted as the relevant theory of classical gravity and has been well tested by many experiments. Despite this success, general relativity does not provide answers to many remaining open questions related to gravity. The ultimate fate of apparent spacetime singularities is one of these open questions.

Possible solutions to spacetime singularities are reviewed in this thesis. For these particular solutions, singularities are replaced by spacetime defects: the black hole singularity is replaced by a space defect and the big bang singularity is replaced by a time defect.

In this thesis, we investigate certain effects which the spacetime defects could produce. We calculate the geodesics of the spacetime defects. For the space defect, we discuss its lensing properties and the corresponding image formation. For the time defect, we investigate the corresponding nonsingular bouncing cosmology. We also present some possible observable effects related to these spacetime defects.

Zusammenfassung

Bis zum heutigen Tag ist die allgemeine Relativitätstheorie weithin als die relevante Theorie der Gravitation anerkannt und wurde durch viele Experimente bestätigt. Trotz dieses Erfolges liefert die allgemeine Relativitätstheorie keine Antwort auf viele offene Fragen, die mit Gravitation zusammenhängen. Das endgültige Schicksal scheinbarer Raumzeit-Singularitäten ist eine dieser offenen Fragen.

Mögliche Lösungen für Raumzeit-Singularitäten werden in dieser Arbeit diskutiert. In diesen speziellen Lösungen werden Singularitäten durch Raumzeitdefekte ersetzt: Die Singularität des Schwarzen Loches wird durch einen Raumdefekt und die Urknall-Singularität wird durch einen Zeitdefekt ersetzt.

In dieser Arbeit untersuchen wir bestimmte Effekte, die Raumzeitdefekte verursachen könnten. Wir berechnen die Geodäten der Raumzeitdefekte. Für den Raumdefekt diskutieren wir seine Linseneigenschaften und die entsprechende Bilderzeugung. Für den Zeitdefekt untersuchen wir die entsprechende nicht singuläre prallende Kosmologie. Wir präsentieren auch einige mögliche beobachtbare Effekte im Zusammenhang mit den Raumzeitdefekten.

List of Publications

This thesis is based on the following publications:

1. F. R. Klinkhamer and Z. L. Wang, “Lensing and imaging by a stealth defect of space-time,” *Mod. Phys. Lett. A* **34** (2019) 1950026, arXiv:1808.02465.
2. F. R. Klinkhamer and Z. L. Wang, “Nonsingular bouncing cosmology from general relativity,” *Phys. Rev. D* **100** (2019) 083534, arXiv:1904.09961.
3. F. R. Klinkhamer and Z. L. Wang, “Nonsingular bouncing cosmology from general relativity: Scalar metric perturbations,” *Phys. Rev. D* **101** (2020) 064061, arXiv:1911.06173.

Conventions

In this thesis, we work in reduced-Planckian units with $G = c = \hbar = 1$, where G is Newton's gravitational constant, c the speed of light in vacuum and \hbar the reduced Planck constant.

In what follows, we consider a four-dimensional spacetime manifold with the metric $g_{\mu\nu}$. We use metric signature $(-, +, +, +)$. The covariant derivative operator is the one compatible with the metric tensor, i.e., $\nabla_\rho g^{\mu\nu} = 0$. The affine connection is given by the following (torsion-free) Christoffel symbol:

$$\Gamma^\lambda{}_{\mu\nu} = \frac{1}{2} g^{\lambda\rho} \left(\frac{\partial g_{\nu\rho}}{\partial x^\mu} + \frac{\partial g_{\mu\rho}}{\partial x^\nu} - \frac{\partial g_{\mu\nu}}{\partial x^\rho} \right), \quad (0.1)$$

where repeated indices are summed over.

The Riemann curvature tensor is

$$R_{\mu\nu\rho}{}^\sigma = \frac{\partial}{\partial x^\nu} \Gamma^\sigma{}_{\mu\rho} - \frac{\partial}{\partial x^\mu} \Gamma^\sigma{}_{\nu\rho} + \Gamma^\alpha{}_{\mu\rho} \Gamma^\sigma{}_{\alpha\nu} - \Gamma^\alpha{}_{\nu\rho} \Gamma^\sigma{}_{\alpha\mu}. \quad (0.2)$$

With our conventions, the Einstein field equation (without cosmological constant) is given by

$$R_{\mu\nu} - \frac{1}{2} R g_{\mu\nu} = 8\pi T_{\mu\nu}, \quad (0.3)$$

where $T_{\mu\nu}$ is the energy-momentum tensor of matter field.

Contents

Abstract	xi
Conventions	xv
1. Introduction	1
2. Singularities in General Relativity	3
2.1. Black hole singularity	3
2.1.1. Schwarzschild solution	3
2.1.2. Extended Schwarzschild–Kruskal–Szekeres solution	4
2.1.3. Black hole singularity	4
2.2. Big bang singularity	4
2.2.1. Robertson-Walker metric	4
2.2.2. Standard FLRW universe	5
2.2.3. Big bang singularity	6
2.3. Singularity theorems	6
2.3.1. Raychaudhuri’s equation	7
2.3.2. Singularity theorems	9
3. Nontrivial topological structure of spacetime	11
3.1. Nontrivial topological structure of spacetime	11
3.1.1. Regularized black hole solution (brief review)	11
3.1.2. Massive remnant from regularized black hole	12
3.1.3. Stealth defect of spacetime (brief review)	14
3.2. Lensing by a stealth defect of spacetime	15
3.2.1. Geodesics of flat-spacetime stealth defect	15
3.2.2. Geodesics of curved-spacetime stealth defect	24
4. Nonsingular bouncing cosmology	31
4.1. Bouncing cosmologies (brief review)	31
4.2. Nonsingular bouncing cosmology	31
4.2.1. Regularized big bang singularity	32
4.2.2. Nonsingular bouncing cosmology	33
4.2.3. Circumventing the singularity theorem	38
4.3. Cosmological perturbations	40
4.3.1. Scalar metric perturbations	40
4.3.2. Cosmological perturbations with conformal coordinates	45
4.3.3. Cosmic microwave background radiation	48
5. Conclusion and Outlook	57
A. Proof of Remark 2 in Sec. 4.2.2.1	59
B. Geodesics for massive particles in nonsingular bouncing cosmology	61
C. Nonsingular bounce with $w = 1$	65
C.1. Basic equations	65

C.2. Null geodesics	66
C.3. Past particle horizon	66
C.4. Modified Hubble diagrams	67
D. Nonsingular bounce from a scalar field with a positive exponential potential	69
E. Primordial anisotropies and initial conditions	71
E.1. Boltzmann equation	71
E.2. Sachs–Wolfe effect	74
E.3. Temperature fluctuations	75
Acknowledgements	79
References	81

CHAPTER 1

Introduction

It was argued by Wheeler [1] that spacetime over small length scales could have large fluctuations of the metric. The resulting large metric fluctuations might lead to a topological change of spacetime [1, 2]. These results suggest a foam-like structure of spacetime [1, 3–5].

In Ref. [6], a simple model of a classical spacetime foam was considered, which consists of identical static defects embedded in Minkowski spacetime. One type of defect discussed in Ref. [6] is obtained by removing the interior of a ball from \mathbb{R}^3 and identifying antipodal points on its boundary. Several investigations on this particular defect of spacetime have been carried out [7–9]. Interestingly, it has been shown in Ref. [7] that the black hole singularity can be removed if we consider the Einstein field equations over the particular defect of spacetime. Recently, the big bang singularity has also been removed [10] by a procedure similar to the regularization of the black hole singularity but with a different spacetime defect.

The main goal of this thesis is to review these two kinds of spacetime defects [7, 8, 10] and to investigate certain novel effects that these defects produce [11–13].

In Chapter 2, we will review two physical singularities in general relativity: the black hole and the big bang singularities. The black hole singularity appears in the extended Schwarzschild solution, and the big bang singularity appears in the Friedmann solution for a homogeneous and isotropic universe. Singularity theorems will also be briefly reviewed in this chapter.

In Chapter 3, a nontrivial topological structure of spacetime will be discussed. Specifically, we will consider a defect in 3-space aimed at regularizing the black hole singularity in general relativity. This particular spacetime defect will lead to a new type of gravitational lensing and may prevent a black hole from complete evaporation.

In Chapter 4, we will consider a defect in time. This defect replaces the singular Friedmann–Lemaître–Robertson–Walker (FLRW) universe by a nonsingular bouncing universe, i.e., a universe which goes from a contraction phase to an expansion phase with a nonvanishing cosmic scale factor at the moment of the bounce. Geodesics and the modified Hubble diagrams of the nonsingular bouncing universe will be presented in this chapter. Then, we will consider cosmological perturbations of the nonsingular bouncing cosmology. Specifically, we will check that the bounce is stable under small perturbations of the metric and matter. Lastly, we will consider a particular nonsingular bouncing universe that could lead to a scale-invariant power spectrum of cosmological perturbations.

In Chapter 5, we present the conclusions of our work, as well as an outlook over possible future work.

The original work of this thesis appears in Sec. 3.1.2, in Sec. 3.2, in part of Sec. 4.2.2, in Sec. 4.2.3, and in part of Sec. 4.3.

Singularities in General Relativity

General relativity (GR), proposed by Albert Einstein in 1915, is a (classical) theory of gravity. It has been well tested by many experiments, e.g., perihelion precession of Mercury, deflection of light by the Sun, gravitational redshift of light, binary pulsars, gravitational lensing [14], and detection of gravitational waves [15]. Although general relativity has achieved great success, many problems remain unsolved. For instance, we do not know what dark energy(ies) is (are), what dark matter is made of, what is at the center of a black hole, and what happened at the beginning of the Universe (if it has a beginning). The last two problems listed above may be related to the black hole singularity and the big bang singularity.

2.1. Black hole singularity

2.1.1. Schwarzschild solution

In 1916, Karl Schwarzschild [16] found a solution of the vacuum Einstein equation for a static, spherically symmetric spacetime. The Schwarzschild solution can be written as follows:

$$ds^2 \Big|_{\text{Schwarzschild metric}} = - \left(1 - \frac{2M}{r}\right) dt^2 + \left(1 - \frac{2M}{r}\right)^{-1} dr^2 + r^2(d\theta^2 + \sin^2\theta d\phi^2), \quad (2.1a)$$

$$t \in \mathbb{R}, \quad (2.1b)$$

$$r \in (0, +\infty), \quad (2.1c)$$

$$\theta \in [0, \pi], \quad (2.1d)$$

$$\phi \in [0, 2\pi). \quad (2.1e)$$

M in (2.1a) is a free parameter, and it can be interpreted as the total mass of the Schwarzschild field.

From the Schwarzschild solution (2.1), we can see that the metric components become singular at both $r = 2M$ and $r = 0$. $r = 2M$ corresponds to a *coordinate singularity*, which can be removed by doing a proper coordinate transformation (see Sec. 2.1.2.) However $r = 0$ is a *spacetime singularity*, which is a true singularity with divergent physical quantities [17] (see Sec. 2.1.3).

2.1.2. Extended Schwarzschild–Kruskal–Szekeres solution

The extended Schwarzschild–Kruskal–Szekeres (SKS) solution has a metric given by [18, 19]

$$ds^2 \Big|_{\text{SKS metric}} = \frac{32M^3 e^{-r/(2M)}}{r} (-dv^2 + du^2) + r^2 (d\theta^2 + \sin^2 \theta d\phi^2), \quad (2.2a)$$

$$u \in \mathbb{R}, \quad (2.2b)$$

$$v \in \mathbb{R}, \quad (2.2c)$$

$$\theta \in [0, \pi], \quad (2.2d)$$

$$\phi \in [0, 2\pi). \quad (2.2e)$$

The relation between the coordinates (r, t) and the coordinates (u, v) is as follows:¹

$$\left(\frac{r}{2M} - 1\right) e^{\frac{r}{2M}} = u^2 - v^2, \quad (2.3a)$$

$$\frac{t}{2M} = \ln\left(\frac{u+v}{u-v}\right). \quad (2.3b)$$

Notice that u and v need to satisfy

$$u^2 - v^2 > -1, \quad (2.4)$$

which is required by $r > 0$.

The extended Schwarzschild–Kruskal–Szekeres solution (2.2a) is well defined at $r = 2M$ ($u = 0$ or $v = 0$), so the coordinate singularity appearing in Schwarzschild solution no longer exists here. However, the spacetime singularity at $r = 0$ still remains in the Schwarzschild–Kruskal–Szekeres solution.

2.1.3. Black hole singularity

The Kretschmann scalar ² (defined in terms of the Riemann curvature tensor) is given by

$$K \equiv R_{\mu\nu\rho\sigma} R^{\mu\nu\rho\sigma}, \quad (2.5)$$

and for the Schwarzschild solution,

$$K \Big|_{\text{SKS}} = 48 \frac{M^2}{r^6}, \quad (2.6)$$

which is divergent as $r \rightarrow 0$.

2.2. Big bang singularity

2.2.1. Robertson–Walker metric

In standard cosmology, a spatially homogeneous and isotropic universe is described by the so-called Robertson–Walker (RW) metric:³

¹Notice that the new coordinates in the SKS metric are usually denoted by (T, X) instead of (u, v) in the literature. We use (u, v) here, as (T, X) will be used in the coming chapters.

²The Ricci tensor and Ricci scalar vanish identically for the Schwarzschild solution.

³Sometimes the metric (2.7) is also called the Friedmann–Lemaître–Robertson–Walker (FLRW) metric.

$$ds^2 \Big|^{RW} = -dt^2 + a^2(t) \left[\frac{dr^2}{1 - kr^2} + r^2(d\theta^2 + \sin^2 \theta d\phi^2) \right], \quad (2.7)$$

which can be written in the following form:

$$ds^2 \Big|^{RW} = -dt^2 + a^2(t) \begin{cases} [d\psi^2 + \sin^2 \psi (d\theta^2 + \sin^2 \theta d\phi^2)], k = 1 \\ [d\psi^2 + \psi^2 (d\theta^2 + \sin^2 \theta d\phi^2)], k = 0 \\ [d\psi^2 + \sinh^2 \psi (d\theta^2 + \sin^2 \theta d\phi^2)], k = -1 \end{cases}, \quad (2.8)$$

with

$$r = \begin{cases} \sin \psi, k = 1 \\ \psi, k = 0 \\ \sinh \psi, k = -1 \end{cases}. \quad (2.9)$$

The function $a(t)$ is the cosmic scale factor. It is dimensionless for $k = 0$, and it has the dimensions of length for $k = \pm 1$. The different values of k in the RW metric correspond to different spatial geometries: $k = 1$ for a three-dimensional sphere; $k = 0$ for three-dimensional flat space; $k = -1$ for a three-dimensional hyperboloid. Note that for $k = 1$, the universe is “closed”, i.e., it has a finite volume at any time but has no boundary [20].

In this thesis, we will only consider the spatially flat universe ($k = 0$).

2.2.2. Standard FLRW universe

As far as we know, the main content of our universe can be described by one or more perfect fluids. (In the Λ CDM model, which is known as the standard model of big bang cosmology, the three major components of our universe are: the cosmological constant, cold dark matter, and ordinary matter. All of these can be viewed as perfect fluids.)

The energy-momentum tensor for a homogeneous perfect fluid (with energy density ρ and pressure P) reads

$$T_{\mu\nu} = \rho U_\mu U_\nu + P(g_{\mu\nu} + U_\mu U_\nu), \quad (2.10)$$

where U_μ is the four-velocity vector.

The dynamical evolution of a homogeneous and isotropic universe can be obtained from the Einstein equation, together with the RW metric. For a spatially flat universe ($k = 0$), the $0 - 0$ component of the Einstein equation gives

$$\frac{1}{a^2(t)} \left(\frac{da(t)}{dt} \right)^2 = \frac{8\pi}{3} \rho(t), \quad (2.11)$$

which is known as the Friedmann equation [21]. The $i - j$ components of the Einstein equation reduce to

$$\frac{1}{a(t)} \frac{d^2 a(t)}{dt^2} + \frac{1}{2} \left(\frac{1}{a(t)} \frac{da(t)}{dt} \right)^2 = -4\pi P(t). \quad (2.12)$$

Standard radiation-dominated universe

For a radiation-dominated universe, we have the equation-of-state parameter

$$w \equiv \frac{P(t)}{\rho(t)} = \frac{1}{3}. \quad (2.13)$$

From (2.11) and (2.12), we get the solution of $a(t)$ and $\rho(t)$ for a radiation-dominated universe:

$$a(t) = \sqrt{\frac{t}{t_0}}, \quad (2.14)$$

$$\rho = \rho_0 \frac{1}{t^2}, \quad (2.15)$$

where the cosmic scale factor $a(t)$ has been normalized to 1 at a given time $t = t_0 > 0$ and where the boundary condition is $\rho(t_0) = \rho_0 > 0$.

Standard matter-dominated universe

For a matter-dominated universe, we have

$$w = 0. \quad (2.16)$$

The solution of $a(t)$ and $\rho(t)$ is given by:

$$a(t) = \sqrt[3]{\frac{t^2}{t_0^2}}, \quad (2.17)$$

$$\rho = \rho_0 \frac{1}{t^2}, \quad (2.18)$$

with normalization $a(t_0) = 1$ at $t = t_0 > 0$ and boundary condition $\rho(t_0) = \rho_0 > 0$.

2.2.3. Big bang singularity

For both the radiation- and matter-dominated universe, we have

$$\lim_{t \rightarrow 0^+} a(t) = 0, \quad (2.19)$$

i.e., the distance between all space points at $t = 0$ is zero.

Moreover, physical quantities are divergent at $t = 0$. For example, the Ricci curvature scalar and energy density for the matter-dominated universe are given by

$$R \propto \frac{1}{t^2}, \quad (2.20a)$$

$$\rho \propto \frac{1}{t^2}, \quad (2.20b)$$

which are divergent at $t = 0$. So, $t = 0$ is referred to as the *big bang singularity*.

2.3. Singularity theorems

There are several singularity theorems in general relativity [17, 22–25]. These theorems suggest that the black hole and big bang singularities as discussed in Sec. 2.1 and Sec. 2.2, are quite general in general relativity if some standard conditions are assumed.

In this thesis, we will consider defects in space and time that may circumvent the singularity theorems. In particular, we will focus on the theorem that relates to the big bang singularity and show how a defect in time may circumvent the singularity theorem. (In principle, we are able to “see” the big bang singularity but not the black hole singularity, as the black hole singularity is, in general, inside an event horizon.) The singularity theorems in a spacetime with nontrivial topology (related to the black hole singularity) have already been discussed in Refs. [26, 27], so we will only give a brief discussion in Chapter 3.

Before stating the singularity theorems, we first briefly introduce some definitions and equations.

2.3.1. Raychaudhuri's equation

Consider a spacetime manifold $(M, g_{\mu\nu})$ and an open subset $O \subset M$. A congruence in O is a family of curves such that through each point $p \in O$ there passes only one curve of this family [17]. Let ξ^μ be the four-velocity vector field which is tangent to a congruence of timelike geodesics. We can define the following ‘‘spatial’’ tensor field [17]

$$B_{\mu\nu} = \nabla_\nu \xi_\mu, \quad (2.21)$$

and ‘‘spatial’’ metric

$$h_{\mu\nu} = g_{\mu\nu} + \xi_\mu \xi_\nu. \quad (2.22)$$

With (2.21) and (2.22), we can define the expansion θ , the shear $\sigma_{\mu\nu}$ and the twist $\omega_{\mu\nu}$ as follows

$$\theta = B^{\mu\nu} h_{\mu\nu}, \quad (2.23a)$$

$$\sigma_{\mu\nu} = \frac{1}{2} (B_{\mu\nu} + B_{\nu\mu}) - \frac{1}{3} \theta h_{\mu\nu}, \quad (2.23b)$$

$$\omega_{\mu\nu} = \frac{1}{2} (B_{\mu\nu} - B_{\nu\mu}). \quad (2.23c)$$

With (2.23), $B_{\mu\nu}$ can be written as

$$B_{\mu\nu} = \frac{1}{3} \theta h_{\mu\nu} + \sigma_{\mu\nu} + \omega_{\mu\nu}. \quad (2.24)$$

The change of $B_{\mu\nu}$ along each geodesic is given by [17],

$$\xi^\rho \nabla_\rho B_{\mu\nu} = -B^\rho{}_\nu B_{\mu\rho} + R_{\rho\nu\mu}{}^\alpha \xi^\rho \xi_\alpha. \quad (2.25)$$

Contracting the μ, ν indices of (2.25) gives

$$\xi^\rho \nabla_\rho \theta = \frac{d\theta}{d\tau} = -\frac{1}{3} \theta^2 - \sigma_{\mu\nu} \sigma^{\mu\nu} + \omega_{\mu\nu} \omega^{\mu\nu} - R_{\mu\nu} \xi^\mu \xi^\nu, \quad (2.26)$$

where τ is the proper time of the geodesic in the congruence. Equation (2.26) is known as the Raychaudhuri equation [17, 28].

For the case

$$\omega_{\mu\nu} = 0, \quad (2.27)$$

and the assumption

$$R_{\mu\nu} \xi^\mu \xi^\nu \geq 0, \quad (2.28)$$

(2.26) reduces to

$$\frac{d\theta}{d\tau} + \frac{1}{3} \theta^2 \leq 0, \quad (2.29)$$

which gives [17]

$$\theta^{-1}(\tau) \geq \theta_0^{-1} + \frac{1}{3} \tau, \quad (2.30)$$

with $\theta_0 = \theta(0)$.

To get (2.29), we have used

$$-\sigma_{\mu\nu} \sigma^{\mu\nu} \leq 0, \quad (2.31)$$

as the $\sigma_{\mu\nu}$ are purely spatial. With the Einstein equation, assumption (2.28) is equivalent to [17]

$$T_{\mu\nu} \xi^\mu \xi^\nu \geq -\frac{1}{2} g^{\mu\nu} T_{\mu\nu}, \quad (2.32)$$

with $T_{\mu\nu}$ being the energy-momentum tensor for matter. Equation (2.32) is known as the strong energy condition.

Note that if the congruence is initially converging, i.e., $\theta_0 < 0$ in (2.30), we have $\theta(\tau) \rightarrow -\infty$ within a proper time $\tau \leq 3/|\theta_0|$. The singularity in θ plays an important role in the proofs of the singularity theorems [17, 29]. In Sec. 4.2.3, we will show explicitly that θ is divergent at the big bang singularity for the standard FLRW universe.

For a spacetime manifold $(M, g_{\mu\nu})$, an edgeless spacelike hypersurface Σ is a Cauchy surface if every causal curve (timelike or lightlike curve) in M intersects Σ . A spacetime $(M, g_{\mu\nu})$ is globally hyperbolic if it has a Cauchy surface [17].

If ξ^μ in (2.21) is (locally) orthogonal to a spacelike hypersurface Σ , the extrinsic curvature of Σ is given by

$$K_{\mu\nu} = \nabla_\mu \xi_\nu = B_{\nu\mu}. \quad (2.33)$$

In this case, it can be proved that the expansion of the geodesic congruence is equal to the trace of the extrinsic curvature [17],

$$\theta = K \equiv h^{\mu\nu} K_{\mu\nu}. \quad (2.34)$$

Conjugate points

Consider a geodesic γ , η^μ is called a Jacobi field on γ if it satisfies the following geodesic deviation equation [17]

$$v^\mu \nabla_\mu (v^\nu \nabla_\nu \eta^\rho) = -R_{\mu\nu\alpha}{}^\rho \eta^\nu v^\mu v^\alpha, \quad (2.35)$$

where v^μ is the tangent vector along the geodesic γ .

For two points $p, q \in \gamma$, if there exists a Jacobi field η^μ (not identically zero) vanishing at p and q ,

$$\eta^\mu(p) = \eta^\mu(q) = 0, \quad (2.36)$$

then p and q are conjugate.

For a spacetime manifold, a necessary condition for a timelike geodesic being a local maximum length curve between two points p and q is that no point on the geodesic (between p and q) is conjugate to p or q (see Ref. [17] for a proof of this statement.)

For later discussion, we introduce the definition of a point p being conjugate to a surface Σ [17]: given a geodesic γ that belongs to a timelike geodesic congruence orthogonal to Σ , a point p (on γ) is conjugate to Σ if there exists a Jacobi field of the congruence that is nonzero on Σ but zero at p .

It can be proven [17] that the sufficient and necessary condition for a point p to be conjugate to Σ is that the expansion of the congruence must go to $-\infty$ at p ,

$$\theta(p) \rightarrow -\infty. \quad (2.37)$$

With this observation, we can make the following remark (Proposition 9.3.4 in Ref. [17]):

Remark 1. *Let $(M, g_{\mu\nu})$ be a spacetime with $R_{\mu\nu} \xi^\mu \xi^\nu \geq 0$ for all timelike ξ^μ . Let Σ be a spacelike hypersurface with $K = \theta < 0$ at a point $q \in \Sigma$. Then with proper time $\tau \leq 3/|K|$ there exists a point p conjugate to Σ along the geodesic γ orthogonal to Σ and passing through q , assuming that γ can be extended that far.*

For a spacetime manifold, a necessary condition for a timelike geodesic γ to be a local maximum length curve between point p and spacelike hypersurface Σ is that γ must be a geodesic orthogonal to Σ and no point on γ (between p and Σ) can be conjugate to Σ .

2.3.2. Singularity theorems

Now, we introduce the following singularity theorem relevant to cosmology (Theorem 9.5.1 in Ref [17]).

Theorem 1. *Let $(M, g_{\mu\nu})$ be a globally hyperbolic spacetime with $R_{\mu\nu} \xi^\mu \xi^\nu \geq 0$ for all timelike ξ^μ . Suppose that there exists a smooth spacelike Cauchy surface Σ for which the trace of the extrinsic curvature (for the past-directed normal geodesic congruence) satisfies $K \leq C < 0$ (with a constant C) everywhere. Then no past-directed timelike curve from Σ can have length greater than $3/|C|$. In particular, all past directed timelike geodesics are incomplete.*

A quick proof of Theorem 1 runs as follows:

Suppose that a past-directed timelike curve λ from Σ can have a length greater than $2/|C|$. For a point p lying beyond length $1/|C|$ from Σ , we can have a maximum length curve γ between the point p and the Cauchy surface Σ . Then, on the one hand, γ must be a geodesic orthogonal to Σ with no point conjugate to Σ between p and Σ . On the other hand, we know from Remark 1 that there exists a point on γ that conjugates to Σ . These two conclusions are contradictory, so the curve λ cannot exist, which finalizes the proof of Theorem 1

A rigorous proof of Theorem 1 and a more generalized theorem can be found in Ref. [17].

The timelike geodesic incompleteness could reveal the existence of a singularity. In Chapter 4, we will give some more details on how Theorem 1 predicts the big bang singularity in the standard FLRW universe, and we will also show how nonsingular bouncing cosmologies may circumvent this singularity theorem.

Penrose's singularity theorem and Gannon's singularity theorem

The first singularity theorem in GR was proposed by Penrose in 1965 [22]. This theorem is relevant to gravitational collapse. It shows geodesic incompleteness for a spacetime that is globally hyperbolic with a noncompact Cauchy surface, has a trapped surface, and satisfies $R_{\mu\nu} k^\mu k^\nu$ for all null vector k^μ .

In 1970, Hawking and Penrose [24] generalized this theorem to a more general spacetime. Five years later, Gannon [30] strengthened the theorem of Hawking and Penrose by showing that a non-simply connected spacetime could also develop a singularity.

Nontrivial topological structure of spacetime

3.1. Nontrivial topological structure of spacetime

3.1.1. Regularized black hole solution (brief review)

In this section, we will introduce a possible regularization of the Schwarzschild solution, which was first proposed in Ref. [7]. The basic idea of this regularization is to *properly* “remove” a small region at the singularity ($r = 0$) in Schwarzschild spacetime.

Instead of the manifold \mathbb{R}^4 , we will consider a noncompact, orientable, non-simply connected manifold $\mathcal{M} = \mathbb{R} \times \mathcal{M}_3$ in this section. To construct \mathcal{M}_3 , we consider first a three-dimensional Euclidean space, remove the interior of a ball with radius b , then identify antipodal points on the defect surface (two-sphere with radius b) of the ball. The first step is to remove the potential singular point in the final manifold, and the second step is to remove the boundary.

Actually, \mathcal{M}_3 has the topology:

$$\mathcal{M}_3 \simeq \mathbb{R}P^3 - \text{point}, \quad (3.1)$$

with $\mathbb{R}P^3$ the three-dimensional real projective plane.⁴ Also, the defect surface has the topology $S^2/\mathbb{Z} \sim \mathbb{R}P^2$.

Because of the nontrivial spatial topology, it is impossible to cover the manifold by using only one chart. As suggested in [7], a relatively simple coordinate system is to use three overlapping charts. In this thesis, we will focus on the chart-2 coordinates. The results and discussions based on the chart-2 coordinates are general and also hold in the other two coordinate systems.

Next, we will show a solution to the Einstein equation over the manifold \mathcal{M} .

⁴Note that $\mathbb{R}P^3$ is topologically equivalent to a three-sphere with antipodal points identified.

The general spherically symmetric *Ansatz* for the metric over manifold M is given by the following line element [7, 8]:

$$ds^2 \Big|_{\text{chart-2}} = -M(W) (dT)^2 + N(W) (dY)^2 + W \left[(dZ)^2 + \sin^2 Z (dX)^2 \right], \quad (3.2a)$$

$$W \equiv b^2 + Y^2, \quad (3.2b)$$

$$M(W) \equiv [\mu(W)]^2, \quad (3.2c)$$

$$N(W) \equiv (1 - b^2/W) [\sigma(W)]^2, \quad (3.2d)$$

where $b > 0$ corresponds to the defect length scale and $Y = 0$ gives the position of the defect surface. The functions $\mu(M)$ and $\sigma(W)$ are determined by the field equations and the boundary conditions. Note that we only show the chart-2 coordinates. The chart-2 spatial coordinates have the following ranges:

$$X \in (0, \pi), \quad (3.3a)$$

$$Y \in (-\infty, \infty), \quad (3.3b)$$

$$Z \in (0, \pi), \quad (3.3c)$$

where X and Z are angular coordinates and Y is a quasi-radial coordinate.

Considering the vacuum Einstein equation and the metric *Ansatz* (3.2), the nonsingular black hole solution has been obtained in Ref. [7] and can be written as follows:

$$ds^2 \Big|_{\text{chart-2}}^{\text{Schwarzschild form}} = - \left(1 - \frac{2M}{\sqrt{b^2 + Y^2}} \right) dT^2 + \left(1 - \frac{2M}{\sqrt{b^2 + Y^2}} \right)^{-1} \frac{Y^2}{b^2 + Y^2} dY^2 + (b^2 + Y^2) (dZ^2 + \sin^2 Z dX^2), \quad (3.4)$$

with parameters

$$2M > b > 0. \quad (3.5)$$

Notice that the metric (3.4) takes precisely the same form as the standard Schwarzschild metric if $Y^2 + b^2$ and r^2 are identified.

In a similar way as for the Schwarzschild solution, the coordinate singularity in metric (3.4) can be removed by introducing Kruskal-Szekeres-type coordinates.

The Kretschmann scalar for the metric(3.4) is given by

$$K = 48 \frac{M^2}{\zeta^6}, \quad (3.6)$$

with $\zeta \equiv \sqrt{b^2 + Y^2}$. For a nonvanishing b , it is clear that the Kretschmann scalar remains finite at $Y = 0$. The black hole singularity that appears in the Schwarzschild metric no longer exists in the metric (3.4). The degenerate metric with nontrivial topology is the key to evade the singularity theorem; cf. Sec. 3.1.5 in Ref. [27]. As a matter of fact, there exist certain geodesics that are ambiguous, i.e., they cannot be extended uniquely (we will show this in detail in Sec. 3.2).

3.1.2. Massive remnant from regularized black hole

As mentioned before, the metric (3.4) takes precisely the same form as the standard Schwarzschild metric if $Y^2 + b^2$ and r^2 are identified. With this observation, the derivation of Hawking radiation [31–33] is expected to be valid for the regularized black hole solution.

The event horizon of the regularized black hole is

$$Y_{\text{H}} \equiv \sqrt{4M^2 - b^2}. \quad (3.7)$$

Considering the region outside the event horizon, in the metric (3.4), we can introduce a new coordinate \tilde{Y} , which measures proper distance from the event horizon. This new coordinate is defined as follows:

$$\begin{aligned} \tilde{Y} &\equiv \int_{Y_{\text{H}}}^Y \sqrt{g_{YY}(Y')} dY' \\ &= \left[\sqrt{\zeta(\zeta - 2M)} + M \ln \left(\sqrt{\zeta(\zeta - 2M)} + \zeta - M \right) \right] \Big|_{2M}^{\zeta}. \end{aligned} \quad (3.8)$$

Near the event horizon, we have

$$\tilde{Y} \approx 2\sqrt{2M(\zeta - 2M)}. \quad (3.9)$$

With (3.9), we can have the following line element near the horizon

$$ds^2 \Big|_{\text{chart-2}}^{\text{Near horizon}} \simeq -\frac{\tilde{Y}^2}{16M^2} dT^2 + d\tilde{Y}^2 + \zeta^2 (dZ^2 + \sin^2 Z dX^2), \quad (3.10)$$

where we have used the approximation

$$1 - \frac{2M}{\zeta} \simeq \left(\frac{\tilde{Y}}{4M} \right)^2 \quad (3.11)$$

for $\tilde{Y} \ll 4M$.

Recall that the angular coordinates can be written as Cartesian coordinates locally. For example, near $(Z, X) = (\pi/2, \pi/2)$, we have

$$\begin{aligned} ds^2_{\mathbb{S}^2} &= \zeta^2 (dZ^2 + \sin^2 Z dX^2) \\ &= \zeta^2 (d\tilde{Z}^2 + \cos^2 \tilde{Z} d\tilde{X}^2) \\ &= \zeta^2 \left(d\tilde{Z}^2 + [1 + \mathcal{O}(\tilde{Z}^2)] d\tilde{X}^2 \right) \\ &\simeq d\zeta_1^2 + d\zeta_2^2, \end{aligned} \quad (3.12)$$

where

$$\tilde{Z} = Z - \frac{\pi}{2}, \quad (3.13)$$

$$\tilde{X} = X - \frac{\pi}{2}, \quad (3.14)$$

$$\zeta_1 = \zeta \tilde{Z}, \quad (3.15)$$

$$\zeta_2 = \zeta \tilde{X}. \quad (3.16)$$

Using (3.12) and taking into account that $\zeta \simeq 2M$ near the event horizon, the metric (3.10) takes the following form:

$$ds^2 \Big|_{\text{chart-2}}^{\text{Local, near horizon}} \simeq -\tilde{Y}^2 d\omega^2 + d\tilde{Y}^2 + d\zeta_1^2 + d\zeta_2^2, \quad (3.17)$$

with

$$\omega = \frac{T}{4M}. \quad (3.18)$$

In fact, (3.17) gives the so-called Rindler coordinates [33]. The Unruh temperature given in terms of Rindler coordinates is

$$\mathcal{T}_U = \frac{1}{2\pi\tilde{Y}}, \quad (3.19)$$

from which we can get the Hawking temperature

$$\mathcal{T}_H = \lim_{\tilde{Y} \rightarrow 0, Y' \rightarrow Y_H, Y \rightarrow +\infty} \mathcal{T}_U \frac{\sqrt{1 - \frac{2M}{\sqrt{b^2 + Y'^2}}}}{\sqrt{1 - \frac{2M}{b^2 + Y^2}}} = \frac{1}{8\pi M}. \quad (3.20)$$

Notice that

$$\frac{\sqrt{1 - \frac{2M}{\sqrt{b^2 + Y'^2}}}}{\sqrt{1 - \frac{2M}{b^2 + Y^2}}}$$

in (3.20) is the gravitational redshift factor.

So, for the nonsingular black hole, the Hawking temperature takes the same value as the one for the standard (singular) black hole. However, something different will happen if we consider the evaporations of singular and nonsingular black holes.

First, let us review the standard (singular) black hole evaporation process. Consider the Hawking radiation of a Schwarzschild black hole with an initial mass M_0 . The black hole will lose mass by the negative energy flux going into the event horizon, and the horizon will shrink. It is expected [17] that the black hole will totally disappear at the end of this process.

However, the nonsingular black hole evaporation may give a different picture.

Consider a nonsingular black hole with initial mass M_0 and constant nonvanishing length defect scale b . The black hole will lose mass through Hawking radiation and the horizon will shrink. Assuming that the mass of the black hole decreases continuously, the nonsingular black hole will cease to shrink when its mass is equal to $b/2$. The reason for this is as follows.

As the mass goes to $b/2$, i.e.,

$$M(T) \rightarrow \frac{b}{2}, \quad (3.21)$$

the horizon Y_H will approach the defect surface, i.e.,

$$Y_H \equiv \sqrt{4M^2 - b^2} \rightarrow 0. \quad (3.22)$$

If $M < b/2$, there will be no event horizon in (3.4) and the ‘‘black hole’’ will no longer lose mass by Hawking radiation.

Hence, the defect may prevent a black hole from complete evaporation and give a remnant with mass $M_{re} = b/2$. A black hole remnant with positive gravitational mass may be of interest for several reasons. It could be a candidate for dark matter [34, 35], and it can also be considered as a solution for the black hole information paradox [36, 37].

3.1.3. Stealth defect of spacetime (brief review)

By considering an $SO(3)$ matter field over the manifold \mathcal{M} , the authors of Refs. [38, 39] have constructed a new type of Skyrmion classical solution. Depending on the boundary conditions, a Skyrmion spacetime defect could have positive or negative or vanishing asymptotic

gravitational mass [38, 39]. For a defect with negative gravitational mass, a distant test particle would suffer a repulsive force, which can be understood as an anti-gravity phenomenon. While a vanishing gravitational-mass defect cannot be detected by a distant test particle (assuming that there are no long-range interactions between the defect and the test particle.) From this point of view, the defect with zero asymptotic gravitational mass can be called a “stealth defect.”

For the rest of this chapter, we will work in the dimensionless chart-2 coordinates. All lengths being measured in units of $1/(ef) > 0$ with f (which has dimensions of length) and e (dimensionless) being two parameters in the action of the Skyrme-type scalar [38, 39]. Specifically, the dimensionless version of the quasi-radial coordinate Y will be denoted by y , and the dimensionless version of the defect length scale b will be denoted by y_0 .

In general, the metric of a particular defect-type solution of the vacuum Einstein equation has been found in Ref. [39], which reads as follows:

$$ds^2 \Big|_{\text{chart-2}}^{(\text{vac. sol.})} = - (1 - l/\sqrt{w}) (dt)^2 + \frac{1 - y_0^2/w}{1 - l/\sqrt{w}} (dy)^2 + w \left[(dz)^2 + \sin^2 z (dx)^2 \right], \quad (3.23a)$$

$$w \equiv y_0^2 + y^2, \quad (3.23b)$$

where the angular coordinates X and Z have been denoted by x and z , respectively.

For a globally regular solution, the real constant l in (3.23a) takes the following values:

$$l \in (-\infty, y_0). \quad (3.24)$$

3.2. Lensing by a stealth defect of spacetime

In this section, we will demonstrate a new type of gravitational lensing, by investigating the geodesics in a stealth defect of spacetime. The main content of this section follows [11].

3.2.1. Geodesics of flat-spacetime stealth defect

From Sec. 2.4 and Fig. 5 in Ref. [39], the simplest stealth-defect solution is given by $l = 0$ in (3.23). Hence, we get the metric for the stealth defect of spacetime

$$ds^2 \Big|_{\text{vac. sol. } l=0} = -(dt)^2 + A(y) (dy)^2 + w \left[(dz)^2 + \sin^2 z (dx)^2 \right], \quad (3.25a)$$

with

$$A(y) = \frac{y^2}{y_0^2 + y^2} \quad (3.25b)$$

and w defined by (3.23b).

Two remarks on (3.25) are in order. First, for a nonvanishing defect length scale b (y_0 is nonzero), the metric from (3.25) is degenerate: $\det g_{\mu\nu} = 0$ at $y = 0$. With a degenerate metric, tensor contraction may not be well defined at the defect surface.

Second, away from the stealth defect, the Riemann curvature tensor is zero, i.e.,

$$R_{\mu\nu\rho}{}^\sigma = 0, \quad (3.26)$$

for $y \neq 0$. With this observation, the metric (3.25) actually represents a flat-spacetime stealth defect.

Next, we will find how particles move in the flat spacetime with a stealth defect. Our calculation follows Sec. 8.4 of Ref. [14].

The nonvanishing Christoffel symbols are [11]

$$\Gamma^y_{yy} = \frac{A'}{2A}, \quad (3.27a)$$

$$\Gamma^y_{zz} = -\frac{w'}{2A}, \quad (3.27b)$$

$$\Gamma^y_{xx} = -\frac{w' \sin^2 z}{2A}, \quad (3.27c)$$

$$\Gamma^z_{yz} = \Gamma^z_{zy} = \frac{w'}{2w}, \quad (3.27d)$$

$$\Gamma^z_{xx} = -\sin z \cos z, \quad (3.27e)$$

$$\Gamma^x_{yx} = \Gamma^x_{xy} = \frac{w'}{2w}, \quad (3.27f)$$

$$\Gamma^x_{zx} = \Gamma^x_{xz} = \cot z, \quad (3.27g)$$

where the prime stands for differentiation with respect to y .

Notice that the first three Christoffel symbols are divergent at the defect surface, but our results will show that the motion of a particle can still be regular.

The geodesic equation [14] with affine parameter λ is given by

$$\frac{d^2 x^\alpha}{d\lambda^2} + \Gamma^\alpha_{\mu\nu} \frac{dx^\mu}{d\lambda} \frac{dx^\nu}{d\lambda} = 0. \quad (3.28)$$

For our flat-spacetime stealth defect, (3.28) gives

$$0 = \frac{d^2 t}{d\lambda^2}, \quad (3.29a)$$

$$0 = \frac{d^2 y}{d\lambda^2} + \Gamma^y_{yy} \left(\frac{dy}{d\lambda}\right)^2 + \Gamma^y_{zz} \left(\frac{dz}{d\lambda}\right)^2 + \Gamma^y_{xx} \left(\frac{dx}{d\lambda}\right)^2, \quad (3.29b)$$

$$0 = \frac{d^2 z}{d\lambda^2} + 2\Gamma^z_{yz} \frac{dy}{d\lambda} \frac{dz}{d\lambda} + \Gamma^z_{xx} \left(\frac{dx}{d\lambda}\right)^2, \quad (3.29c)$$

$$0 = \frac{d^2 x}{d\lambda^2} + 2\Gamma^x_{yx} \frac{dy}{d\lambda} \frac{dx}{d\lambda} + 2\Gamma^x_{zx} \frac{dz}{d\lambda} \frac{dx}{d\lambda}. \quad (3.29d)$$

We can choose the normalization of λ so that the solution of (3.29a) has

$$\frac{dt}{d\lambda} = 1. \quad (3.30)$$

With the normalization (3.30), λ can be replaced by t in (3.29b), (3.29c), and (3.29d).

Since the metric is spherically symmetric, to simplify the calculations, we need only consider the case $z = \pi/2$.

First, consider the general case with $dx/dt \neq 0$. For this case, divide (3.29d) by dx/dt and use the Christoffel symbols from (3.27). We obtain the following relation between angular coordinate x and quasi-radial coordinate y :

$$\frac{d}{dt} \left(\ln \frac{dx}{dt} + \ln w \right) = 0, \quad (3.31)$$

which gives a real constant (up to a sign),

$$J \equiv w \frac{dx}{dt}. \quad (3.32)$$

With (3.27), (3.32), and multiplying (3.29b) by $2A dy/dt$, we find

$$\frac{d}{dt} \left[A \left(\frac{dy}{dt} \right)^2 + \frac{J^2}{w} \right] = 0. \quad (3.33)$$

Hence, we arrive at the following constant of motion:

$$E \equiv A \left(\frac{dy}{dt} \right)^2 + \frac{J^2}{w}. \quad (3.34)$$

By elimination of t from (3.32) and (3.34), we get y as a function of x ,

$$\frac{A}{w^2} \left(\frac{dy}{dx} \right)^2 + \frac{1}{w} = \frac{E}{J^2}. \quad (3.35)$$

From (3.32), (3.34), and $z = \pi/2$, the metric (3.25) along the geodesic can now be written as

$$ds^2 = (-1 + E)(dt)^2. \quad (3.36)$$

With our notation, we have from (3.36) that

$$E = 1, \quad \text{for a massless particle,} \quad (3.37a)$$

$$E \in [0, 1), \quad \text{for a massive particle.} \quad (3.37b)$$

Radial geodesics

Now, let us consider the case with $dx/dt = 0$. In particular, we want to obtain the geodesic equation for a particle moving in the negative y direction (going from right to left in Fig. 3.1). From the definition of J in (3.32), it follows immediately that $J = 0$, even though J was initially defined as a nonzero quantity [see the sentence at the start of the paragraph above (3.31)].

The corresponding energy-type constant of motion is

$$E = \frac{y^2}{y_0^2 + y^2} \left(\frac{dy}{dt} \right)^2. \quad (3.38)$$

The solutions of (3.38) are

$$y = \pm \sqrt{-y_0^2 + \left(+\sqrt{E}t + C_1 \right)^2}, \quad (3.39a)$$

$$y = \pm \sqrt{-y_0^2 + \left(-\sqrt{E}t + C_2 \right)^2}, \quad (3.39b)$$

with C_1 and C_2 being real constants which depend on the initial conditions. An example of a radial geodesic is shown in Fig. 3.2

Two remarks are in order. First, by making appropriate time shifts (or setting $C_1 = C_2 = y_0$) and defining $B \equiv \sqrt{E}/y_0$, the solutions (3.39) reproduce the results of Sec. 3 in Ref. [7].

Second, we find a constant y solution, i.e., the particle is at rest in (t, y, x, z) coordinates, for $E = 0$ in (3.39).

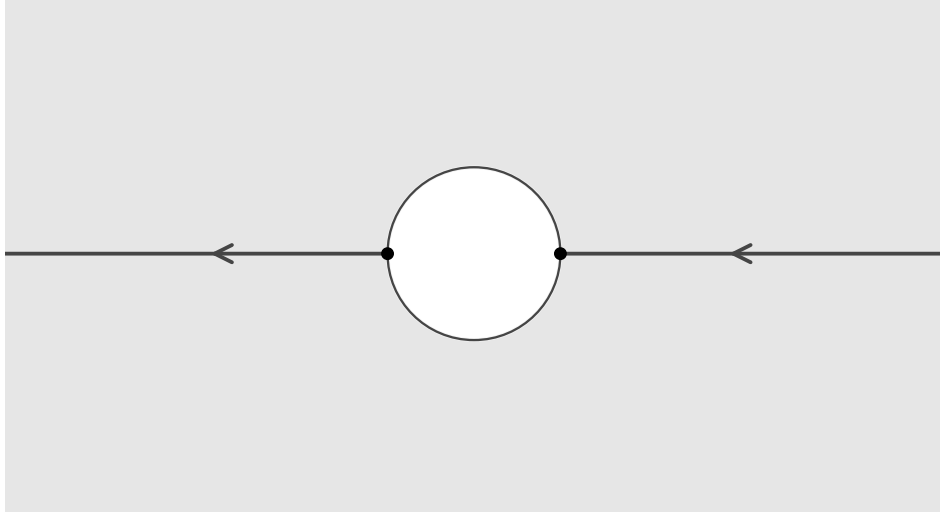


Figure 3.1.: Radial geodesic for the stealth defect (3.25). Part of the 3-dimensional space manifold is indicated by the shaded area, and antipodal points (dots) on the defect surface are identified.

Nonradial geodesics

We have shown that particles moving exactly in the radial direction can pass through the defect. Next, we will show the geodesics of particles that move in the nonradial direction.

Nonradial geodesics actually exist in two types, those that reach the defect and those that do not.

As we have mentioned before (see (3.26)), outside the defect surface, the spacetime (3.25) is Minkowskian. So, geodesics that do not cross the defect surface should be straight lines with standard Cartesian coordinates. Next, we will show this explicitly.

From (3.35), we find the following relation between angular coordinate x and quasi-radial coordinate y

$$\int dx = \pm \int \frac{y dy}{(y_0^2 + y^2) \sqrt{(E/J^2)(y_0^2 + y^2) - 1}}. \quad (3.40)$$

Define the quasi-radial coordinate y_1 corresponding to the point on the line closest to the defect surface (cf. Fig. 3.3 with $y_1 > 0$), so that $|y_1|$ can be understood as an “impact parameter.”

Since $d\sqrt{w}/dx$ and dy/dx must vanish at y_1 , (3.35) reduces to

$$\frac{1}{y_0^2 + y_1^2} = \frac{E}{J^2}. \quad (3.41)$$

Then, (3.40) can be written as

$$x(y) = x(\infty) \pm \int_y^\infty \frac{y dy}{(y_0^2 + y^2) \sqrt{(y_0^2 + y^2)/(y_0^2 + y_1^2) - 1}}. \quad (3.42)$$

At $y = y_1$, (3.42) gives

$$|x(y_1) - x(\infty)| = \pi/2, \quad (3.43)$$

i.e., the angular coordinate x has changed by an amount $\pi/2$ when the particle moves from infinity to the point closest to the defect surface. The result (3.43) shows that geodesics, which are nonradial and nonintersecting with the defect surface, are indeed straight lines.

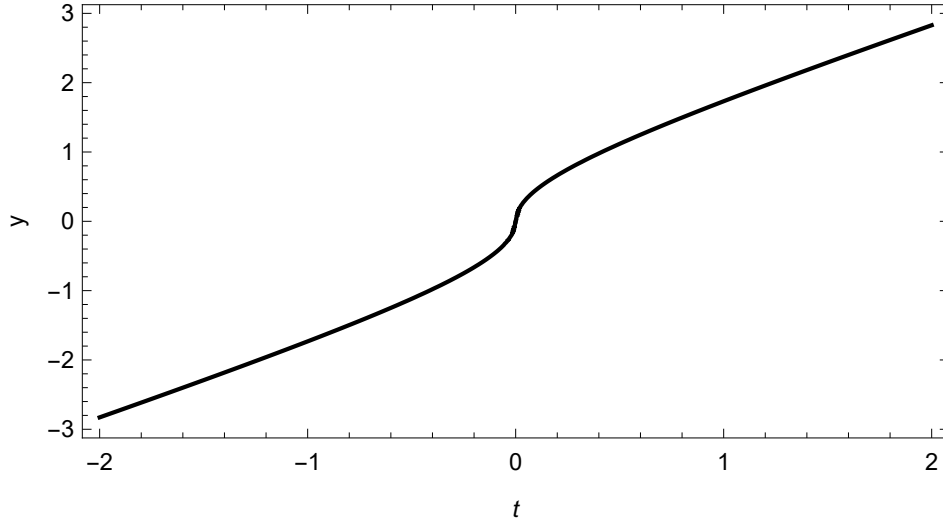


Figure 3.2: Null radial geodesic for the stealth defect (3.25). The geodesic is given by (3.39) with a plus sign in (3.39a) and a minus sign in (3.39b). Also, we have set $C_1 = C_2 = y_0 = 1$, and $E = 1$ in (3.25).

Now, we will consider nonradial geodesics that cross the defect surface.

If we use in (3.35) the replacement

$$\frac{dy}{dx} = \frac{1}{2y} \frac{dy^2}{dx}, \quad (3.44)$$

we find the following two solutions for y^2 :

$$y^2 = \frac{\tan^2(x_1 + x) + 1}{E/J^2} - y_0^2, \quad (3.45a)$$

$$y^2 = \frac{\tan^2(x_2 - x) + 1}{E/J^2} - y_0^2, \quad (3.45b)$$

where x_1 and x_2 are real constants.

Recall that the metric (3.25) has a spherically symmetric form and the corresponding “radial” coordinate is given by

$$\sqrt{w} \in [y_0, \infty). \quad (3.46)$$

After a shift of the constants, the solutions (3.45) can be written as

$$\sqrt{w} \sin(x_1 - x) = \pm \frac{J}{\sqrt{E}}, \quad (3.47a)$$

$$\sqrt{w} \sin(x_2 + x) = \pm \frac{J}{\sqrt{E}}, \quad (3.47b)$$

with $\sqrt{w} \geq y_0$. Three comments on the solutions (3.47) are in order:

- (i) mathematically, the solutions are straight lines or straight-line segments in polar-type coordinates (\sqrt{w}, x) ;
- (ii) the solutions are regular at the defect surface, $\sqrt{w} = y_0$;
- (iii) to find the complete geodesic of a given particle among these solutions, we must remember the antipodal identifications at the defect surface $\sqrt{w} = y_0$.

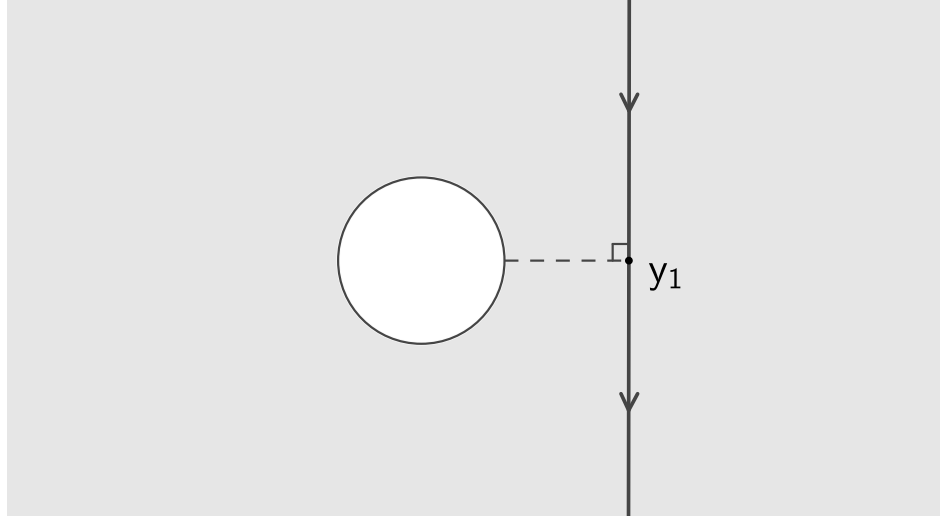


Figure 3.3.: Nonradial geodesic that does not cross the defect surface and defines the quasi-radial coordinate $y_1 > 0$.

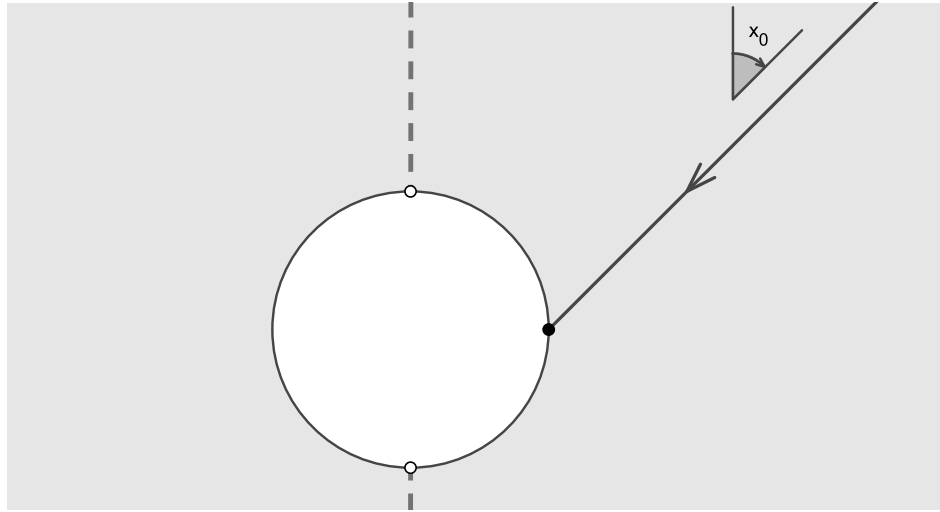


Figure 3.4.: Ingoing line (3.48) lying in the domain of the chart-2 coordinates. The dashed line shows the x_3 Cartesian axis, which does not belong to the domain of the chart-2 coordinates.

For a nonradial ingoing line, it is convenient to choose coordinates so that the end of the ingoing line has $x = \pi/2$ (Fig. 3.4). In these coordinates, the ingoing line is given by

$$\sqrt{w} \sin(x_0 - x) = -y_0 \cos x_0, \quad (3.48a)$$

with

$$0 < x_0 < x \leq \pi/2. \quad (3.48b)$$

Notice that we have included the end point of the ingoing line, i.e., $x = \pi/2$, in (3.48b). It is easy to see that the formula (3.48) indeed corresponds to one of the solutions (3.47).

For the ingoing line (3.48), there will exist, among the solutions (3.47), a unique outgoing line (Fig. 3.5) if the following two conditions are met:

1. the beginning of the outgoing line and the end of the ingoing line must be antipodal points at the defect surface (these points are identified);

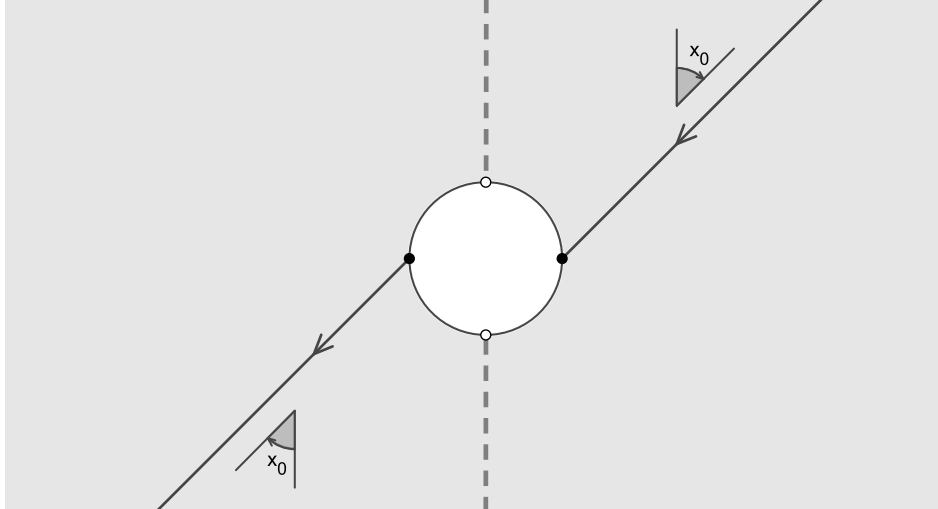


Figure 3.5.: Nonradial geodesic crossing the defect surface.

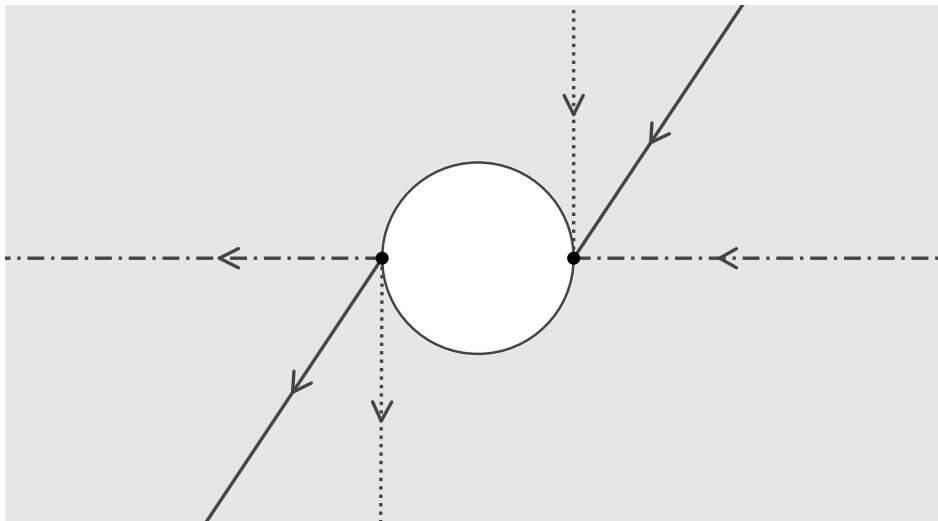


Figure 3.6.: Family of geodesics crossing the defect surface.

2. the complete geodesic must be a straight line if $y_0 = 0$.

Observe that with a nonradial ingoing line as in Fig. 3.5, the quantity J will change sign after crossing the defect surface (see Ref. [40] for further discussion of the anomalous angular-momentum behavior of scattering solutions).

Based on the above discussion, Fig. 3.6 shows three geodesics from a continuous family of geodesics crossing the defect surface: the family ranges continuously from a radial geodesic (dot-dashed line in Fig. 3.6) to a tangent geodesic (dotted line in Fig. 3.6).

Now, consider a tangent ingoing line (solid line in Fig. 3.7). On the one hand, according to the dotted line in Fig. 3.6, we have a “shifting tangent outgoing line” (dotted line in Fig. 3.7). On the other hand, from the limiting case of the geodesic in Fig. 3.3 with $y_1 \rightarrow 0^+$, we could obtain an “ongoing tangent line” (dot-dashed line in Fig. 3.7). With this observation, we conclude that “certain geodesics at the defect surface $y = 0$ cannot be continued uniquely,” as mentioned in the second remark of Sec. VI in Ref. [38] (further discussion can be found in Sec. 3.1.5 of Ref. [27]).

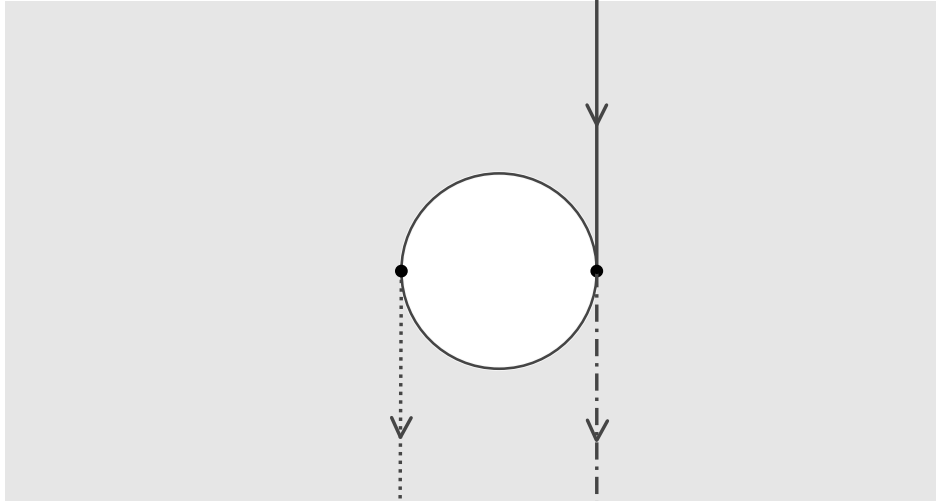


Figure 3.7.: Geodesic at the defect surface that cannot be continued uniquely.

Image formation by a flat-spacetime stealth defect

Fig. 3.5 has actually presented a crucial effect caused by the spacetime stealth defect: for a nonradial geodesic reaching the defect surface, the defect can make a parallel shift of the geodesic in the ambient space (i.e., the Euclidean 3-space away from the defect surface). In this subsection, we will show that this nontrivial effect can lead to the phenomenon of image formation.

To show the image formation explicitly, we consider first the geodesics that start from a point P at one side of the defect (see Fig. 3.8, where the point P is on the right-hand side of the defect). For geodesics that cross the defect surface, according to the parallel shift shown in Fig. 3.5, there will be an intersection point P' at the other side of the defect (see the left-hand side of Fig. 3.8). In fact, P and P' are reflection points about the “center” of the defect. The different paths connecting P and P' have, in general, different values for the time-of-flight.⁵

Similarly to Fig. 3.8, a permanent luminous object on one side of the defect will have a real image on the other side of the defect (Fig. 3.9).

Five remarks on Fig. 3.8 and the image formation are in order.

- (i) The image is inverted and the image and object have the same size. Note that this is also the case if an object in Minkowski spacetime is located at a double focal length of a standard thin double-convex lens (see Ref. [41]).
- (ii) If we consider the image from a static luminous source, then the irradiance of the image depends on both the defect scale b and the location of the source (the irradiance is defined as the power per unit receiving area; cf. Secs. 5.3.2 and 5.3.5 in Ref. [42]). The irradiance will be larger if b is increased for an unchanged source position (larger “white disk” in Fig. 3.9) or if the source is brought closer to the defect for an unchanged defect scale (object and image closer to the “white disk” in Fig. 3.9): in both cases, the flux captured and transmitted by the defect is larger.
- (iii) Returning to the analogy with standard lenses in Minkowski spacetime as mentioned in the first remark, recall the standard lens equation $1/d_{\text{object}} + 1/d_{\text{image}} = 1/f$ in

⁵Taking into account the particle–wave duality, we can interpret the three geodesics crossing the defect surface in Fig. 3.8 as coherent light emitted from the source P . Then, due to the different values for the time-of-flight, these coherent-light bundles will have a constant (time-independent) phase difference at P' , which leads to stationary interference. In this sense, the defect resembles some types of interferometers.

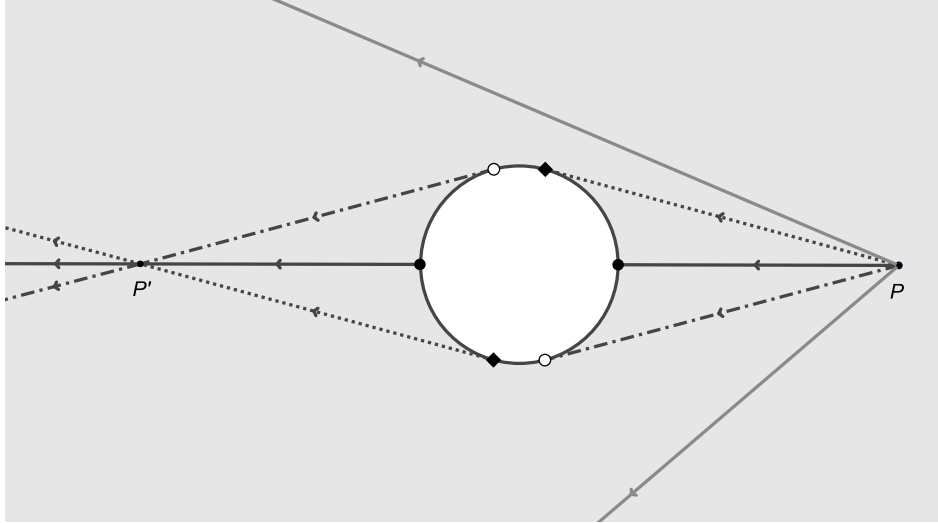


Figure 3.8.: Geodesics with intersection points P and P' .

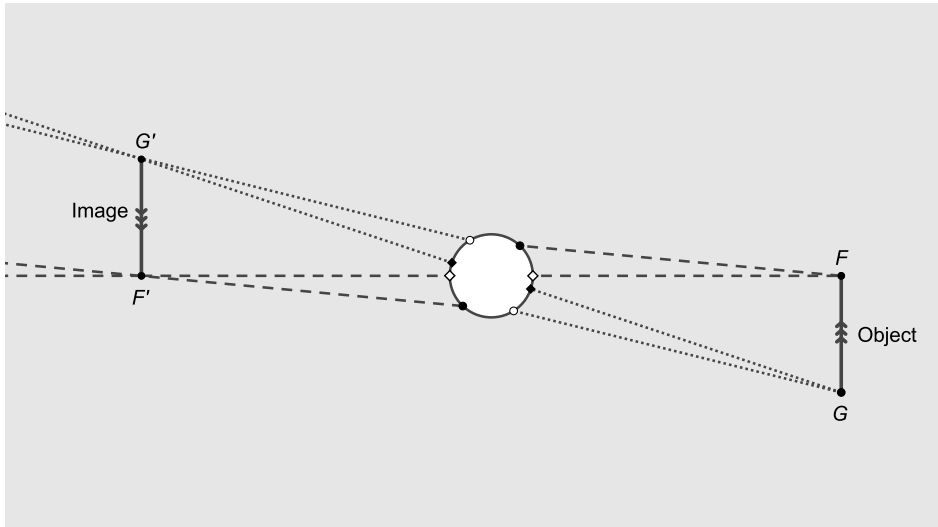


Figure 3.9.: Image formation by a stealth defect.

Minkowski spacetime [41]. The defect actually has an effective focal length f_{eff} given by

$$2f_{\text{eff}} = \sqrt{b^2 + (Y_{\text{object}})^2} \in (b, \infty), \quad (3.49)$$

where $Y_{\text{object}} \equiv y_{\text{object}}/(ef) \neq 0$ is the dimensional chart-2 quasi-radial coordinate of a small object away from the defect surface.

- (iv) Consider the case that a permanent pointlike light source is located at point P of Fig. 3.8. Then what an observer at point P' will see is not a point but a luminous disk. This phenomenon is of course different from the Einstein ring [43–47].
- (iv) Needless to say, the unusual ingredient for the lensing behavior is the spacetime defect (i.e., the nontrivial topological structure of spacetime). Then, it would be interesting to compare the above results with the lensing results from wormholes (see Refs. [48–51] and references therein). For the case of the wormholes, the unusual ingredient is the exotic matter.

So far, we have shown the geodesics of a flat-spacetime stealth defect, and the corresponding lensing behavior. In the following subsection, we will show the geodesics of a curved-spacetime stealth defect.

3.2.2. Geodesics of curved-spacetime stealth defect

The logic of this subsection is as follows.

First, we will start with a general spacetime defect. Then, calculations will show that the lensing behavior can still hold in a general spacetime defect. At last, we will show the geodesics of a given curved-spacetime stealth defect and the corresponding lensing behavior.

General results

Recall that the general spherically symmetric *Ansatz* for the spacetime of defect is given by (3.2). (Based on (3.2), the following calculations are quite general and do not depend on the explicit form of $\mu(w)$ and $\sigma(w)$.)⁶

Without loss of generality, the spherical symmetry allows us to consider the particle moving in the equatorial plane, i.e., $z = \pi/2$.

In this case, the nonvanishing Christoffel symbols are given by

$$\Gamma^t_{ty} = \Gamma^t_{yt} = -\frac{1}{2M} \frac{dM}{dy}, \quad (3.50a)$$

$$\Gamma^y_{tt} = -\frac{1}{2N} \frac{dM}{dy}, \quad (3.50b)$$

$$\Gamma^y_{yy} = \frac{1}{2N} \frac{dN}{dy}, \quad (3.50c)$$

$$\Gamma^y_{xx} = -\frac{1}{2N} \frac{dw}{dy}, \quad (3.50d)$$

$$\Gamma^x_{xy} = \Gamma^x_{yx} = \frac{1}{2w} \frac{dw}{dy}. \quad (3.50e)$$

With the procedure we have used in Sec. 3.2.1, the geodetic equation gives

$$\frac{dt}{d\lambda} = M, \quad (3.51a)$$

$$w \frac{dx}{d\lambda} = \tilde{J}, \quad (3.51b)$$

$$N \left(\frac{dy}{d\lambda} \right)^2 + \frac{\tilde{J}^2}{w} - \frac{M^3}{3} = \tilde{E}, \quad (3.51c)$$

where \tilde{J} and \tilde{E} are real constants and λ is the affine parameter.

By elimination of λ from (3.51b) and (3.51c), we have

$$\frac{\tilde{J}^2 N(w)}{w^2} \left(\frac{dy}{dx} \right)^2 + \frac{\tilde{J}^2}{w} - \frac{[M(w)]^3}{3} = \tilde{E}. \quad (3.52)$$

⁶The functions $\mu(w)$ and $\sigma(w)$ are determined by the field equations and the boundary conditions.

With the the help of (3.44), (3.52) can be written as

$$\frac{\tilde{J}^2 N(w)}{4y^2 w^2} \left(\frac{dy^2}{dx} \right)^2 + \frac{\tilde{J}^2}{w} - \frac{[M(w)]^3}{3} = \tilde{E}, \quad (3.53)$$

with the constants \tilde{J} and \tilde{E} from (3.51).

The orbit of a particle moving in the equatorial plane $z = \pi/2$ is described by (3.53). Observe that $N(w)$ and $M(w)$ are functions of w and, hence, functions of y^2 . If the solution of (3.53) exists, x must be a function of y^2 : $x = x(y^2)$. Recall that the chart-2 coordinate ranges are given by

$$x \in (0, \pi), \quad y \in (-\infty, \infty), \quad z \in (0, \pi). \quad (3.54)$$

For a particular solution $x = x(y^2)$ in the $z = \pi/2$ plane of the chart-2 domain, there will exist two branches of this solution: one branch with $y \geq 0$ and the other one with $y \leq 0$. To be specific, the lines that correspond to these two branches of the solution are symmetrical about the ‘‘center’’ of the defect surface. If the orbit of a given particle which does not cross the defect surface, then this orbit is usually described by only one of these two branches. But, if the particle crosses the defect surface, then we argue that the ingoing and outgoing lines are given by two different branches. Note that, in flat spacetime, this argument is consistent with the two conditions for the existence of a unique outgoing line as discussed in Sec. 3.2.1.

Based on the above discussion, a defect in a curved spacetime has the same lensing behavior as discussed in Sec. 3.2.1 for the flat-spacetime case. Still, there is one exception: a black hole may occur for this defect spacetime [7]. Then, the metric (3.2) is not globally regular and (3.53) cannot properly describe the orbit of the particle reaching the defect surface. In fact, the particle will be confined within the black-hole horizon once it crosses the horizon. (It may be of interest to consider null geodesics in the spacetime with a massive black hole remnant discussed in Sec. 3.1.2. Then, the lensing behavior discussed above could be a possible observable effect for the black hole remnant.)

Next, we will give an explicit example of the geodesics in a curved-spacetime stealth defect for illustrative purposes.

Explicit calculation

The numerical stealth-defect solution from Fig. 4 of Ref. [39] has metric functions $\sigma(w)$ and $\mu(w)$ in (3.2) with approximately the following form:

$$\sigma(w) = 1 - \frac{1}{2w}, \quad (3.55a)$$

$$\mu(w) = 1, \quad (3.55b)$$

for $y_0 = 1$ (giving $w \equiv 1 + y^2$).

Now, we will give the analytic solutions of (3.51) and (3.53) from the explicit choice of functions in (3.55).

For the radial geodesic ($\tilde{J} = 0$), the general solutions of (3.51c) are given as follows:

$$\frac{2w(2w+1) \sqrt{(-2w+1)^2/w^3}}{2w-1} = +4t \sqrt{\tilde{E} + 1/3} + \tilde{C}_1, \quad (3.56a)$$

$$\frac{2w(2w+1) \sqrt{(-2w+1)^2/w^3}}{2w-1} = -4t \sqrt{\tilde{E} + 1/3} + \tilde{C}_2, \quad (3.56b)$$

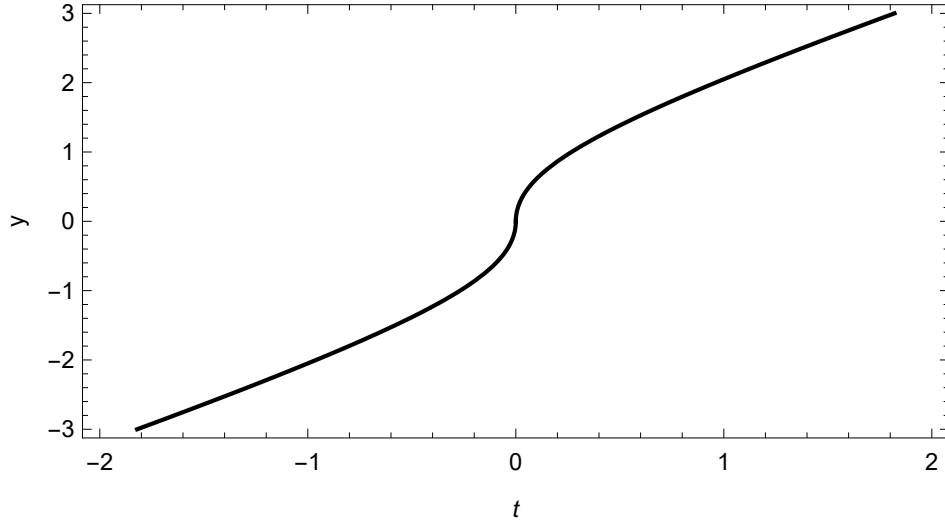


Figure 3.10.: Null radial geodesic for the stealth defect (3.2) with metric functions (3.55). The geodesic is given by (3.56) with $\tilde{C}_1 = \tilde{C}_2 = 6$, $y_0 = 1$, and $\tilde{E} = 2/3$.

where \tilde{C}_1 and \tilde{C}_2 are real constants. An example of the null radial geodesic is shown in Fig. 3.10.

For a nonradial geodesic, the solutions of (3.53) are

$$\pm x = \frac{1}{4} \left((4 - D) \arctan(\sqrt{Dw - 1}) - \frac{\sqrt{Dw - 1}}{w} \right) + \tilde{x}_4, \quad (3.57a)$$

with the definition

$$D \equiv \frac{\tilde{E} + 1/3}{\tilde{J}^2} \quad (3.57b)$$

and a real constant \tilde{x}_4 .

As the spacetime is curved, geodesics that do not cross the defect surface will not be straight lines in general. In this case, we can calculate the change in x (as we have done in Sec. 3.2.1),

$$\Delta x \equiv |x(y_1) - x(\infty)| = \frac{\pi}{2} \left(1 - \frac{1/4}{1 + y_1^2} \right), \quad (3.58)$$

where y_1 corresponds to the point on the line closest to the defect surface. For small y_1 (i.e., the line coming close to the defect surface), (3.58) shows that the line is bent away from the defect surface. This observation agrees with the fact that the effective mass near the defect surface is negative (for more details, see the $l(w)$ panel in Fig. 4 of Ref. [39]).

Note that (3.57) can be rewritten in the following way:

$$\pm \frac{1}{\sqrt{D}} = \sqrt{w} \cos \left[\frac{4(x - x_4) + \sqrt{Dw - 1}/w}{4 - D} \right], \quad (3.59a)$$

$$\pm \frac{1}{\sqrt{D}} = \sqrt{w} \cos \left[\frac{4(-x + x_5) + \sqrt{Dw - 1}/w}{4 - D} \right], \quad (3.59b)$$

with real constants x_4 and x_5 . As a concrete example, we first consider the solution corresponding to the upper sign on the left-hand side of (3.59a), that is,

$$\frac{1}{\sqrt{D}} = \sqrt{w} \cos \left[\frac{4(x - x_4) + \sqrt{Dw - 1}/w}{4 - D} \right]. \quad (3.60)$$

For given values of D and x_4 , the solution (3.60) has, in general, two branches: one branch lies in the upper half-plane ($y > 0$) and the other in the lower half-plane ($y < 0$). The solid lines in Fig. 3.11 correspond to the orbits of two different particles, while the dotted line corresponds to the orbit of a third particle. Even though the points on the solid lines which are closest to the defect surface have $x = \pi/2$, these solid lines are not symmetrical about the line $x = \pi/2$ for $w \sim 2$, as can be verified in (3.60) with $x' = \pi - x$ and $w(x') \neq w(x)$.

Fig. 3.12 shows a family of geodesics to illustrate the lensing property of the curved-spacetime defect (cf. Fig. 3.8 for the lensing of the flat-spacetime defect).

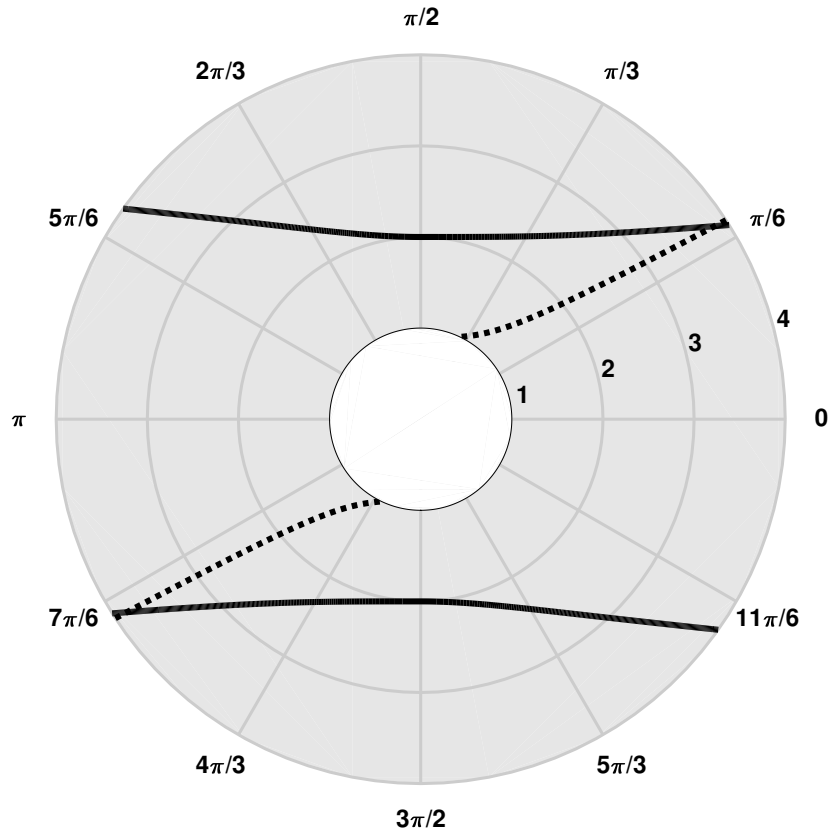


Figure 3.11.: Geodesics in polar coordinates (\sqrt{w}, ϕ) . The geodesics are given by (3.60). With the chart-2 coordinates x and y , the azimuthal angle ϕ is defined by $\phi = x$ if $y > 0$ and $\phi = x + \pi$ if $y < 0$. The defect surface is given by the circle $w = 1$ and part of the 3-dimensional space manifold (3.2) (with metric functions (3.55)), is indicated by the shaded area. The solid lines have constants $D = 0.25$ and $x_4 = \pi/2$, and the dotted-line segments have constants $D = 1.25$ and $x_4 = \pi/2$. The points on the solid lines that are closest to the defect surface have polar coordinates $(2, \pi/2)$ and $(2, 3\pi/2)$, corresponding to the original coordinates $(y, x) = (\pm\sqrt{3}, \pi/2)$.

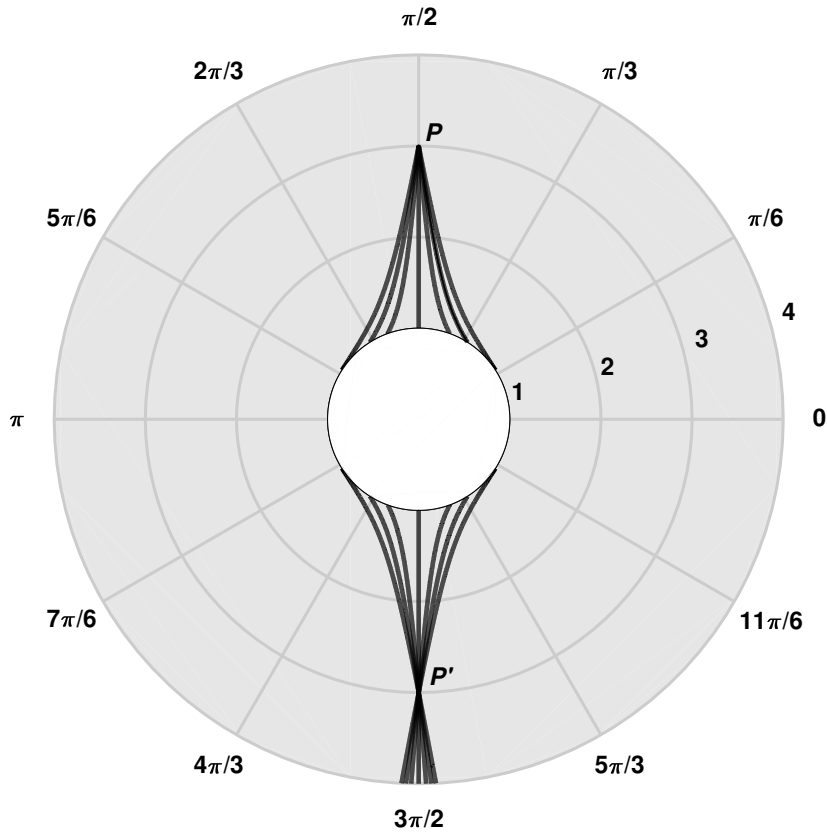


Figure 3.12.: Family of geodesics in polar coordinates (\sqrt{w}, ϕ) , where the geodesics are given by (3.59) with plus signs on the left-hand sides. The defect surface is given by the circle $w = 1$. The parameters of the six curved geodesics in the upper half-plane are, from left to right, $(D = 1, x_4 = 2.57258)$, $(D = 1.2, x_4 = 2.5408766)$, $(D = 1.5, x_4 = 2.4784766)$, $(D = 1.5, x_5 = \pi - 2.4784766)$, $(D = 1.2, x_5 = \pi - 2.5408766)$, and $(D = 1, x_5 = \pi - 2.57258)$. In terms of the original (y, x) coordinates, the focal points P and P' are given by $(y, x)_P = (\sqrt{8}, \pi/2)$ and $(y, x)_{P'} = (-\sqrt{8}, \pi/2)$.

Nonsingular bouncing cosmology

4.1. Bouncing cosmologies (brief review)

By bouncing cosmologies, we mean universes that go from a contraction to an expansion, with or without a big bang singularity. The history of bouncing cosmologies dates back to the work of Friedmann [21], who introduced the possibility of a closed cyclic universe. (By cyclic universe, we mean the cosmic scale factor $a(t)$ that oscillates between some minimal value (zero or nonzero) and some large finite value.)

In the scientific literature of bouncing cosmologies [52], a regular bounce can be derived either from general relativity (with unusual energy condition of matter) or from the theories beyond general relativity, e.g., modified gravity, loop quantum gravity, and string theory.

General features of bouncing cosmologies are given as follows:

- 1 avoid the big bang singularity by having a nonvanishing cosmic scale factor at the bounce;
- 2 solve the horizon problem by having an infinite past particle horizon;
- 3 solve the flatness problem;
- 4 make timelike and lightlike geodesics complete.

For different bouncing cosmologies, there may exist other advantages. For example, the matter bounce scenario [53] may produce a scale-invariant power spectrum for cosmological perturbation, and the Ekpyrotic scenario [54] can avoid the anisotropy problem (a brief introduction to the anisotropy problem will be given in App. C.)

4.2. Nonsingular bouncing cosmology

Actually, most of the bouncing models in the context of general relativity require the violation of the strong energy condition [52]. In this section, we will introduce a bouncing model [10, 12] without violation of the strong energy condition for matter. This new nonsingular bouncing model is based on general relativity but allows for degenerate metrics.

4.2.1. Regularized big bang singularity

The new nonsingular bouncing model discussed in this chapter actually comes along with a particular regularization of the big bang singularity. So, before we start to present the nonsingular bouncing cosmology, we first review the regularized big bang singularity.

The particular regularization of the big bang singularity is based on the following *Ansatz* for the metric [10, 12, 55] :

$$ds^2 \Big|_{\text{mod. RW}} \equiv g_{\mu\nu}(x) dx^\mu dx^\nu \Big|_{\text{mod. RW}} = -\frac{T^2}{b^2 + T^2} dT^2 + a^2(T) \delta_{ij} dx^i dx^j, \quad (4.1a)$$

$$b^2 > 0, \quad (4.1b)$$

$$T \in (-\infty, \infty), \quad (4.1c)$$

$$x^i \in (-\infty, \infty), \quad (4.1d)$$

where the spatial indices i, j run over $\{1, 2, 3\}$.

In fact, (4.1a) is a modified version of spatially flat RW metric (2.7). First, it precisely gives the standard spatially flat RW metric if $b = 0$. Second, for a nonvanishing b (as required by (4.1b)), by defining the new coordinate

$$t(T) = \begin{cases} +\sqrt{b^2 + T^2}, & \text{for } T \geq 0, \\ -\sqrt{b^2 + T^2}, & \text{for } T \leq 0, \end{cases} \quad (4.2)$$

we can write the line element (4.1a) in a standard spatially flat RW metric form:

$$ds^2 \Big|_{\text{mod. RW}} = -dt^2 + \tilde{a}^2(t) \delta_{ij} dx^i dx^j, \quad (4.3a)$$

$$t \in (-\infty, -b] \cup [b, +\infty). \quad (4.3b)$$

Two remarks are in order. First, the coordinate transformation from T to t is not a diffeomorphism,⁷ so that the differential structure of the metric (4.1) is different from the standard spatially flat RW metric (4.3).

Second, the t domains $(-\infty, -b]$ and $[b, +\infty)$ are disconnected and t is multivalued at $T = 0$, so the boundary conditions at $t = \pm b$ require special care if we do calculations in t coordinate (see Ref. [40] for a related discussion.)

With the metric (4.1) and taking the energy-momentum tensor of a homogeneous perfect fluid (2.10), the Einstein gravitational field equation leads to the following modified spatially flat Friedmann equation and unmodified energy-conservation equation:

$$\left(1 + \frac{b^2}{T^2}\right) \left(\frac{1}{a(T)} \frac{da(T)}{dT}\right)^2 = \frac{8\pi}{3} \rho(T), \quad (4.4a)$$

$$\frac{d}{da} \left[a^3 \rho \right] + 3 a^2 P = 0. \quad (4.4b)$$

Remark that (4.4a) is singular at $T = 0$, but, as we will show soon, it can have nonsingular solutions.

⁷A diffeomorphism is, by definition, an invertible function that maps one manifold to another manifold such that the function and its inverse function are C^∞ functions.

In general, the solutions $a(T)$ of (4.4) could be even or odd in T [10]. The T -odd solution could be of interest for a CPT -symmetric universe [56]. The T -even solution, with positive definite cosmic scale factor, naturally gives a nonsingular bouncing universe. So, in this chapter, we will focus on the T -even solution.

For a radiation-dominated universe ($w = P/\rho = 1/3$), we have the following solutions for $a(T)$ and $\rho(T)$:

$$a(T)\Big|_{\text{mod. FLRW}}^{(w=1/3)} = \sqrt[4]{\frac{b^2 + T^2}{b^2 + T_0^2}}, \quad (4.5)$$

$$\rho\Big|_{\text{mod. FLRW}}^{(w=1/3)} = \rho_0 \frac{b^2 + T_0^2}{b^2 + T^2}, \quad (4.6)$$

where the cosmic scale factor $a(T)$ has been normalized to unity at $T = T_0 > 0$ and where the boundary condition $\rho(T_0) = \rho_0 > 0$.

For a matter-dominated universe ($w = 0$), we have

$$a(T)\Big|_{\text{mod. FLRW}}^{(w=0)} = \sqrt[3]{\frac{b^2 + T^2}{b^2 + T_0^2}}, \quad (4.7)$$

$$\rho\Big|_{\text{mod. FLRW}}^{(w=0)} = \rho_0 \frac{b^2 + T_0^2}{b^2 + T^2}, \quad (4.8)$$

with boundary conditions $a(T_0) = 1$ and $\rho_0 > 0$ at $T = T_0 > 0$.

The energy density $\rho(T)$ for both radiation-dominated and matter-dominated universe take the same expression, which is *finite* at $T = 0$ for finite boundary condition and nonvanishing b . The curvature of these two universes are also finite at $T = 0$. For example, the Ricci curvature scalar R and the Kretschmann curvature scalar K for matter-dominated universe are

$$R(T)\Big|_{\text{mod. FLRW}}^{(w=0)} \propto \frac{1}{b^2 + T^2}, \quad (4.9a)$$

$$K(T)\Big|_{\text{mod. FLRW}}^{(w=0)} \propto \frac{1}{(b^2 + T^2)^2}, \quad (4.9b)$$

which are finite at $T = 0$, provided $b \neq 0$. Hence, the big bang curvature singularity has been removed.

Historically, the above regularization of the big bang singularity is motivated by the method of regularizing Schwarzschild singularity that we discussed in Sec. 3.1.1 [10]. Specifically, in Sec. 3.1.1, we have introduced a (three-dimensional) space defect [10]. While a defect in time (one dimension) has been introduced in this section. To see this defect in time, we can consider a co-moving observer in the spacetime manifold (4.1), then the proper time parameter of this observer would have a ‘‘jump’’ at $T = 0$; see (4.3b) for the range of coordinate t .

4.2.2. Nonsingular bouncing cosmology

As we can see from (4.5) or (4.7), the bouncing behavior of the positive scale factor is manifest: $a(T)$ decreases for negative T approaching $T = 0^-$, the bounce occurs at $T = 0$ with a minimal value of the cosmic scale factor (nonvanishing), and $a(T)$ increases for positive T moving away from $T = 0^+$. The bouncing solutions for a radiation-dominated universe and a matter-dominated universe are shown in Fig. 4.1 and Fig. 4.2, respectively.

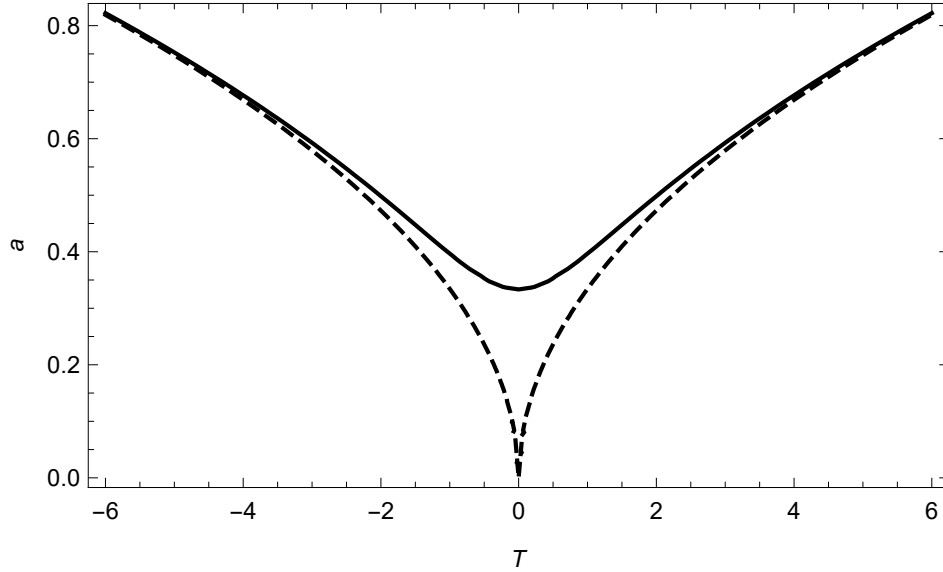


Figure 4.1.: Cosmic scale factor (full curve) of the modified, spatially flat FLRW universe with relativistic matter, as given by (4.5) with $b = 1$ and $T_0 = 4\sqrt{5}$. Also shown is the cosmic scale factor (dashed curve) of the standard FLRW universe with an extended cosmic time coordinate T , as given by (2.14) with $t_0 = 4\sqrt{5}$.

4.2.2.1. Geodesics

In a standard matter-dominated or radiation-dominated universe, null geodesics and timelike geodesics are incomplete in the past direction because of the presence of a big bang singularity.⁸ In this section, we will show that the null geodesic can be extended uniquely at $T = 0$ in the nonsingular bouncing cosmology. Similar conclusions can also be obtained for timelike geodesics; the discussion is given in App. B.

For the metric (4.1), we have the following remark.

Remark 2. *Particles travel on straight lines in the coordinate system $\{T, x^1, x^2, x^3\}$.*

The proof of this remark is given in App. A. Without loss of generality, we can consider geodesics that start at $T = T_1 < 0$ and end at $T = T_0 > 0$, while moving in the $x^1 \equiv X$ direction.

For massless particles, e.g., photons and gravitons, the reduced metric is

$$0 = ds^2 \Big|_{\text{mod. RW}}^{(\text{light})} = -\frac{T^2}{b^2 + T^2} dT^2 + a^2(T) dX^2. \quad (4.10)$$

For relativistic matter, the cosmic scale factor $a(T)$ is given by (4.5). With boundary condition $X(0) = 0$, we have the following solution for null geodesic from (4.10):

$$X(T) = \begin{cases} +2 \sqrt[4]{b^2 + T_0^2} \left[\sqrt[4]{T^2 + b^2} - \sqrt{b} \right], & \text{for } T > 0, \\ -2 \sqrt[4]{b^2 + T_0^2} \left[\sqrt[4]{T^2 + b^2} - \sqrt{b} \right], & \text{for } T \leq 0. \end{cases} \quad (4.11)$$

A plot of this null geodesic is given in Fig. 4.3.

⁸It has been shown in [57] that inflationary spacetimes are also incomplete in null and timelike past directions.

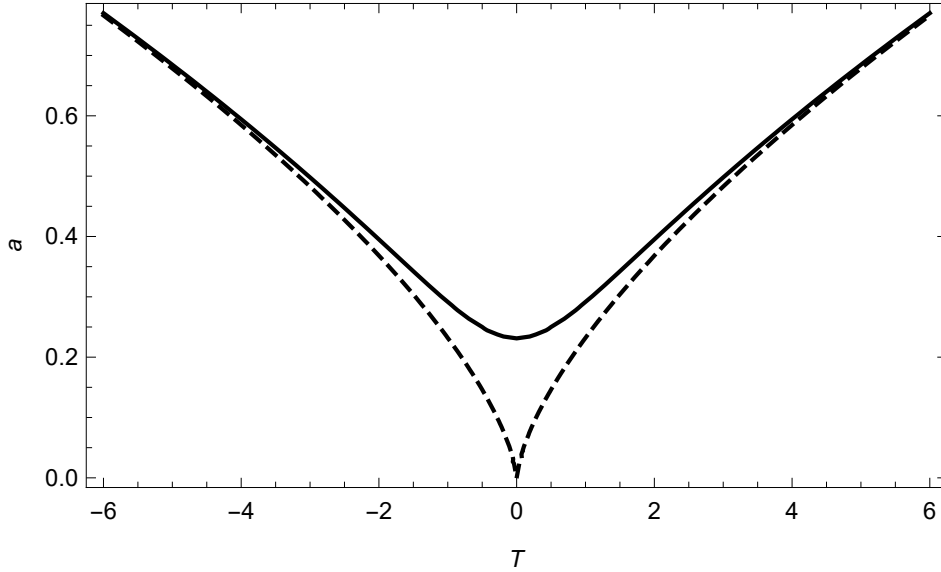


Figure 4.2.: Cosmic scale factor (full curve) of the modified, spatially flat FLRW universe with nonrelativistic matter, as given by (4.7) with $b = 1$ and $T_0 = 4\sqrt{5}$. Also shown is the cosmic scale factor (dashed curve) of the standard FLRW universe with an extended cosmic time coordinate T , as given by (2.17) with $t_0 = 4\sqrt{5}$.

4.2.2.2. Past particle horizon

The particle horizon at cosmic time $T_0 > 0$ reads

$$d_{\text{hor}}(T_0) = a(T_0) \lim_{t_1 \rightarrow -\infty} \left[\int_{t_1}^{-b} \frac{dt''}{a(t'')} + \int_b^{t(T_0)} \frac{dt'}{a(t')} \right], \quad (4.12)$$

where $t(T_0) \equiv t_0$ is given by (4.2) and $a(t) = a(t(T))$.

For positive and finite values of b and t_0 , the particle horizon for radiation-dominated universe is

$$\begin{aligned} d_{\text{hor}}(T_0) &= 2 a(T_0) \lim_{t_1 \rightarrow -\infty} \left(\sqrt{-t_1 t_0} - 2 \sqrt{b t_0} + \sqrt{t t_0} \right) \\ &= 2 a(T_0) \lim_{t_1 \rightarrow -\infty} \sqrt{-t_1 t_0}. \end{aligned} \quad (4.13)$$

Similarly, the particle horizon for matter-dominated universe is given by

$$d_{\text{hor}}(T_0) = 3 a(T_0) \lim_{t_1 \rightarrow -\infty} \sqrt[3]{-t_1 t_0^2}. \quad (4.14)$$

In general, for a bouncing universe with

$$a(T) = \left(\frac{T^2 + b^2}{T_0^2 + b^2} \right)^{q/2}, \quad (4.15)$$

where $0 < q < 1$. We have the following expression for past particle horizon (for positive and finite values of b and t_0):

$$d_{\text{hor}}(T_0) = \frac{1}{1-q} a(T_0) \lim_{t_1 \rightarrow -\infty} (-t_1)^{1-q} t_0^q, \quad (4.16)$$

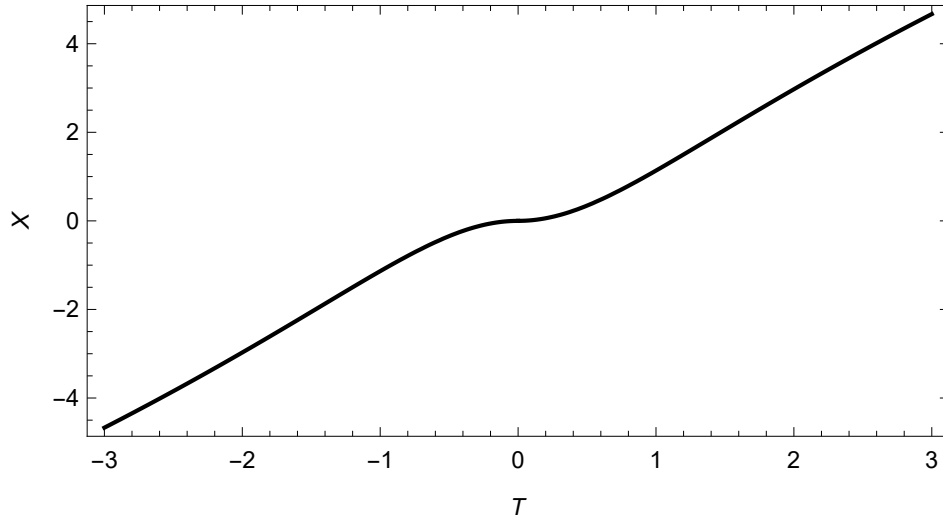


Figure 4.3.: Null geodesic (4.11) with $b = 1$ and $T_0 = 4\sqrt{5}$. Recall that X is the co-moving coordinate, the physical length is given by $a(T)X$. For timelike geodesics, see Fig. B.1 in App. B.

which goes to $+\infty$.

The result of (4.16) implies that, the past particle horizon at a finite positive time T_0 diverges for the nonsingular bouncing cosmologies with cosmic scale factor (4.15).

An infinite past particle horizon provides an alternative solution to the horizon and flatness problems. This solution, of course, is different from the solution provided by inflation [58–60].

4.2.2.3. Modified Hubble diagram

With the evolution of the cosmic scale factor, we can calculate the luminosity distance d_L and d_A for the nonsingular bouncing universe.

First, for bouncing cosmologies, we need to distinguish the following two cases:

1. the light is emitted by a co-moving galaxy in the expanding phase of the universe ($T_1 > 0$);
2. the light is emitted by a co-moving galaxy in the contracting phase of the universe ($T_1 \leq 0$).

Notice that, in both cases, the light is detected by a co-moving observer in the expanding phase at cosmic time $T_0 > 0$ with $T_0 > T_1$.

In what follows, we will use the auxiliary time coordinate t from (4.2) to simplify calculations.

Assume that light is emitted at cosmic time $t = t_1$ (with $t_1 > b$ for case 1 and $t_1 \leq -b$ for case 2) and observed at $t = t_0 > b > 0$ with $t_0 > t_1$. Then, the luminosity distance (for the definition of luminosity distance, see Secs. 14.4 and 14.6 of Ref. [14]) is given by

$$d_L(t_1, t_0) \Big|_{\text{case 1}} = \frac{a^2(t_0)}{a(t_1)} \int_{t_1}^{t_0} \frac{dt'}{a(t')}, \quad (4.17a)$$

$$d_L(t_1, t_0) \Big|_{\text{case 2}} \equiv d_L^{(\text{pre})}(t_1) + d_L^{(\text{post})}(t_0) \equiv \frac{a^2(-b)}{a(t_1)} \int_{t_1}^{-b} \frac{dt''}{a(t'')} + \frac{a^2(t_0)}{a(b)} \int_b^{t_0} \frac{dt'}{a(t')}. \quad (4.17b)$$

The corresponding expression for the angular diameter distance d_A is given by

$$d_A(t_1, t_0) \Big|_{\text{case 1}} = \frac{a^2(t_1)}{a^2(t_0)} d_L(z) \Big|_{\text{case 1}}, \quad (4.18a)$$

$$d_A(t_1, t_0) \Big|_{\text{case 2}} \equiv \frac{a^2(t_1)}{a^2(-b)} d_L^{(\text{pre})}(t_1) + \frac{a^2(b)}{a^2(t_0)} d_L^{(\text{post})}(t_0). \quad (4.18b)$$

Define the redshift as

$$z \equiv \sqrt{a^2(t_0)/a^2(t_1)} - 1 = a(t_0)/a(t_1) - 1. \quad (4.19)$$

With (4.19) and (4.17), the luminosity distance for radiation-dominated nonsingular bouncing universe is given by (see Fig. 4.4)

$$d_L(z) \Big|_{\text{case 1}} = 2 t_0 z, \quad \text{for } z \in [0, z_{\text{max}}), \quad (4.20a)$$

$$d_L(z) \Big|_{\text{case 2}} = 2b \frac{z_{\text{max}} - z}{1 + z_{\text{max}}} + 2 t_0 z_{\text{max}}, \quad \text{for } z \in (-1, z_{\text{max}}], \quad (4.20b)$$

with definition

$$z_{\text{max}} \equiv a(t_0)/a(b) - 1 = \sqrt{t_0/b} - 1. \quad (4.20c)$$

With (4.19) and (4.20), (4.18) gives the following expression for the angular diameter distance of a radiation-dominated nonsingular bouncing universe:

$$d_A(z) \Big|_{\text{case 1}} = 2 t_0 \frac{z}{(1+z)^2}, \quad \text{for } z \in [0, z_{\text{max}}), \quad (4.21a)$$

$$d_A(z) \Big|_{\text{case 2}} = 2 t_0 \left(\frac{1}{(1+z)^2} - \frac{1}{(1+z_{\text{max}})^2} + \frac{1}{1+z_{\text{max}}} \frac{z}{1+z} \right), \quad \text{for } z \in (-1, z_{\text{max}}]. \quad (4.21b)$$

Values of d_A as a function of z is plotted in Fig. 4.5.

In App. C, we present a nonsingular bouncing cosmology with $w = 1$ (the reason for this choice of w is discussed there). The corresponding geodesics and modified Hubble diagrams are also presented in this appendix.

Several remarks are in order.

First, in order to display the main characteristics of the modified Hubble diagrams, we have given a relatively small value of z_{max} in Figs. 4.4 and 4.5. If a cosmic bounce has really occurred, z_{max} must be much larger than the value given in Figs. 4.4 (Recall that the cosmic microwave background has a redshift of $z \approx 1100$). It was calculated in Ref. [12] that in order to reproduce the hot-big-bang model with TeV temperature, z_{max} must be larger than 10^{15} .

Second, observe that there exists nonsmooth behavior for luminosity distance d_L or angular diameter distance at $z = z_{\text{max}}$ (see modified Hubble diagram Figs. 4.4 and 4.5.) These cusp-type nonsmooth behavior are caused by the sharp change in the slope of $a(t)$ between $t \leq -b$ and $t \geq b$, which traces back to the ‘‘jump’’ of the proper time for a co-moving observer at $T = 0$ (See the last paragraph in Sec. 4.2.1). These nonsmooth behaviors are direct manifestations of the defect.

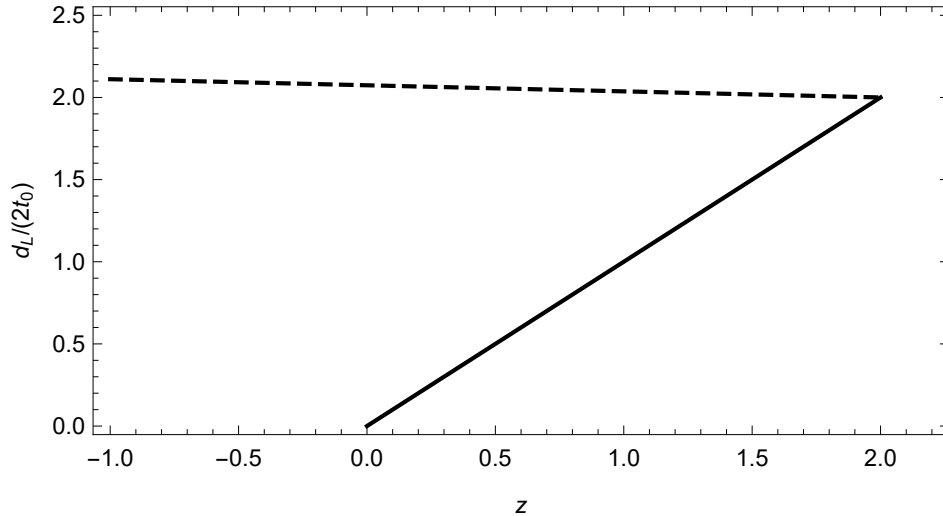


Figure 4.4.: Hubble diagram with the luminosity distance d_L from (4.20) for $b/t_0 = 1/9$ and $z_{\max} = 2$. With an observer in the expanding phase, the full curve corresponds to case 1 (light emitted by a co-moving galaxy in the expanding phase of the universe) and the dashed curve to case 2 (light emitted by a co-moving galaxy in the contracting phase). Note that the luminosity distance $d_L(z)$ has a cusp-type behaviour around $z = z_{\max}$.

Third, our description of the luminosity distance and angular diameter distance is complete, which, to the best of our knowledge, has not yet been obtained in other bouncing models. For example, the authors in Ref. [61] did calculate the luminosity distances for different contracting phases but not the complete description, from contraction to expansion.

Fourth, the dashed lines in Figs. 4.4 and 4.5 are supposed to represent the signals emitted by luminous standard candles in the contracting phase. These light signals would inevitably come across the hot plasma in the standard hot big bang phase. Any light from the standard candles would be strongly scattered by the hot plasma. That is to say, images of these luminous standard candles are impossible to obtain for observers in the post-bounce phase. But, it may very well be that the required standard candles emit gravitational waves [15, 61] instead of electromagnetic waves. In this sense, the dashed lines in Figs. 4.4 and 4.5 concern gravitational standard candles.

4.2.3. Circumventing the singularity theorem

In this subsection, we will show how the nonsingular bouncing cosmology discussed in Sec. 4.2.2 can circumvent the singularity theorem (Theorem 1 of Sec. 2.3, in particular).

Consider the curves given by the world lines of all co-moving observers in the modified RW metric (4.1a). A family of these curves is, of course, a congruence of timelike geodesics.

Then, the vector field ξ^μ that is tangent to the congruence is given by

$$\xi^0 = -\sqrt{\frac{b^2 + T^2}{T^2}}, \quad (4.22a)$$

$$\xi^i = 0. \quad (4.22b)$$

Notice that ξ^μ is actually opposite to the four-velocity of the co-moving observers, as we are interested in the past-directed normal geodesic congruence.

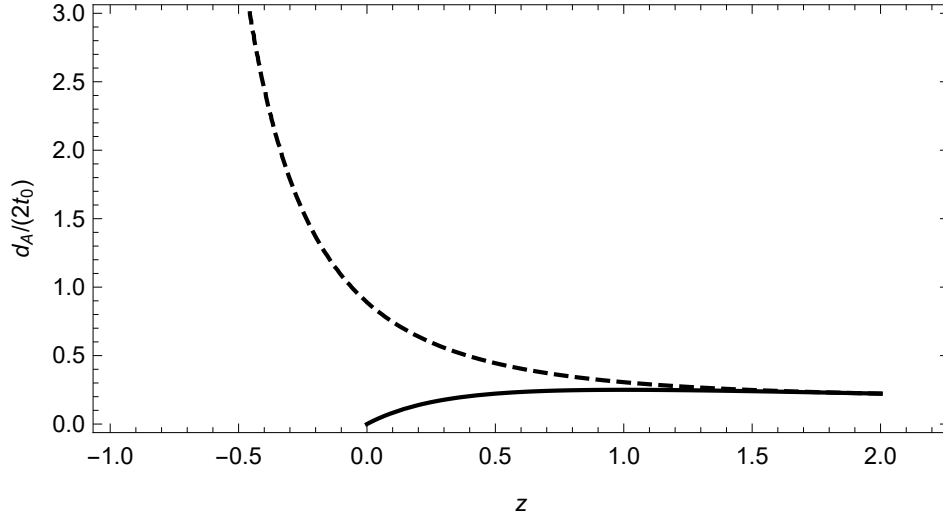


Figure 4.5.: Same as Fig. 4.4, but with the angular diameter distance d_A from (4.21).

With (4.22), it is straightforward to calculate $B_{\mu\nu}$ and $h_{\mu\nu}$ from (2.21) and (2.22), respectively. The nonvanishing components of $B_{\mu\nu}$ and $h_{\mu\nu}$ are as follows:

$$B_{ij} = -a \frac{da}{dT} \sqrt{\frac{b^2 + T^2}{T^2}}, \quad (4.23a)$$

$$h_{ij} = g_{ij}. \quad (4.23b)$$

Finally, we have the expression for the expansion of the congruence

$$\begin{aligned} \theta &= B^{\mu\nu} h_{\mu\nu} \quad (4.24) \\ &= B_{ij} h^{ij} \\ &= -3 \sqrt{\frac{b^2 + T^2}{T^2}} \frac{1}{a} \frac{da}{dT}. \end{aligned}$$

For radiation-dominated universe ($a(T)$ given by (4.5)) and matter-dominated universe ($a(T)$ given by (4.7)), we have

$$\theta(T) \Big|_{\text{mod. FLRW}}^{(w=1/3)} = -\frac{3}{2} \frac{T/|T|}{\sqrt{b^2 + T^2}}, \quad (4.25a)$$

$$\theta(T) \Big|_{\text{mod. FLRW}}^{(w=0)} = -2 \frac{T/|T|}{\sqrt{b^2 + T^2}}. \quad (4.25b)$$

Notice that, in both (4.25a) and (4.25b), θ are negative for positive T .

Four remarks are in order.

First, the expansion of the congruence for the standard FLRW universe is given by (4.25) with $b = 0$. Then, (4.25) (with $b = 0$) implies that $\theta \rightarrow -\infty$ when $T \rightarrow 0^+$. For a given constant $T = T_1 > 0$ hypersurface Σ , the “point” $T = 0^+$ is conjugate to Σ ; see the paragraph above (2.37). Hence, no past-directed co-moving observer’s curve from Σ can have length greater than $-3/\theta(T_1)$. So, we have incomplete timelike geodesics, and the singularity theorem cannot be avoided.

Second, for a nonsingular bouncing cosmology ($b \neq 0$), $\theta(T)$ from (4.25) is always *finite*. Then, for a given constant $T = T_1 > 0$ hypersurface Σ , the point conjugate to Σ does not

exist. The length of the past-directed co-moving observer's curve could have no upper bound. The singularity theorem would be circumvented.

Third, for nonsingular bouncing cosmology ($b \neq 0$), θ , as a function of T , is discontinuous at $T = 0$. This discontinuity is a direct manifestation of the spacetime defect.

Fourth, even though we have only shown that the co-moving timelike geodesics in nonsingular bouncing cosmologies can be extended indefinitely in the past direction, the results should also hold for general timelike geodesics. For general timelike geodesics in the nonsingular bouncing cosmology, see App. B.

As the last part of this subsection, we would like to compare the nonsingular bouncing cosmology discussed in Sec. 4.2.2 with other bouncing cosmologies.

In the context of general relativity, most bouncing cosmologies [52] in the literature require a violation of the strong energy condition.⁹ The violation of the strong energy condition¹⁰ directly invalidates (2.30), so that the expansion θ can remain finite and the singularity theorem is avoided.

In short, the singularity theorem 1 can be circumvented by a finite expansion θ along timelike geodesics. A finite expansion can be realized by a violation of the strong energy condition or by a spacetime defect.

4.3. Cosmological perturbations

Having obtained nonsingular bouncing cosmologies in Sec. 4.2.2, we now turn to analyze the stabilities of the bouncing models. Specifically, we will focus on the linear cosmological perturbations of the metric and matter.

4.3.1. Scalar metric perturbations

In this section, the background metric (4.1) will be called the unperturbed metric. The perturbed metric can then be written as

$$g_{\mu\nu}(x) \Big|_{\text{mod. RW}}^{(\text{perturbed})} = \bar{g}_{\mu\nu}(T) + h_{\mu\nu}(x), \quad (4.26)$$

where $h_{\mu\nu} = h_{\nu\mu}$ is a small perturbation compared to the unperturbed metric $\bar{g}_{\mu\nu}$ from (4.1a). Henceforth, a bar over a quantity denotes its unperturbed value.

We know that the spatially isotropic and homogeneous background allows us to decompose the metric perturbations into scalars, divergenceless vectors, and divergenceless traceless symmetric tensors [63, 64].

For the modified spatially flat RW unperturbed metric (4.1a), the *Ansatz* for the perturbed metric with scalar perturbations is taken as follows [13]

$$ds^2 \Big|_{\text{mod. RW}}^{(\text{scalar pert.})} = - (1 + E) \frac{T^2}{b^2 + T^2} dT^2 + 2\bar{a} \frac{\partial F}{\partial x^i} dx^i dt + \bar{a}^2 \left[(1 + A) \delta_{ij} + \frac{\partial B^2}{\partial x^i \partial x^j} \right] dx^i dx^j, \quad (4.27a)$$

where the perturbations E , F , A and B are functions of all spacetime coordinates $\{T, x^1, x^2, x^3\}$ and the background scale factor \bar{a} is a function of only T .

⁹For perfect fluids, the strong energy condition implies $\rho + P \geq 0$ and $\rho + 3P \geq 0$.

¹⁰The violation of strong energy condition may lead to instabilities and problems, as regards microcausality [52, 62].

4.3.1.1. Newtonian gauge

Consider the following transformation of the spacetime coordinates:

$$x^\mu \rightarrow \tilde{x}^\mu = x^\mu + \varepsilon^\mu, \quad (4.28)$$

where the parameters $\varepsilon^\mu \equiv \varepsilon^\mu(x)$ are infinitesimal functions of the spacetime coordinates. By decomposing the spatial part of ε^μ into the gradient of a spatial scalar and a divergenceless vector [63, 64],

$$\varepsilon^i = \partial^i \varepsilon_S + \varepsilon_V^i, \quad (4.29a)$$

$$\partial_i \varepsilon_V^i = 0, \quad (4.29b)$$

we have the following transformations of the metric functions from (4.27a) under the change of coordinates (4.28):

$$\tilde{E} = E - \frac{2b^2}{T} \varepsilon^0 - \frac{\partial \varepsilon^0}{\partial T}, \quad (4.30a)$$

$$\tilde{F} = F - \frac{\bar{a}}{2} \frac{\partial \varepsilon_S}{\partial T} + \frac{T^2}{b^2 + T^2} \frac{\varepsilon^0}{2\bar{a}}, \quad (4.30b)$$

$$\tilde{A} = A - \frac{2\dot{\bar{a}}}{\bar{a}} \varepsilon^0, \quad (4.30c)$$

$$\tilde{B} = B - 2\varepsilon_S, \quad (4.30d)$$

where the overdot stands for the partial derivative with respect to T . Note that only ε^0 and ε_S contribute to the transformations of scalar metric perturbations.

Following Sec. 7.1.2 of Ref. [63], we can construct the following gauge-invariant quantities:

$$2\Phi \equiv E - \frac{\partial}{\partial T} \left[2\bar{a} \frac{b^2 + T^2}{T^2} \left(F - \frac{\bar{a}}{4} \dot{B} \right) \right] - \frac{2b^2}{T} \left[2\bar{a} \frac{b^2 + T^2}{T^2} \left(F - \frac{\bar{a}}{4} \dot{B} \right) \right], \quad (4.31a)$$

$$2\Psi \equiv A - 4\dot{\bar{a}} \frac{b^2 + T^2}{T^2} \left(F - \frac{\bar{a}}{4} \dot{B} \right). \quad (4.31b)$$

In this section, we will use the Newtonian gauge (the origin of the name will become clear later on),

$$F = B = 0, \quad (4.32)$$

which can be reached by, first, choosing an appropriate ε_S in (4.30d) and, then, an appropriate ε^0 in (4.30b).

In the Newtonian gauge, the line element (4.27a) reduces to

$$ds^2 \Big|_{\text{mod. RW}}^{(\text{scalar pert. Newtonian-gauge})} = -(1 + 2\Phi) \frac{T^2}{b^2 + T^2} dT^2 + \bar{a}^2 (1 + 2\Psi) \delta_{ij} dx^i dx^j. \quad (4.33)$$

Note that, after choosing the Newtonian gauge, there is no further freedom to make coordinate transformations, while remaining within the *Ansatz* (4.33).

4.3.1.2. Hydrodynamic matter perturbations

Now, consider a perfect fluid with the energy-momentum tensor given by (2.10).

With the perturbed metric (4.33), the first-order perturbations of the 00 and ij components of the energy-momentum tensor are given by

$$\delta T_{00} = 2 \frac{T^2}{b^2 + T^2} \bar{\rho} \Phi + \frac{T^2}{b^2 + T^2} \delta \rho, \quad (4.34a)$$

$$\delta T_{ij} = 2 \bar{a}^2 \bar{P} \Psi \delta_{ij} + \bar{a}^2 \delta P \delta_{ij}. \quad (4.34b)$$

From (4.34), together with (4.33), we obtain

$$\delta T^0_0 = -\delta \rho, \quad (4.35a)$$

$$\delta T^i_j = \delta P \delta^i_j. \quad (4.35b)$$

After a straightforward calculation of the perturbed Einstein tensor from the perturbed metric (4.33), together with (4.35), we can get the following perturbed Einstein equations (up to first-order perturbations):

$$8\pi \left(\bar{\rho} + 2\Phi \bar{\rho} + \delta \rho \right) = 3 \frac{b^2 + T^2}{T^2} \frac{\dot{\bar{a}}^2}{\bar{a}^2} + 6 \frac{b^2 + T^2}{T^2} \frac{\dot{\bar{a}}}{\bar{a}} \dot{\Psi} - \frac{2\Delta \Psi}{\bar{a}^2}, \quad (4.36a)$$

$$\begin{aligned} 8\pi \left(\bar{P} + 2\Psi \bar{P} + \delta P \right) \delta_{ij} = & \left[\frac{2b^2}{T^3} \dot{\Psi} - 2 \frac{b^2 + T^2}{T^2} \ddot{\Psi} - 6 \frac{b^2 + T^2}{T^2} \frac{\dot{\bar{a}}}{\bar{a}} \dot{\Psi} + 2 \frac{b^2 + T^2}{T^2} \frac{\dot{\bar{a}}}{\bar{a}} \dot{\Phi} \right. \\ & + 2 \left(\frac{b^2}{T^3} \frac{\dot{\bar{a}}}{\bar{a}} - \frac{b^2 + T^2}{T^2} \frac{\ddot{\bar{a}}}{\bar{a}} \right) (1 + 2\Psi - 2\Phi) + \frac{\Delta(\Phi + \Psi)}{\bar{a}^2} \\ & \left. - \frac{b^2 + T^2}{T^2} \frac{\dot{\bar{a}}^2}{\bar{a}^2} (1 + 2\Psi - 2\Phi) \right] \delta_{ij} - \frac{1}{\bar{a}^2} \frac{\partial^2}{\partial x^i \partial x^j} (\Phi + \Psi), \end{aligned} \quad (4.36b)$$

where Δ is the Laplace operator in three-dimensional Euclidean space.

From (4.36b) for $i \neq j$, we obtain

$$\frac{\partial^2}{\partial x^i \partial x^j} (\Phi + \Psi) = 0. \quad (4.37)$$

For plane-wave metric perturbations, (4.37) leads to

$$k_i k_j (\Phi_{\mathbf{k}} + \Psi_{\mathbf{k}}) = 0, \quad (4.38)$$

where $\Phi_{\mathbf{k}}$ and $\Psi_{\mathbf{k}}$ are amplitudes of the plane-wave scalar metric perturbations. The only way to get (4.38) is to have

$$\Phi_{\mathbf{k}} + \Psi_{\mathbf{k}} = 0, \quad (4.39)$$

from which we obtain

$$\Psi = -\Phi. \quad (4.40)$$

For more details on obtaining (4.40), see Sec. 5.2 in [65].

Without perturbations, the leading order terms in (4.36) give

$$\left(1 + \frac{b^2}{T^2}\right) \left(\frac{\dot{\bar{a}}}{\bar{a}}\right)^2 = \frac{8\pi}{3} \bar{\rho}, \quad (4.41a)$$

$$\left(1 + \frac{b^2}{T^2}\right) \left[\frac{2\ddot{\bar{a}}}{\bar{a}} + \frac{\dot{\bar{a}}^2}{\bar{a}^2}\right] - \frac{2b^2}{T^3} \frac{\dot{\bar{a}}}{\bar{a}} = -8\pi \bar{P}. \quad (4.41b)$$

Equation (4.41a) is just (4.4a), while (4.41b) can be derived from energy-conservation equation (4.4b) with the help of (4.4a).

From the first-order perturbations in (4.36), together with the background equations (4.41) and the result (4.40), we get the following equations of motion for scalar metric perturbations:

$$4\pi \delta\rho = \frac{\Delta\Phi}{\bar{a}^2} - 3 \frac{\dot{\bar{a}}^2}{\bar{a}^2} \frac{b^2 + T^2}{T^2} \Phi - 3 \frac{\dot{\bar{a}}}{\bar{a}} \frac{b^2 + T^2}{T^2} \dot{\Phi}, \quad (4.42a)$$

$$4\pi \delta P = \frac{b^2 + T^2}{T^2} \ddot{\Phi} + \frac{b^2 + T^2}{T^2} \left(\frac{\dot{\bar{a}}^2}{\bar{a}^2} + \frac{2\ddot{\bar{a}}}{\bar{a}}\right) \Phi + 4 \frac{\dot{\bar{a}}}{\bar{a}} \frac{b^2 + T^2}{T^2} \dot{\Phi} - 2 \frac{b^2}{T^3} \frac{\dot{\bar{a}}}{\bar{a}} \Phi - \frac{b^2}{T^3} \dot{\Phi}. \quad (4.42b)$$

Note that (4.42a) for constant $\bar{a}(T)$ reproduces the Poisson equation of Newtonian gravity, which explains the name of the gauge [63].

Consider adiabatic perturbations,

$$\delta P = c_s^2 \delta\rho, \quad (4.43)$$

where c_s^2 is the square of the speed of sound [63].

Combining (4.42) and (4.43), we get the following equation of motion for the gravitational potential $\Phi(T, \mathbf{x})$:

$$\begin{aligned} & \frac{b^2 + T^2}{T^2} \ddot{\Phi} - c_s^2 \frac{\Delta\Phi}{\bar{a}^2} + \frac{b^2 + T^2}{T^2} \left[\frac{\dot{\bar{a}}^2}{\bar{a}^2} \left(1 + 3c_s^2\right) + \frac{2\ddot{\bar{a}}}{\bar{a}}\right] \Phi + \frac{\dot{\bar{a}}}{\bar{a}} \frac{b^2 + T^2}{T^2} \left(4 + 3c_s^2\right) \dot{\Phi} \\ & - 2 \frac{b^2}{T^3} \frac{\dot{\bar{a}}}{\bar{a}} \Phi - \frac{b^2}{T^3} \dot{\Phi} = 0, \end{aligned} \quad (4.44)$$

which is the basic equation for adiabatic perturbations.

Equations (4.42) and (4.44) are *singular* differential equations (the singularity appears at $T = 0$), but they have *nonsingular* solutions that will be presented shortly.

Note that, for nonrelativistic matter ($w = 0$), background solution are given by:

$$P = c_s^2 = 0, \quad (4.45a)$$

$$\bar{\rho}(T) \propto [\bar{a}(T)]^{-3}, \quad (4.45b)$$

$$\bar{a}(T) = \sqrt[3]{\frac{b^2 + T^2}{b^2 + T_0^2}}, \quad (4.45c)$$

where $\bar{a}(T)$ has been normalized to unity at $T = T_0 > 0$.

In this case, (4.44) has the solution

$$\Phi(T, \mathbf{x}) = C_1(\mathbf{x}) + \frac{b^{5/3} C_2(\mathbf{x})}{(b^2 + T^2)^{5/6}}, \quad (4.46)$$

where $C_1(\mathbf{x})$ and $C_2(\mathbf{x})$ are arbitrary dimensionless functions of the spatial coordinates \mathbf{x} (The second term on the right hand side of (4.46) does not vanish if $b = 0$, this is because of the fact that the dimensionless function $C_2(\mathbf{x})$ also depends on b .)

Remark that both modes in (4.46) are nonsingular at $T = 0$, which is different from the result obtained from standard FLRW universe [63].

As a special case of (4.46), consider a plane-wave perturbation with a single comoving wave vector \mathbf{k} ,

$$C_{1,2}(\mathbf{x}) = \widehat{C}_{\mathbf{k},1,2} \exp(i\mathbf{k} \cdot \mathbf{x}), \quad (4.47)$$

where $\widehat{C}_{\mathbf{k},1}$ and $\widehat{C}_{\mathbf{k},2}$ are the dimensionless amplitudes. The amplitude of such a plane-wave scalar metric perturbation is given by

$$\Phi_{\mathbf{k}}(T) = \widehat{C}_{\mathbf{k},1} + \frac{b^{5/3} \widehat{C}_{\mathbf{k},2}}{(b^2 + T^2)^{5/6}}. \quad (4.48)$$

From (4.42a), the corresponding energy density perturbation has the following amplitude:

$$\begin{aligned} \frac{\delta\rho_{\mathbf{k}}(T)}{\bar{\rho}(T)} = & - \left[2 + \frac{3}{2} k^2 (b^2 + T_0^2)^{2/3} (b^2 + T^2)^{1/3} \right] \widehat{C}_{\mathbf{k},1} \\ & + \left[3 - \frac{3}{2} k^2 (b^2 + T_0^2)^{2/3} (b^2 + T^2)^{1/3} \right] \frac{b^{5/3} \widehat{C}_{\mathbf{k},2}}{(b^2 + T^2)^{5/6}}, \end{aligned} \quad (4.49)$$

with $k \equiv |\mathbf{k}|$. The perturbation results for different wave vectors \mathbf{k} can be superposed, in order to obtain localized wave packets.

The results of (4.46) and (4.49) show that the scalar metric perturbations and the plane-wave adiabatic density perturbations are always finite (for finite $C_1(\mathbf{x})$ and $C_2(\mathbf{x})$), in particular, they remain *finite* at the moment of the bounce, $T = 0$. But, the metric perturbations and density perturbations $\delta\rho/\bar{\rho}$ are required to be much less than unity, so as to keep the background metric essentially unchanged. (For the metric perturbations larger than 1, the calculations of first-order perturbations make no sense.)

For $T \neq 0$ and a physical wavelength much larger than the Hubble horizon ($1/H \equiv \bar{a}/\dot{\bar{a}}$),

$$\frac{\bar{a}^2}{k^2} \gg \frac{1}{H^2} > \frac{T^2/(b^2 + T^2)}{H^2}, \quad (4.50)$$

we have from (4.49)

$$\left. \frac{\delta\rho_{\mathbf{k}}(T)}{\bar{\rho}(T)} \right|^{(\text{long-wavelength})} \sim -2\widehat{C}_{\mathbf{k},1} + \frac{3\widehat{C}_{\mathbf{k},2}}{(1 + T^2/b^2)^{5/6}}. \quad (4.51a)$$

For a short physical wavelength, we get

$$\left. \frac{\delta\rho_{\mathbf{k}}(T)}{\bar{\rho}(T)} \right|^{(\text{short-wavelength})} \sim -\frac{3}{2} k^2 (T_0 + b^2)^{2/3} \left[\widehat{C}_{\mathbf{k},1} \sqrt[3]{b^2 + T^2} + \frac{b^{2/3} \widehat{C}_{\mathbf{k},2}}{\sqrt{1 + T^2/b^2}} \right]. \quad (4.51b)$$

Observe that, as happens for the standard matter-dominated FLRW universe (see Eq. (7.56) of Ref. [63]), the growing mode in (4.51b) is proportional to the cosmic scale factor $\bar{a}(T)$.

4.3.2. Cosmological perturbations with conformal coordinates

In Sec. 4.3.1, we have shown *directly* that matter-dominated nonsingular bounce could have regular behavior under scalar metric perturbations. In this section, we will present more results on the cosmological perturbations of nonsingular bouncing cosmologies.

To simplify calculations, we will use the so-called conformal coordinates in this section.

In terms of conformal coordinates, the modified spatially flat RW metric (4.1a) can be written as the following form:

$$ds^2 \Big|_{\text{mod. RW}} = \tilde{g}_{\mu\nu} d\tilde{x}^\mu d\tilde{x}^\nu = \Omega^2(\eta) \left(-d\eta^2 + \delta_{ij} dx^i dx^j \right), \quad (4.52a)$$

$$\Omega(\eta) d\eta \equiv \sqrt{\frac{T^2}{b^2 + T^2}} dT, \quad (4.52b)$$

with η being the conformal time and where $\Omega^2(\eta)$ is the conformal factor.

Cosmological perturbations of the conformally flat metric (4.52a) have been widely studied in the literature; see, in particular, Ref. [63].

For the nonsingular bouncing cosmologies discussed in Sec. 4.2.2, the metric perturbation solutions take the same form as in the standard FLRW model but with the conformal time η given by (4.52b).

4.3.2.1. Scalar metric perturbations

For scalar metric perturbations, the perturbed metric in conformal-Newtonian gauge is given as follows [63]:

$$ds^2 \Big|_{\text{mod. RW}}^{\text{perturbed}} = \Omega^2(\eta) \left[-(1 + 2\tilde{\Phi})d\eta^2 + (1 + 2\tilde{\Psi})\delta_{ij} dx^i dx^j \right], \quad (4.53)$$

with η given by (4.52b).

For nonrelativistic hydrodynamic matter, the solution for gravitational potential is

$$\tilde{\Phi}(\eta, \mathbf{x}) = \tilde{C}_1(\mathbf{x}) + \frac{\tilde{C}_2(\mathbf{x}) \text{sgn}(\eta)}{\eta^5}, \quad (4.54)$$

with $\tilde{C}_1(\mathbf{x})$ and $\tilde{C}_2(\mathbf{x})$ are arbitrary functions of the spatial coordinates \mathbf{x} (the extra sign factor multiplying $\tilde{C}_2(\mathbf{x})$ is needed to get the correct boundary conditions at the spacetime defect, as will be explained below).

The corresponding plane-wave adiabatic energy density perturbations have the following solutions [63]:

$$\frac{\delta\rho_{\mathbf{k}}(\eta)}{\bar{\rho}(\eta)} \Big|_{\text{(long-wavelength)}} \sim -2\tilde{C}_{\mathbf{k},1} + 3\tilde{C}_{\mathbf{k},2} \text{sgn}(\eta) \eta^{-5}, \quad (4.55a)$$

$$\frac{\delta\rho_{\mathbf{k}}(\eta)}{\bar{\rho}(\eta)} \Big|_{\text{(short-wavelength)}} \sim -\frac{k^2}{6} \left(\tilde{C}_{\mathbf{k},1} \eta^2 + \tilde{C}_{\mathbf{k},2} \text{sgn}(\eta) \eta^{-3} \right), \quad (4.55b)$$

with $k \equiv |\mathbf{k}|$ and constants $\tilde{C}_{\mathbf{k},1,2}$.

Notice that

$$\Omega^2(\eta(T)) = a^2(T). \quad (4.56)$$

Inserting the scale factor for the nonrelativistic matter-dominated universe (4.45c) into (4.56) and using (4.52b), we obtain

$$\Omega(\eta) = \frac{1}{9} \frac{\eta^2}{b^2 + T_0^2}, \quad (4.57a)$$

$$\eta = \begin{cases} +3 \sqrt[3]{b^2 + T_0^2} \sqrt[6]{b^2 + T^2}, & \text{for } T \geq 0, \\ -3 \sqrt[3]{b^2 + T_0^2} \sqrt[6]{b^2 + T^2}, & \text{for } T \leq 0, \end{cases} \quad (4.57b)$$

$$\eta \in (-\infty, \eta_-] \cup [\eta_+, \infty), \quad (4.57c)$$

$$\eta_{\pm} \equiv \pm 3 \sqrt[3]{b(b^2 + T_0^2)}. \quad (4.57d)$$

The coordinate transformation (4.57b) is not a diffeomorphism, as happens for the coordinate transformation between t and T (see (4.2)). There are different values η_{\pm} for the single point $T = 0$. For the nonsingular bouncing cosmologies, T from (4.1) is a good coordinate, but η from (4.57b) is *not*. Still, η appears to be a useful auxiliary coordinate. First, it is well defined away from the spacetime defect at $\eta = \eta_{\pm}$. Second, with correct boundary conditions at $\eta = \eta_{\pm}$, the results calculated in η coordinate can agree with the results calculated in T coordinate (we will show this point in the coming paragraph).

Actually, the extra minus signs for the \tilde{C}_2 terms in (4.58) are responsible for correct boundary conditions at $\eta = \eta_{\pm}$. Inserting the η expression from (4.57b) into the perturbations (4.58), the final expressions for gravitational potential is

$$\tilde{\Phi}(\eta, \mathbf{x}) = \tilde{C}_1(\mathbf{x}) + \frac{1}{3^5 (b^2 + T_0^2)^{5/3}} \frac{\tilde{C}_2(\mathbf{x})}{(b^2 + T^2)^{5/6}}, \quad (4.58)$$

in agreement with our previous result (4.46).

For completeness, we also present here the scalar metric perturbations for relativistic hydrodynamic matter.

The amplitude of a plane-wave gravitational potential for adiabatic perturbations is given by [65],

$$\tilde{\Phi}_{\mathbf{k}}(\eta) = \frac{1}{\eta^3} \{ B_{\mathbf{k},1} [\omega\eta \cos(\omega\eta) - \sin(\omega\eta)] + B_{\mathbf{k},2} [\omega\eta \sin(\omega\eta) + \cos(\omega\eta)] \}, \quad (4.59)$$

with $\omega \equiv k/\sqrt{3}$ and constants $B_{\mathbf{k},1,2}$.

The corresponding energy density perturbations are

$$\begin{aligned} \frac{\delta\rho_{\mathbf{k}}}{\bar{\rho}}(\eta) = & \frac{4B_{\mathbf{k},1}}{\eta^3} \left\{ [(\omega\eta)^2 - 1] \sin(\omega\eta) + \omega\eta \left[1 - \frac{1}{2}(\omega\eta)^2 \right] \cos(\omega\eta) \right\} \\ & + \frac{4B_{\mathbf{k},2}}{\eta^3} \left\{ [1 - (\omega\eta)^2] \cos(\omega\eta) + \omega\eta [1 - (\omega\eta)^2] \sin(\omega\eta) \right\}. \end{aligned} \quad (4.60)$$

The conformal factor Ω^2 and the conformal time η are given by

$$\Omega^2(\eta) = \frac{1}{4} \frac{\eta^2}{b^2 + T_0^2}, \quad (4.61a)$$

$$\eta = \begin{cases} +2 \sqrt[4]{b^2 + T_0^2} \sqrt[4]{b^2 + T^2}, & \text{for } T \geq 0, \\ -2 \sqrt[4]{b^2 + T_0^2} \sqrt[4]{b^2 + T^2}, & \text{for } T \leq 0, \end{cases} \quad (4.61b)$$

$$\eta \in (-\infty, \eta_-] \cup [\eta_+, \infty), \quad (4.61c)$$

$$\eta_{\pm} \equiv \pm 2 \sqrt[4]{b^2 (b^2 + T_0^2)}, \quad (4.61d)$$

where the points $\eta = \eta_-$ and $\eta = \eta_+$ are identified.

For long-wavelength perturbations ($\omega\eta \ll 1$), we have

$$\tilde{\Phi}_{\mathbf{k}}(\eta) = \frac{1}{\eta^3} \left[-\frac{B_{\mathbf{k},1} \omega^3}{3} \eta^3 + B_{\mathbf{k},2} \right], \quad (4.62)$$

and

$$\frac{\delta\rho_{\mathbf{k}}}{\bar{\rho}}(\eta) = \frac{4}{\eta^3} \left(\frac{B_{\mathbf{k},1} \omega^3}{6} \eta^3 + B_{\mathbf{k},2} \right). \quad (4.63)$$

During an expansion phase, we should see that the nondecaying modes of $\tilde{\Phi}$ and $\delta\rho/\bar{\rho}$ are constants in the long-wavelength limit,

$$\delta\rho/\bar{\rho} \simeq -2\tilde{\Phi} \simeq \text{constant}. \quad (4.64)$$

Notice that the gravitational potential $\tilde{\Phi}$ could take different values at different spatial locations.

4.3.2.2. Vector and tensor metric perturbations

For the discussion of vector and tensor perturbations, we can follow Sec. 7 in Ref. [63].

For vector perturbations, the perturbed metric is given as follows [63]:

$$ds^2 \Big|_{\text{mod. RW}}^{\text{vector perturb.}} = \Omega^2(\eta) \left[-d\eta^2 - 2 S_i dx^i d\eta + \left(\delta_{ij} - \frac{\partial H_i}{\partial x^j} - \frac{\partial H_j}{\partial x^i} \right) dx^i dx^j \right], \quad (4.65)$$

where the perturbations S_i and H_i are 3-vectors on spacetime coordinates satisfying

$$\frac{\partial (\delta^{ij} S_j)}{\partial x^i} = 0, \quad (4.66a)$$

$$\frac{\partial (\delta^{ij} H_j)}{\partial x^i} = 0. \quad (4.66b)$$

So, there are four independent functions for vector perturbations. Only two of them have physical importance; the other two are gauge redundancy (coordinates freedom), as happens for scalar perturbations.

The gauge-invariant variable for vector perturbations is

$$V_i = S_i - \frac{\partial H_i}{\partial \eta}. \quad (4.67)$$

For a perfect fluid, the solution for vector perturbations are given by (cf. Eq. (7.93) in Ref. [63])

$$V_i \propto a^{-2}(T), \quad (4.68)$$

which decay for an expanding phase.

Turning to tensor perturbations, the perturbed metric is given as follows

$$ds^2 \Big|_{\text{mod. RW}}^{\text{tensor perturb.}} = \Omega^2(\eta) [-d\eta^2 + (\delta_{ij} - D_{ij})dx^i dx^j], \quad (4.69)$$

with D_{ij} satisfying

$$\delta^{ij} D_{ij} = 0, \quad (4.70a)$$

$$\frac{\partial(\delta^{ik} D_{jk})}{\partial x^i} = 0. \quad (4.70b)$$

From (4.70), we can see that there are only two independent functions for tensor perturbations. Recall that the tensor perturbations actually describe gravitational waves (with two polarizations).

The solution of plane-wave tensor metric perturbations for the radiation-dominated case is as follows (see Eq. (7.98) in Ref. [63]):

$$D_{\mathbf{k}}^{ij} = \frac{1}{\eta} \left[\tilde{C}_{\mathbf{k},4} \sin(k\eta) + \tilde{C}_{\mathbf{k},5} \text{sgn}(\eta) \cos(k\eta) \right] e_{\mathbf{k}}^{ij}, \quad (4.71a)$$

$$\eta = \begin{cases} +2 \sqrt[4]{b^2 + T_0^2} \sqrt[4]{b^2 + T^2}, & \text{for } T \geq 0, \\ -2 \sqrt[4]{b^2 + T_0^2} \sqrt[4]{b^2 + T^2}, & \text{for } T \leq 0, \end{cases} \quad (4.71b)$$

$$\eta \in (-\infty, \tilde{\eta}_-] \cup [\tilde{\eta}_+, \infty), \quad (4.71c)$$

$$\tilde{\eta}_{\pm} \equiv \pm 2 \sqrt[4]{b^2 (b^2 + T_0^2)}, \quad (4.71d)$$

with $k \equiv |\mathbf{k}|$ and constant polarization tensor $e_{\mathbf{k}}^{ij}$ (the polarization may be different for different wave vectors \mathbf{k}). The sign factor to the coefficient $\tilde{C}_{\mathbf{k},5}$ in (4.71a) is added to get the correct boundary conditions at $\eta = \tilde{\eta}_{\pm}$.

From (4.71a), we see that the evolution for the gravitational wave is regular at the bounce moment ($T = 0$). In other words, the gravitational wave originating from cosmological perturbations in the pre-bounce phase can safely cross the bounce.

4.3.3. Cosmic microwave background radiation

The cosmic microwave background (CMB), discovered in 1964 by Arno Penzias and Robert Wilson [66], is landmark evidence for the standard big bang theory.¹¹ The spectrum of the CMB can be described by a blackbody radiation with temperature $\mathcal{T} = 2.725$ K [67]. The universe described by the CMB is almost isotropic. The anisotropies are at the level of about one part in 10^{-5} . However, these anisotropies give important constraints on cosmological parameters and lead us to a deep understanding of our universe. The primordial anisotropies, i.e., anisotropies at the scale which spans much larger than 1° on the sky of today, imply a nearly scale-invariant power spectrum of gravitational potential [63, 67, 68].

¹¹The other two crucial pieces of evidence for the standard big bang theory are Hubble's law (expansion of the Universe) and the abundance of primordial elements [64].

In this section, we will discuss two mechanisms that can produce a scale-invariant power spectrum, namely inflation and matter contraction. In both of the two scenarios, primordial perturbations originated from quantum fluctuations at small scales. For a brief review of the CMB primordial anisotropies, see App. E. In the same appendix, we will also show how primordial anisotropies imply a scale-invariant power spectrum.

The background (unperturbed) metric is considered to be the modified spatially flat RW metric (4.1). As regards inflation, we mean an exponential expansion of the cosmic scale factor which starts at $T > 0$. As for matter contraction, we mean a bouncing model with a matter contraction phase, i.e., $a(T) \propto \sqrt[3]{T^2 + b^2}$ for $T < 0$.

Assuming that we are working in the region far from the “defect”, we have

$$H \equiv \frac{\dot{a}}{a} \equiv \frac{da/dT}{a} = \sqrt{T^2/(T^2 + b^2)} \frac{da/dt}{a} \cong \frac{da/dt}{a}. \quad (4.72)$$

So in the later discussion in this chapter, the overdot will stand for differentiation with respect to t .

To simplify the calculations, we will be working in the conformal coordinates as we introduced in Sec. 4.3.2.

To discuss the origin of cosmological fluctuations, we consider a scalar field with the following action:

$$S_\varphi = \int \sqrt{-\tilde{g}} dx^4 \left[-\frac{1}{2} \tilde{g}^{\mu\nu} \partial_\mu \varphi \partial_\nu \varphi - V(\varphi) \right], \quad (4.73)$$

where $\tilde{g}_{\mu\nu}$ is given by the metric (4.52). By varying the action with respect to the metric tensor, we can get the energy-momentum tensor for the scalar field

$$T_\varphi^{\mu\nu} = -\tilde{g}^{\mu\nu} \left[\frac{1}{2} \tilde{g}^{\alpha\beta} \partial_\alpha \varphi \partial_\beta \varphi + V(\varphi) \right] + \tilde{g}^{\mu\alpha} \tilde{g}^{\nu\beta} \partial_\alpha \varphi \partial_\beta \varphi. \quad (4.74)$$

By comparing (4.74) and the energy-momentum tensor of a perfect fluid (2.10), we can get the energy density and pressure for the scalar field as follows:

$$\rho_\varphi = -\frac{1}{2} \tilde{g}^{\mu\nu} \partial_\mu \varphi \partial_\nu \varphi + V(\varphi), \quad (4.75)$$

$$p_\varphi = -\frac{1}{2} \tilde{g}^{\mu\nu} \partial_\mu \varphi \partial_\nu \varphi - V(\varphi). \quad (4.76)$$

4.3.3.1. Background fields

For scalar perturbations, we consider the metric background to be (4.52), where the homogeneous universe is characterized completely by the conformal factor $\Omega^2(\eta)$ (remember that $\Omega(\eta) = \Omega(\eta(T)) = a(T)$).

For the scalar field, the homogeneous *Ansatz* is

$$\varphi(\eta, \mathbf{x}) = \bar{\varphi}(\eta). \quad (4.77)$$

The background equations of motion for Ω and $\bar{\varphi}$ are the Klein–Gordon equation, Friedmann equation and the energy-momentum conservation

$$\bar{\varphi}'' + 2\mathcal{H}\bar{\varphi}' + \Omega^2 \frac{\partial V}{\partial \varphi} = 0, \quad (4.78a)$$

$$\frac{8\pi}{3} \Omega^2 \bar{\rho}_\varphi = \mathcal{H}^2, \quad (4.78b)$$

$$-3\mathcal{H}(\bar{\rho}_\varphi + \bar{P}_\varphi) = \bar{\rho}_\varphi', \quad (4.78c)$$

where the prime stands for differentiation with respect to the conformal time η and where

$$\mathcal{H} \equiv \Omega' / \Omega. \quad (4.79)$$

4.3.3.2. Perturbed fields

The perturbed metric is given by (4.53) with Ω given by (4.52b). The scalar field is assumed to be decomposed into two parts,

$$\varphi = \bar{\varphi}(\eta) + \delta\varphi(\eta, \mathbf{x}), \quad (4.80)$$

with $\delta\varphi(\eta, \mathbf{x})$ being a small perturbation satisfying $|\delta\varphi(\eta, \mathbf{x})| \ll \bar{\varphi}(\eta)$. The equations of motion for the gravitational potential and the perturbation of the scalar field are [63]

$$-3\mathcal{H}(\tilde{\Phi}' + \mathcal{H}\tilde{\Phi}) + \Delta\tilde{\Phi} = 4\pi\Omega^2(\bar{\rho}_\varphi + \bar{P}_\varphi) \left[\left(\frac{\delta\varphi'}{\bar{\varphi}'} \right) - 2\mathcal{H} \frac{\delta\varphi}{\bar{\varphi}} - \tilde{\Phi} \right], \quad (4.81a)$$

$$\mathcal{H}\tilde{\Phi} + \tilde{\Phi}' = 4\pi\Omega^2(\bar{\rho}_\varphi + \bar{P}_\varphi) \frac{\delta\varphi}{\bar{\varphi}'}, \quad (4.81b)$$

where the background equations of motion (4.78) have been used and where we have also used

$$\tilde{\Psi} = -\tilde{\Phi}, \quad (4.82)$$

as follows from the perturbed off-diagonal spatial Einstein equation.

Following Sec. 8.3.1 of [63], we can define the following two variables

$$u(\eta, \mathbf{x}) \equiv \frac{\tilde{\Phi}}{4\pi\sqrt{\bar{\rho}_\varphi + \bar{P}_\varphi}}, \quad (4.83a)$$

$$v(\eta, \mathbf{x}) \equiv \Omega \left(\delta\varphi + \frac{\bar{\varphi}'}{\mathcal{H}} \tilde{\Phi} \right). \quad (4.83b)$$

As we will see later, the v variable introduced here is to make the action of the cosmological perturbations to have canonical kinetic terms. While the u variable is proportional to the gravitational potential $\tilde{\Phi}$ for a given conformal time. Using (4.83), together with (4.78), (4.81) can be written as

$$\Delta u = z \left(\frac{v}{z} \right)', \quad (4.84a)$$

$$v = \theta \left(\frac{u}{\theta} \right)', \quad (4.84b)$$

with definitions

$$z(\eta) \equiv \frac{\Omega^2 \sqrt{\bar{\rho}_\varphi + \bar{P}_\varphi}}{\mathcal{H}}, \quad (4.85a)$$

$$\theta(\eta) \equiv \frac{1}{z}. \quad (4.85b)$$

Adding Δ on both sides of (4.84b) and using (4.84a), we obtain

$$v'' - \Delta v - \frac{z''}{z} v = 0. \quad (4.86)$$

Recall that Δ in (4.86) is the Laplace operator in three-dimensional Euclidean space.

It can be shown that, up to total derivative terms, the action that could reproduce the equations of motion (4.86) is [63]

$$S_v = \frac{1}{2} \int d\eta d^3x \left[v'^2 + v\Delta v + \frac{z''}{z} v^2 \right]. \quad (4.87)$$

Equation (4.87) is the action for the cosmological perturbations; as we mentioned before, this action has canonical kinetic terms. The canonical variable v evolves like a scalar field with a time-dependent mass in Minkowski space.

The canonical quantization of cosmological perturbation with action (4.87) can be found in Sec. 8.3.3 of Ref. [63]. The resulting operator \hat{v} can be written in the following form:

$$\hat{v}(\eta, \mathbf{x}) = \frac{1}{\sqrt{2}} \int \left[v_{\mathbf{k}}^*(\eta) e^{i\mathbf{k}\mathbf{x}} \hat{a}_{\mathbf{k}}^- + v_{\mathbf{k}}(\eta) e^{-i\mathbf{k}\mathbf{x}} \hat{a}_{\mathbf{k}}^+ \right] \frac{d^3k}{(2\pi)^{3/2}}, \quad (4.88)$$

with $\hat{a}_{\mathbf{k}}^+$ and $\hat{a}_{\mathbf{k}}^-$ being creation and annihilation operators. More details can be found in Ref. [63].

The mode functions $v_{\mathbf{k}}(\eta)$ in (4.88) satisfy

$$v_{\mathbf{k}}'' + \left(k^2 - \frac{z''}{z} \right) v_{\mathbf{k}} = 0. \quad (4.89)$$

The initial conditions for $v_{\mathbf{k}}$ are given by [63]

$$v_{\mathbf{k}}(\eta_0) = \frac{1}{\sqrt{\omega_k}}, \quad (4.90a)$$

$$v_{\mathbf{k}}'(\eta_0) = i\sqrt{\omega_k}. \quad (4.90b)$$

Considering the initial quantum fluctuations originate on small scales, i.e., $k^2 \gg z''/z$, we have

$$\omega_k \simeq k. \quad (4.91)$$

With (4.90) and (4.91), the initial conditions for $u_{\mathbf{k}}$ can be obtained from (4.84)

$$u_{\mathbf{k}}(\eta_0) \simeq -\frac{i}{\sqrt[2]{k^3}}, \quad (4.92a)$$

$$u_{\mathbf{k}}'(\eta_0) \simeq \frac{1}{\sqrt{k}}. \quad (4.92b)$$

Assume that the equation of state of the background field is constant, i.e.,

$$w \equiv \frac{\bar{P}}{\bar{\rho}} = \text{constant}. \quad (4.93)$$

With (4.78b) and (4.93), (4.85a) reduces to

$$z(\eta) = \frac{3}{8\pi} \bar{\rho} \sqrt{1 + \bar{P}/\bar{\rho}} \propto \Omega(\eta). \quad (4.94)$$

With (4.93) and (4.78b), we also have

$$\sqrt{\bar{\rho}_\varphi + \bar{P}_\varphi} \propto \frac{|\Omega'|}{\Omega^2} \propto |H|. \quad (4.95)$$

4.3.3.3. Scale-invariant power spectrum from inflation

In this section, we will briefly discuss the scale-invariant power spectrum from inflation. A more complete and rigorous derivation of cosmological perturbations from inflation can be found in Ref. [63].

We know that during inflation, H is almost constant,

$$0 \approx \dot{H} = \frac{\ddot{a}}{a} - \frac{\dot{a}^2}{a^2}. \quad (4.96)$$

Then, we have

$$\frac{z''}{z} = \frac{\Omega''}{\Omega} \approx 2\mathcal{H}^2, \quad (4.97)$$

where (4.96) has been used.

Notice that

$$\frac{a^2}{k^2} \ll \frac{1}{H^2} \quad (4.98)$$

is equivalent to

$$k^2 \gg \mathcal{H}^2. \quad (4.99)$$

So, for a physical wavelength much smaller than the Hubble horizon, (4.86) gives

$$v_{\mathbf{k}}'' + k^2 v_{\mathbf{k}} = 0. \quad (4.100)$$

The solution of (4.100) is

$$v_{\mathbf{k}}(\eta) = e^{ik(\eta-\eta_0)} v_{\mathbf{k}}(\eta_0). \quad (4.101)$$

With (4.100), the solution for u can be obtained from (4.84a). In small-wavelength limit, the solution for $u_{\mathbf{k}}$ is

$$u_{\mathbf{k}}(\eta) \Big|^{(\text{short-wavelength})} \simeq -\frac{i}{k} e^{ik(\eta-\eta_0)} v_{\mathbf{k}}(\eta_0). \quad (4.102)$$

For a physical wavelength much larger than the Hubble horizon, (4.86) reduces to

$$v_{\mathbf{k}}'' - \frac{z''}{z} v_{\mathbf{k}} = 0, \quad (4.103)$$

which has the solution

$$v_{\mathbf{k}}(\eta) \propto z(\eta). \quad (4.104)$$

With (4.94), (4.84b) reduces to

$$v = u' + \frac{\Omega'}{\Omega} u. \quad (4.105)$$

From (4.84b) and (4.104), together with (4.104), we have the evolution of $u_{\mathbf{k}}$ for a physical wavelength much larger than the Hubble horizon

$$u_{\mathbf{k}} \Big|^{(\text{long-wavelength})} \propto \frac{\Omega^2}{\Omega'} \propto \frac{1}{H}. \quad (4.106)$$

The power spectrum of the gravitational potential is given by the following dimensionless quantity [63]

$$\delta_{\tilde{\Phi}}^2(\eta, k) \equiv \frac{|\tilde{\Phi}_k|^2 k^3}{2\pi^2}. \quad (4.107)$$

The initial quantum fluctuations originating beyond the Hubble horizon are given by (4.90). Then, from (4.101), we find that $v_{\mathbf{k}}$ will undergo oscillations with constant amplitude on sub-Hubble scales. Equation (4.104) implies that $v_{\mathbf{k}}$ will stop to oscillate after the length scale crosses the Hubble horizon. The time $t_H(k)$ when the mode with wavenumber k crosses the Hubble horizon is given by

$$\frac{a(t_H)}{k} = \frac{1}{H(t_H)}. \quad (4.108)$$

Notice that for different modes, t_H is different in general.

Finally, the power spectrum of the gravitational potential at a very late time η is

$$\begin{aligned} \delta_{\Phi}^2(\eta, k) &= \frac{|\tilde{\Phi}_k|^2 k^3}{2\pi^2} \\ &\simeq \frac{k^3}{2\pi^2} |4\pi H(\eta) u_{\mathbf{k}}(\eta)|^2 \\ &\simeq \frac{k^3}{2\pi^2} |4\pi H(\eta)|^2 \left| \frac{u_{\mathbf{k}}(\eta_H)}{H(\eta)} H(\eta_H) \right|^2 \\ &\simeq \frac{k^3}{2\pi^2} |4\pi H(\eta)|^2 k^{-3} \frac{H^2(\eta_H)}{H^2}, \end{aligned} \quad (4.109)$$

where we have used

$$u_{\mathbf{k}}(\eta_H) \simeq -\frac{i}{k} e^{ik\eta_H - \eta_0} v_{\mathbf{k}}(\eta_0). \quad (4.110)$$

With the approximation that H is almost constant during inflation, we have

$$\delta_{\Phi}^2(\eta, k) \propto H^2, \quad (4.111)$$

which is independent of k . So, the exponential expansion of the inflationary scenario can actually lead to a scale-invariant power spectrum of the gravitational potential.

4.3.3.4. Scale-invariant power spectrum from matter contraction

Inflation may not be the only theory that can lead to a scale-invariant power spectrum of the cosmological perturbations. Several bouncing cosmological models are also able to produce scale-invariant perturbations [53, 62, 69, 70]. In this section, we will show that a matter-contraction phase may also lead to a scale-invariant power spectrum [62].

Before we start, we have two remarks in order.

First, do not confuse the matter contraction discussed here with a contracting phase dominated by nonrelativistic hydrodynamic matter. The latter cannot convert quantum fluctuation into a scale-invariant power spectrum of cosmological perturbations.

Second, the fact that a matter-contracting phase can be realized by a scalar field with an exponential potential was already noted in Ref [53]. But in that work [53], a bounce cannot occur with the exponential potential. The new result presented here is that we can have a matter contraction (which produces a scale-invariant power spectrum) and a nonsingular bounce in a *single* model. The details of a nonsingular bounce from a scalar field with a positive exponential potential are given in App. D.

For matter contraction, we have

$$\Omega(\eta) \propto \eta^2 \quad (4.112a)$$

$$\mathcal{H} = \frac{2}{\eta}. \quad (4.112b)$$

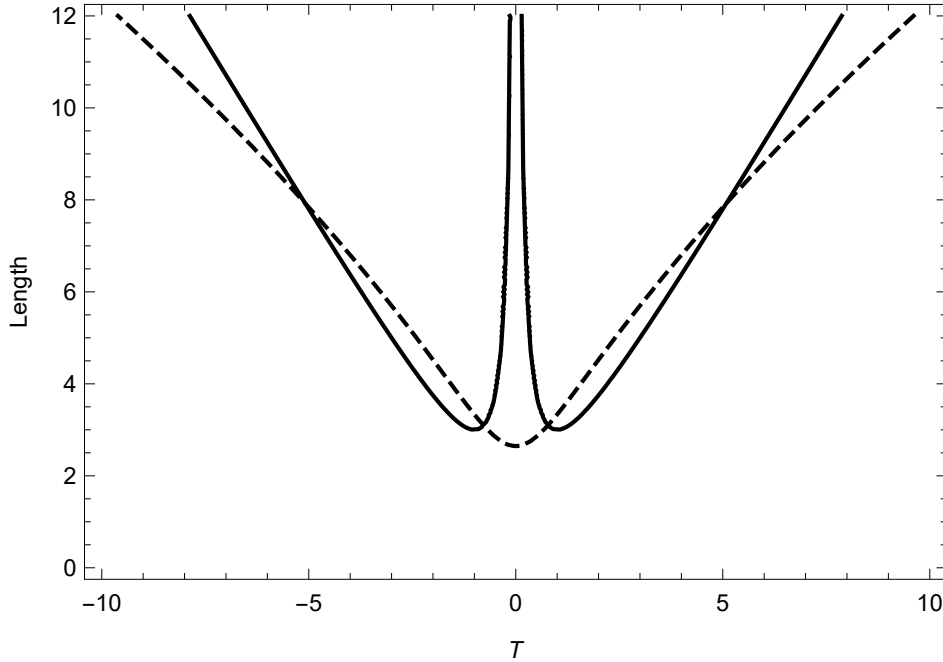


Figure 4.6.: The evolution of the Hubble horizon (full curve) and a physical wave (dashed curve) in the modified, spatially flat FLRW universe. The scale factor is given by (D.5a) with $b = 1$ and $T_0 = 1$. The Hubble horizon R_H is defined by $R_H \equiv 1/|H| = a(T)/(|da(T)/dT|)$. The physical wave is specified by a wavelength $\lambda = a/k$ with $k = 0.3$.

Assume that the lengths of physical waves are smaller than the Hubble horizon $1/|H|$ at $T \rightarrow -\infty$. Remark that this assumption is easy to be satisfied for matter contraction because

$$\frac{1}{|H|} \propto (-T)^{1/3} a(T) \quad (4.113)$$

is larger than a/k at $T \rightarrow -\infty$ for nonvanishing k . See Fig. 4.6 and Fig. 4.7 for the evolution of the Hubble horizon and physical waves in the modified, spatially flat FLRW universe.

From (4.112), we have

$$\frac{z''}{z} = \frac{\Omega''}{\Omega} = \frac{2}{\eta^2} = \frac{\mathcal{H}^2}{2}. \quad (4.114)$$

So, for a physical wavelength much smaller than the Hubble horizon, z''/z in (4.89) is negligible compared to the k^2 term. Hence, (4.89) reduces to (4.100). The corresponding solution is also given by (4.101). The solution for $u_{\mathbf{k}}$ is given as (4.102) in short wavelength limit.

For a physical wavelength much larger than the Hubble horizon, (4.86) reduces to

$$v_{\mathbf{k}}'' - \frac{2}{\eta^2} v_{\mathbf{k}} = 0. \quad (4.115)$$

The solution for $v_{\mathbf{k}}(\eta)$ from (4.115) are given by

$$v_{\mathbf{k}}(\eta) = c_{\mathbf{k},7} \eta^2 + c_{\mathbf{k},8} \eta^{-1}, \quad (4.116)$$

where $c_{\mathbf{k},7}$ and $c_{\mathbf{k},8}$ are constants and need to be determined by the initial conditions given at the time of horizon crossing.

Notice that the first mode in (4.116) is decaying during contraction, as it is proportional to the scale factor a . The second term, which is proportional to $1/\sqrt{a}$, is the growing term¹² during the contracting phase.

¹²In this case, $|c_{\mathbf{k},8} \eta^{-1}|^2$ is growing during contraction.

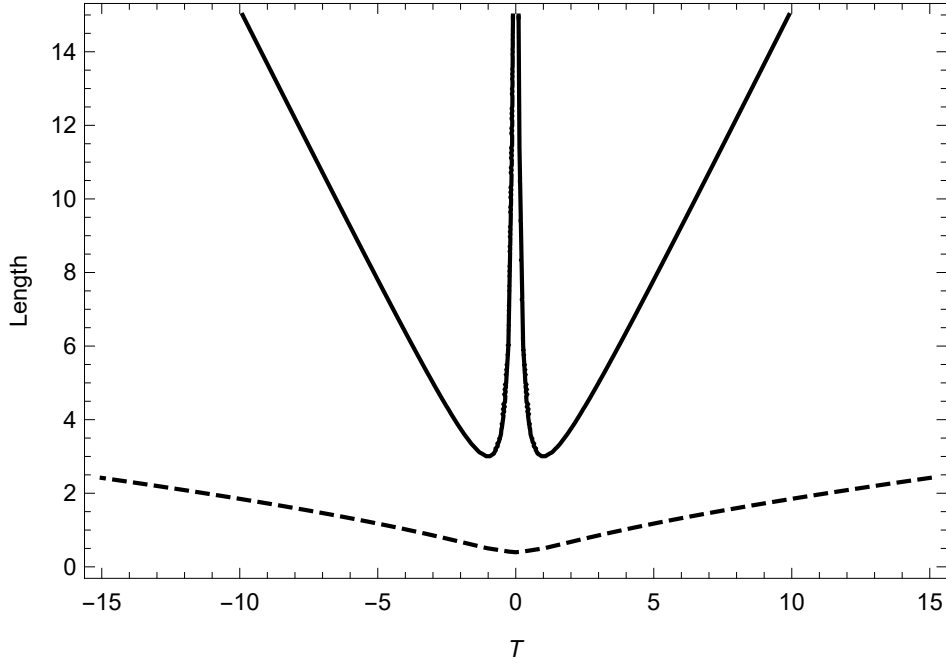


Figure 4.7.: Same as Fig. 4.6, but the physical wave is specified by a larger wave number $k = 2$. This figure shows the case in which the physical wave is always smaller than the Hubble horizon. This case is not of interest here, as it cannot contribute to super-horizon perturbations.

In the following discussion, we will neglect the decaying mode and focus on the growing mode, i.e., we take

$$v_{\mathbf{k}}(\eta) = c_{\mathbf{k},8} \eta^{-1}. \quad (4.117)$$

The constant $c_{\mathbf{k},8}$ is given by

$$v_{\mathbf{k}}(\eta_H) = e^{ik(\eta_H - \eta_0)} v_{\mathbf{k}}(\eta_0) \simeq \frac{c_{\mathbf{k},8}}{\eta_H}, \quad (4.118)$$

which gives

$$c_{\mathbf{k},8} \simeq \eta_H e^{ik(\eta_H - \eta_0)} v_{\mathbf{k}}(\eta_0). \quad (4.119)$$

Then, $\eta_H(\mathbf{k})$ can be found by solving

$$\mathcal{H}^2(\eta_H) = k^2, \quad (4.120)$$

which gives

$$\eta_H(\mathbf{k}) = -\frac{2}{k}. \quad (4.121)$$

For $v_{\mathbf{k}} = c_{\mathbf{k},8} \eta^{-1}$, (4.84b) gives to

$$c_{\mathbf{k},8} \eta^{-1} \simeq u'_{\mathbf{k}} + \frac{2}{\eta} u_{\mathbf{k}}, \quad (4.122)$$

where we have used

$$\theta \equiv \frac{1}{z} \propto \frac{1}{\Omega(\eta)}. \quad (4.123)$$

The solution of (4.122) is

$$u_{\mathbf{k}}(\eta) = \frac{c_{\mathbf{k},8}}{2} + \frac{c_{\mathbf{k},9}}{\eta^2}, \quad (4.124)$$

where $c_{\mathbf{k},9}$ is constant. In (4.124), the first mode is time-independent, while the second mode is growing during contraction.

To calculate the power spectrum of cosmological perturbations, we use the approximation that $u_{\mathbf{k}}(\eta)$ is given by (4.102) before crossing the Hubble horizon. At the time of crossing the Hubble horizon, we have from (4.106)

$$u_{\mathbf{k}}(\eta_H) \simeq -\frac{i}{k} e^{ik(\eta_H - \eta_0)} v_{\mathbf{k}}(\eta_0). \quad (4.125)$$

With $c_{\mathbf{k},8}$ given by (4.119) and (4.125), from (4.124), we have the evolution of $u_{\mathbf{k}}$ after crossing the Hubble horizon (up to an irrelevant phase factor)

$$u_{\mathbf{k}}(\eta) \simeq \frac{1}{k^{3/2}}, \quad (4.126)$$

where $c_{\mathbf{k},9}$ has been set to zero to match the boundary condition at the horizon crossing.

From (4.83a), we can get the power spectrum of the gravitational potential for a matter contracting universe

$$\begin{aligned} \delta_{\tilde{\Phi}}^2(\eta, k) &\equiv \frac{|\tilde{\Phi}_{\mathbf{k}}|^2 k^3}{2\pi} \\ &= \frac{|4\pi\sqrt{\bar{\rho} + \bar{P}} u_{\mathbf{k}}(\eta)|^2 k^3}{2\pi^2} \\ &\simeq 8(\bar{\rho} + \bar{P}) \\ &\propto H^2, \end{aligned} \quad (4.127)$$

where (4.95) and (4.126) have been used.

Even though the final result in (4.127) has the same expression as the result in (4.111), the Hubble parameter H in (4.127) behaves like $1/t^2$, while H is almost constant in (4.111). In a matter contracting universe, the initial vacuum fluctuation at sub-Hubble scales early in the contracting phase can actually be converted into a scale-invariant power spectrum of the gravitational potential, and the amplitude of the spectrum increases in proportion to a^{-3} .

Conclusion and Outlook

In this thesis, we have reviewed possible solutions to certain apparent singularities of general relativity. Specifically, the regularized Schwarzschild solution and the regularized Friedmann solution were discussed. The theory involved here is standard general relativity but allowing for degenerate metrics. More precisely, the metrics obey the standard Einstein equation but have a vanishing determinant over a spacetime defect. (Mathematically, the spacetime defect is a submanifold of the spacetime manifold.)

For the regularized black hole solution, we are actually dealing with general relativity in a spacetime manifold with a nontrivial topological structure. An $\mathbb{R}P^3$ defect in space is responsible for the nontrivial topological structure of spacetime. Through the study of geodesics for this space defect, we obtained a new type of gravitational lensing. Different from the standard gravitational lensing, which is due to the nonvanishing curvature of spacetime, the lensing from a flat-spacetime defect (Fig. 3.8) is entirely due to the nontrivial topology from the defect.

The second effect brought about by the space defect is a massive black hole remnant. For a singular black hole solution, by emitting Hawking radiation, a black hole would totally disappear at the end. However, for the regularized black hole solution, the defect could prevent a black hole from complete evaporation leaving a remnant with mass $bc^2/(2G)$, with b being the length scale of the defect, c the speed of light in vacuum and G Newton's gravitational constant. These massive remnants could be a candidate for dark matter and may or may not provide a solution for the black hole information paradox.

Motivated by the method of regularizing the black hole singularity, the big bang singularity was regularized by introducing a defect in the time coordinate of the standard Robertson–Walker metric. More precisely, a defect was introduced in the classical proper time of the co-moving observer of the standard Robertson–Walker metric. This defect replaced the big bang singularity by a nonsingular bounce. This particular nonsingular bounce modified the Hubble diagram by presenting a cusp-type behavior at the bounce, which could lead to observable effects. The calculations of Sec. 4.3.1 indicated that the nonsingular bounce could be regular under small perturbations of the metric and matter.

For any cosmological model aiming to describe the evolution of the very early universe, it is crucial to be able to produce a scale-invariant power spectrum of cosmological perturbations. In the thesis, we have presented a particular bouncing model that might do the job

(details are given in App. D and Sec. 4.3.3.4). For this particular bouncing model, the matter contraction generated the scale-invariant power spectrum of the gravitational potential and the nonsingular bounce (produced by the spacetime defect) transferred this spectrum to the expansion phase giving the initial conditions for temperature fluctuations.

For most of the bouncing cosmologies in the scientific literature, the singularity theorem is avoided by the violation of strong energy condition. However, for the nonsingular bouncing cosmology discussed in Sec. 4.2, the energy condition for matter is entirely standard. The degenerate-metric bounce scenario circumvented the singularity theorem in a particular way: the spacetime defect guarantees the absence of conjugate points over the spacetime manifold, which results in the absence of an upper bound on the length of timelike geodesics.

The nonsingular bouncing cosmologies we presented in this thesis are far from perfect. For example, a nonsingular bouncing cosmology with a matter contraction could produce a scale-invariant power spectrum of cosmological perturbations but cannot avoid the shear problem (anisotropy problem). Needless to say, to get a complete bounce scenario, which could not only predict the correct cosmological observations but also be free of any problems, is far from trivial. The nontrivial result from the degenerate-metric scenario is that it gives a new mechanism to produce a regular bounce.

In this thesis, the length scales of the two different spacetime defects are both represented by the parameter b , but they may or may not take the same value. For the time defect, we have qualitative bounds: $l_{\text{planck}} \lesssim b \lesssim 10^{-3}$ m. The upper bound is necessary to reproduce the hot big-bang model with temperatures $\mathcal{T} \lesssim \text{TeV}$ and the lower bound is demanded to make classical Einstein theory applicable. As regards a single space defect, little is known for sure about its length scale. It might be possible that the spacetime defects trace back to the underlying (unknown) theory of “quantum spacetime”. In loop quantum gravity [71, 72], there does exist something like a “quantum of space” (space has a discrete spectrum of area and volume) and a “quantum of cosmic time” (cosmological evolution is discrete), but the classical limit of the theory is not yet well understood. It is rather interesting that spacetime may emerge from the master field of a nonperturbative formulation of string theory [73], and the emerging spacetime may be described by the degenerate metric discussed in Chapter 4. The physical origin of the spacetime defects remains an interesting topic for future research.

Proof of Remark 2 in Sec. 4.2.2.1

We will prove that, for the background (4.1), particles travel on straight lines in the coordinate system $\{x^0 \equiv T, x^1, x^2, x^3\}$.

The geodesic equation is given by (3.28), which we copy here:

$$\frac{d^2 x^\alpha}{d\lambda^2} + \Gamma^\alpha_{\mu\nu} \frac{dx^\mu}{d\lambda} \frac{dx^\nu}{d\lambda} = 0, \quad (\text{A.1})$$

with λ being the proper time for massive particle or λ being the affine parameter for massless particle. (Note that that the proper time for a massless particle is not well defined; the parameter λ should be understood as the time told by some other freely falling clock. See Appendix B of Ref. [64] for more discussion about proper time.)

Defining a four-velocity vector

$$U^\mu \equiv \frac{dx^\mu}{d\lambda}, \quad (\text{A.2})$$

for a massive particle (for a massless particle, U^μ should be understood as an energy-momentum four-vector [64],) (A.1) gives

$$\frac{dU^\alpha}{d\lambda} + \Gamma^\alpha_{\mu\nu} U^\mu U^\nu = 0. \quad (\text{A.3})$$

Notice that

$$\begin{aligned} \frac{dU^\alpha}{d\lambda} &= \frac{d(g^{\alpha\beta} U_\beta)}{d\lambda} \\ &= g^{\alpha\beta} \frac{dU_\beta}{d\lambda} + U_\beta \frac{dg^{\alpha\beta}}{d\lambda}. \end{aligned} \quad (\text{A.4})$$

With (A.4), (A.3) can be written as

$$g^{\alpha\beta} \frac{dU_\beta}{d\lambda} + U_\beta \frac{dg^{\alpha\beta}}{d\lambda} + \Gamma^\alpha_{\mu\nu} U^\mu U^\nu = 0. \quad (\text{A.5})$$

Contracting (A.5) with $g_{\alpha\rho}$, we have

$$\frac{dU_\rho}{d\lambda} - U^\alpha \frac{dg_{\alpha\rho}}{d\lambda} + \frac{1}{2}(g_{\rho\nu,\beta} + g_{\rho\beta,\nu} - g_{\nu\beta,\rho})U^\nu U^\beta = 0, \quad (\text{A.6})$$

where we have the definition of Christoffel symbol

$$\Gamma^\mu_{\nu\rho} = \frac{1}{2}g^{\mu\sigma}(g_{\sigma\nu,\rho} + g_{\rho\sigma,\nu} - g_{\nu\rho,\sigma}) \quad (\text{A.7})$$

and where

$$0 = \frac{d\delta_\sigma^\alpha}{d\lambda} = g^{\mu\alpha} \frac{dg_{\nu\sigma}}{d\lambda} + g_{\mu\sigma} \frac{dg^{\mu\alpha}}{d\lambda} \quad (\text{A.8})$$

has been used.

Notice that

$$\begin{aligned} g_{\rho\nu,\beta}U^\beta &\equiv \frac{\partial g_{\rho\nu}}{\partial x^\beta} \frac{dx^\beta}{d\lambda} \\ &= \frac{dg_{\rho\nu}}{d\lambda}. \end{aligned} \quad (\text{A.9})$$

With the help of (A.9), (A.6) reduces to

$$\frac{dU_\rho}{d\lambda} - \frac{1}{2} \frac{\partial g_{\nu\beta}}{\partial x^\rho} U^\nu U^\beta = 0. \quad (\text{A.10})$$

Recall that

$$g_{00} = \frac{-T^2}{T^2 + b^2}, \quad (\text{A.11a})$$

$$g_{ij} = a^2(T)\delta_{ij}, \quad (\text{A.11b})$$

which are independent of spatial coordinates. Hence, from the geodesic equation (A.10), we have

$$\frac{dU_i}{d\lambda} = 0, \quad (\text{A.12})$$

i.e., spatial components of U_μ are constants along the geodesic in the coordinate system $\{T, x^1, x^2, x^3\}$. For later discussion, we write these constants as

$$U_1 \equiv c_1, \quad U_2 \equiv c_2, \quad U_3 = c_3. \quad (\text{A.13})$$

From the definition of U^i , we have

$$\frac{dx^1}{d\lambda} = \frac{c_1}{a^2(T)}, \quad (\text{A.14a})$$

$$\frac{dx^2}{d\lambda} = \frac{c_2}{a^2(T)}, \quad (\text{A.14b})$$

$$\frac{dx^3}{d\lambda} = \frac{c_3}{a^2(T)}, \quad (\text{A.14c})$$

from which we can get

$$\frac{dx^i}{dx^j} = \frac{dx^i/d\lambda}{dx^j/d\lambda} = \frac{c_i}{c_j}. \quad (\text{A.15})$$

From (A.15), we can get the following parametric representation of a straight line

$$x^1 = x^1, \quad (\text{A.16a})$$

$$x^2 = \frac{c_2}{c_1}x^1 + b_2, \quad (\text{A.16b})$$

$$x^3 = \frac{c_3}{c_1}x^1 + b_3, \quad (\text{A.16c})$$

with x^1 being the parameter and $b_{2,3}$ real constants.

Geodesics for massive particles in nonsingular bouncing cosmology

In Sec. 4.2.2.1, we have presented the null geodesics in nonsingular bouncing cosmology. In this appendix, we will calculate the timelike geodesics.

As particles travel on straight lines in the coordinate system $\{T, x^1, x^2, x^3\}$ (see proof of this statement in App. A), we can consider timelike geodesics that start at $T = T_1 < 0$ and end at $T = T_0 > 0$, while moving in the $x^1 \equiv X$ direction. So, we take $c_2 = c_3 = 0$ and $c_1 = v > 0$ in (A.16a).

Notice that

$$\frac{dX}{dT} = \frac{dX/d\lambda}{dT/d\lambda} = \frac{U^1}{U^0}. \quad (\text{B.1})$$

For a massive particle, we have

$$g_{\mu\nu}U^\mu U^\nu = -1, \quad (\text{B.2})$$

which gives

$$(U^0)^2 = \left(1 + \frac{v^2}{a^2}\right) \frac{b^2 + T^2}{T^2}. \quad (\text{B.3})$$

Taking into account that $U^1 = g^{11}U_1 = v/a^2$ and (B.3), (B.1) gives

$$dX = \frac{v/a^2}{\sqrt{1 + v^2/a^2}} \sqrt{\frac{T^2}{b^2 + T^2}} dT. \quad (\text{B.4})$$

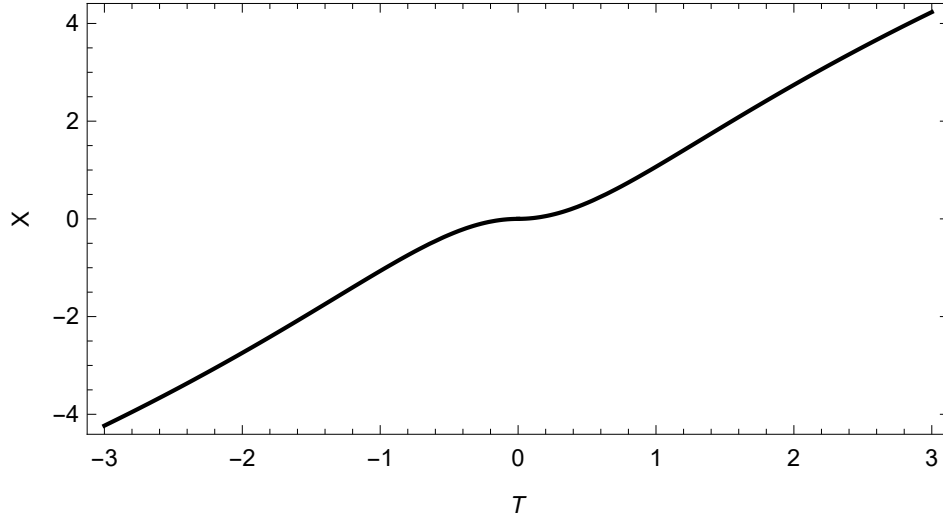


Figure B.1.: Timelike geodesic (B.5) with $b = 1$, $T_0 = 4\sqrt{5}$, $v = 1$, and $c_4 = -18 \tanh^{-1} \left(1/\sqrt{10} \right) = -c_5$.

For radiation-dominated universe, $a(T)$ is given by (4.5), the solution of (B.4) is as follows

$$X(T) = \begin{cases} +2 \frac{v \sqrt{\sqrt{\frac{b^2+T^2}{b^2+T_0^2}} + v^2} \tanh^{-1} \left(\frac{\sqrt[4]{\frac{b^2+T^2}{b^2+T_0^2}}}{\sqrt{\sqrt{\frac{b^2+T^2}{b^2+T_0^2}} + v^2}} \right)}{\sqrt{\frac{1}{b^2+T^2}} \left(\frac{b^2+T^2}{b^2+T_0^2} \right)^{3/4} \sqrt{\frac{v^2}{\frac{b^2+T^2}{b^2+T_0^2}} + 1}} + c_4, & \text{for } T > 0, \\ -2 \frac{v \sqrt{\sqrt{\frac{b^2+T^2}{b^2+T_0^2}} + v^2} \tanh^{-1} \left(\frac{\sqrt[4]{\frac{b^2+T^2}{b^2+T_0^2}}}{\sqrt{\sqrt{\frac{b^2+T^2}{b^2+T_0^2}} + v^2}} \right)}{\sqrt{\frac{1}{b^2+T^2}} \left(\frac{b^2+T^2}{b^2+T_0^2} \right)^{3/4} \sqrt{\frac{v^2}{\frac{b^2+T^2}{b^2+T_0^2}} + 1}} + c_5, & \text{for } T \leq 0, \end{cases} \quad (\text{B.5})$$

where c_4 is an arbitrary real constant and where

$$c_5 = 4b \frac{v \sqrt{\sqrt{\frac{b^2}{b^2+T_0^2}} + v^2} \tanh^{-1} \left(\frac{\sqrt[4]{\frac{b^2}{b^2+T_0^2}}}{\sqrt{\sqrt{\frac{b^2}{b^2+T_0^2}} + v^2}} \right)}{\left(\frac{b^2}{b^2+T_0^2} \right)^{3/4} \sqrt{\frac{v^2}{\frac{b^2}{b^2+T_0^2}} + 1}} + c_4. \quad (\text{B.6})$$

The energy of a particle with mass m as determined by a co-moving observer with 4-velocity u^μ is

$$E = -mU_\mu u^\mu, \quad (\text{B.7})$$

In the rest frame of the co-moving observer, the spatial components of the 4-velocity vanish

$$u^i = 0, \quad (\text{B.8})$$

and we have

$$g_{\mu\nu} u^\mu u^\nu = g_{00} u^0 u^0 = -1, \quad (\text{B.9})$$

which gives

$$u^0 = \frac{1}{\sqrt{-g_{00}}}. \quad (\text{B.10})$$

Finally, we have

$$E = -mU_0u^0 = m\sqrt{1 + \frac{v^2}{a^2}}. \quad (\text{B.11})$$

From (B.11), we could find that the energy of a particle measured by a co-moving observer is always *finite* in the nonsingular bouncing cosmology.

Nonsingular bounce with $w = 1$

C.1. Basic equations

Consider now that the equation-of-state parameter $W(T)$ satisfies

$$W(T) \equiv \frac{P(T)}{\rho(T)} = w = 1, \quad (\text{C.1})$$

and we have the T -even bounce-type solution $a(T)$ from (4.4) with normalization $a(T_0) = 1$ at $T_0 > 0$

$$a(T) \Big|_{\text{mod. FLRW}}^{(w=1, T\text{-even sol.})} = \sqrt[6]{(b^2 + T^2)/(b^2 + T_0^2)}, \quad (\text{C.2})$$

which is perfectly smooth at $T = 0$ as long as $b \neq 0$ (see Fig. C.1 for a comparison with the singular solution). The corresponding Kretschmann curvature scalar $K \equiv R^{\mu\nu\rho\sigma} R_{\mu\nu\rho\sigma}$ and matter energy density ρ are then finite at $T = 0$, provided $b \neq 0$,

$$K(T) \propto (b^2 + T^2)^{-2}, \quad (\text{C.3a})$$

$$\rho(T) \propto (b^2 + T^2)^{-1}. \quad (\text{C.3b})$$

The particular value $w \geq 1$ is to avoid instabilities in the prebounce phase (see the third and fourth paragraphs of Sec. 4 in Ref. [54]). In particular, a contracting phase with $w \geq 1$ can avoid the anisotropy problem (shear problem). The idea is that, if an initial classical shear is present, the shear (anisotropic part in a homogeneous universe) will be about a^{-6} . During a contracting phase, the shear could dominate over matter (a^{-3}) or radiation (a^{-4}) near the bounce, which may ruin the RW metric. However, a slow contraction with $w \geq 1$ could overcome the anisotropy and preserve the RW metric approximation.¹³ See Sec. 5.4 in Ref [62] for more details on the anisotropy problem.

In terms of the auxiliary coordinate t from (4.2), the bounce solution reads

$$a(t) \Big|_{\text{mod. FLRW}}^{(w=1, t\text{-even sol.})} = \sqrt[6]{t^2/t_0^2}, \quad (\text{C.4})$$

with $t_0^2 \equiv b^2 + T_0^2$.

¹³Recall that, the energy density for a component with equation of state w is about $\rho \propto a^{-3(1+w)}$.

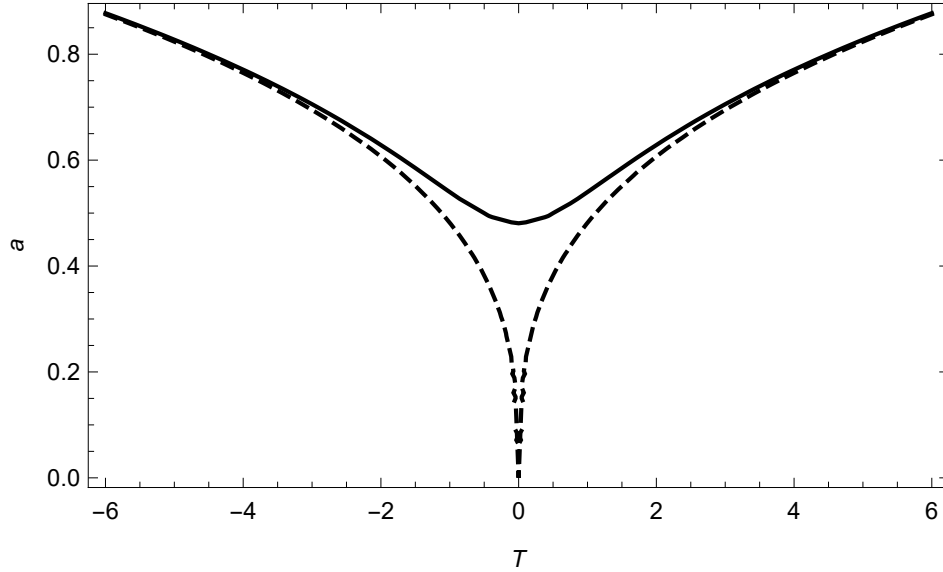


Figure C.1.: Cosmic scale factor (full curve) of the modified spatially flat FLRW universe with $w = 1$ matter, as given by (C.2) with $b = 1$ and $T_0 = 4\sqrt{5}$. Also shown is the cosmic scale factor (dashed curve) of the standard FLRW universe with an extended cosmic time coordinate T , as given by (C.2) with $b = 0$ and $T_0 = 4\sqrt{5}$.

C.2. Null geodesics

Consider geodesics of light that start at $T = T_1 < 0$ and end at $T = T_0 > 0$, while moving in the $x^1 \equiv X$ direction. With boundary condition $X(0) = 0$, we have the following geodesic solution $X = X(T)$ from the reduced metric (4.10) and the cosmic scale factor (C.2):

$$X(T) = \begin{cases} +\frac{3}{2} \sqrt[6]{b^2 + T_0^2} \left[\sqrt[3]{T^2 + b^2} - \sqrt[3]{b^2} \right], & \text{for } T > 0, \\ -\frac{3}{2} \sqrt[6]{b^2 + T_0^2} \left[\sqrt[3]{T^2 + b^2} - \sqrt[3]{b^2} \right], & \text{for } T \leq 0. \end{cases} \quad (\text{C.5})$$

A plot of this null geodesic is given in Fig. C.2.

C.3. Past particle horizon

For this particular bounce-type universe, the particle horizon at $T_0 > 0$ reads as

$$d_{\text{hor}}(T_0) = a(T_0) \lim_{t_1 \rightarrow -\infty} \left[\int_{t_1}^{-b} \frac{dt''}{a(t'')} + \int_b^{t(T_0)} \frac{dt'}{a(t')} \right], \quad (\text{C.6})$$

where $t(T_0) \equiv t_0$ is given by (4.2) and $a(t)$ by (C.4). For positive and finite values of b and t_0 , we get

$$\begin{aligned} d_{\text{hor}}(T_0) &= \frac{3}{2} a(T_0) \lim_{t_1 \rightarrow -\infty} \left(\sqrt[3]{t_1^2 t_0} - 2 \sqrt[3]{b^2 t_0} + t_0 \right) \\ &= \frac{3}{2} a(T_0) \lim_{t_1 \rightarrow -\infty} \sqrt[3]{t_1^2 t_0}, \end{aligned} \quad (\text{C.7})$$

which goes to $+\infty$.

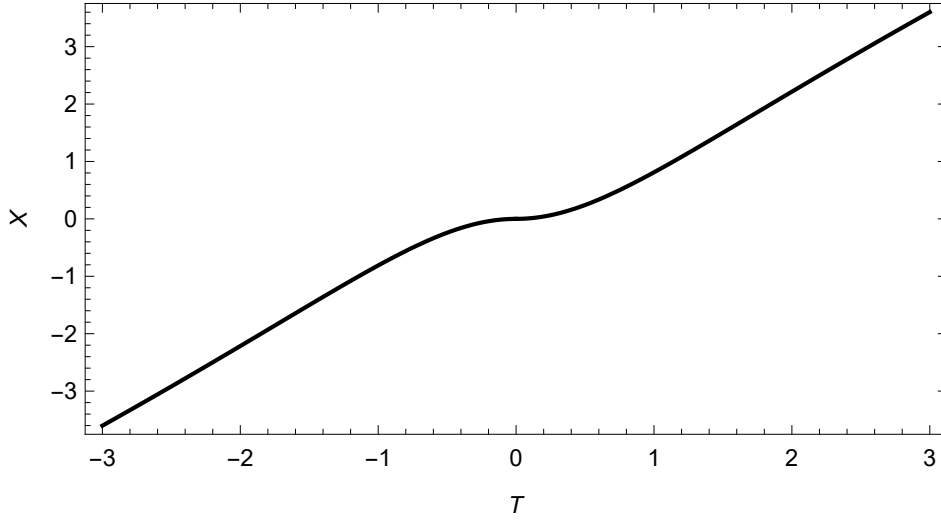


Figure C.2.: Null geodesic (C.5) with $b = 1$ and $T_0 = 4\sqrt{5}$.

C.4. Modified Hubble diagrams

Taking the positive function $a(t)$ from (C.4), the integrals in (4.17) give

$$d_L(z) \Big|_{z \in [0, z_{\max}]}^{(\text{case 1})} = 3 t_0 \frac{1}{2} \left[1 + z - \frac{1}{1+z} \right], \quad (\text{C.8a})$$

$$d_L(z) \Big|_{z \in (-1, z_{\max}]}^{(\text{case 2})} = 3 t_0 \frac{1}{2} \left[1 + z_{\max} - \frac{1}{1+z_{\max}} + \frac{1}{(1+z_{\max})^2} \left(\frac{1}{1+z} - \frac{1+z}{(1+z_{\max})^2} \right) \right], \quad (\text{C.8b})$$

with the definition

$$z_{\max} \equiv a(t_0)/a(b) - 1 = \sqrt[3]{t_0/b} - 1. \quad (\text{C.8c})$$

The corresponding angular diameter distance d_A is

$$d_A(z) \Big|_{z \in [0, z_{\max}]}^{(\text{case 1})} = 3 t_0 \frac{1}{2} \frac{1}{(1+z)^2} \left[1 + z - \frac{1}{1+z} \right], \quad (\text{C.9a})$$

$$d_A(z) \Big|_{z \in (-1, z_{\max}]}^{(\text{case 2})} = 3 t_0 \frac{1}{2} \left[\frac{1}{(1+z)^3} - \frac{1}{(1+z_{\max})^3} + \frac{z_{\max} + z(1+z_{\max})}{(1+z_{\max})^2(1+z)} \right]. \quad (\text{C.9b})$$

The modified Hubble diagram with the luminosity distance $d_L(z)$ is plotted in Fig. C.3 and the one with the angular diameter distance $d_A(z)$ in Fig. C.4.

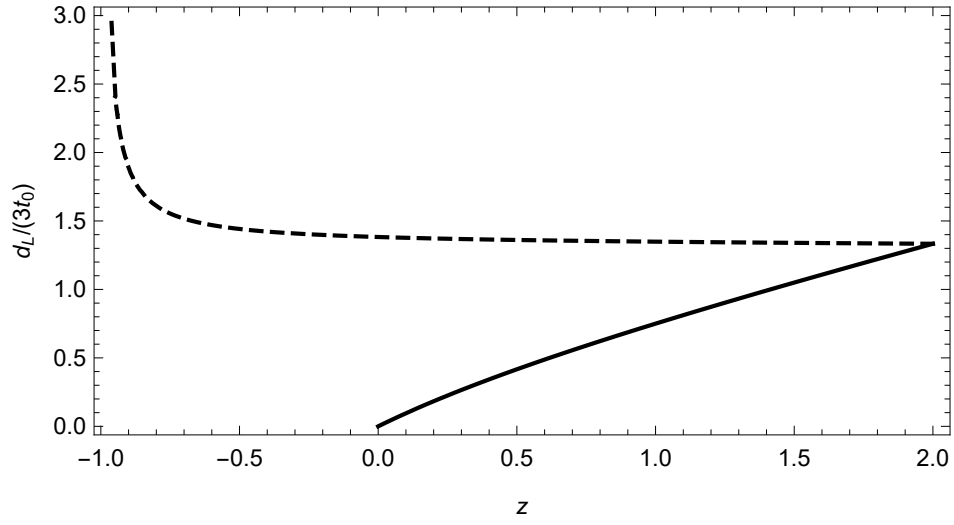


Figure C.3.: Hubble diagram with the luminosity distance d_L from (C.8) for $b/t_0 = 1/27$ and $z_{\max} = 2$. With an observer in the expanding phase, the full curve corresponds to case 1 (light emitted by a co-moving galaxy in the expanding phase of the universe) and the dashed curve to case 2 (light emitted by a co-moving galaxy in the contracting phase).

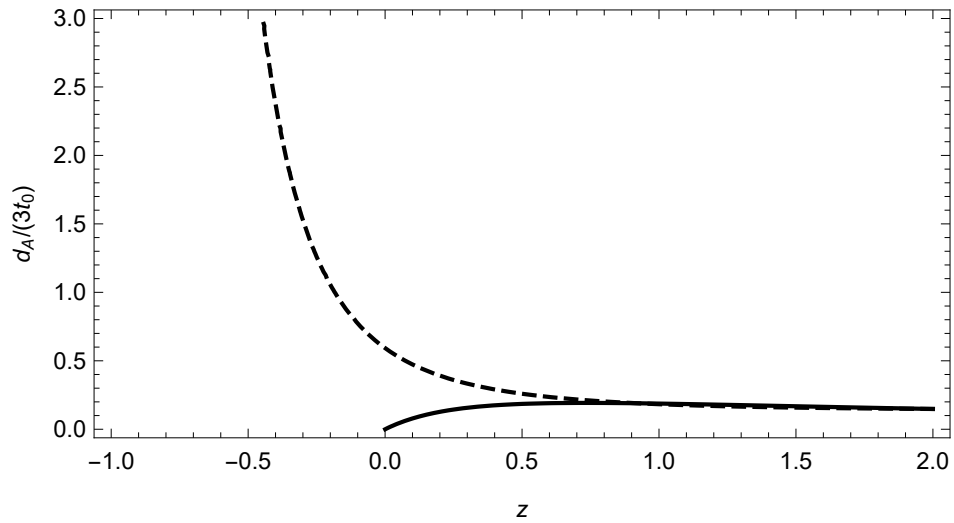


Figure C.4.: Same as Fig. C.3, but with the angular diameter distance d_A from (C.9).

Nonsingular bounce from a scalar field with a positive exponential potential

In Sec. (4.3.3.4). we showed that a matter contraction can lead to a scale-invariant power spectrum. In this appendix, we will show one realization of the matter contraction, namely a single scalar field with a positive exponential potential.

Before we start, we remark that a positive exponential potential that can lead to a contracting universe dominated by cold matter was already discussed in Ref. [53]. However, that model itself [53] cannot produce a nonsingular bounce. It is assumed in Ref. [53] that modifications to general relativity are supposed to yield a bounce. In our case, the bounce is given by the defect and we still remain within the domain of general relativity (but allow for degenerate metrics).

We will use the t coordinate to simplify the calculations. The final results can be easily represented in terms of the T coordinate by using the coordinate transformation (4.2).

For a single scalar field φ with potential $V(\varphi)$, the equations of motion are given by (4.78). In terms of the t coordinate, the equations of motion are as follows:

$$\frac{d^2\varphi}{dt^2} + \frac{3}{a} \frac{da}{dt} \frac{d\varphi}{dt} + \frac{\partial V}{\partial \varphi} = 0, \quad (\text{D.1a})$$

$$\frac{8\pi G}{3} \left[\frac{1}{2} \left(\frac{d\varphi}{dt} \right)^2 + V(\varphi) \right] = \left(\frac{1}{a} \frac{da}{dt} \right)^2, \quad (\text{D.1b})$$

$$-3 \frac{1}{a} (\rho_\varphi + P_\varphi) \frac{da}{dt} = \frac{d\rho_\varphi}{dt}, \quad (\text{D.1c})$$

with

$$\rho_\varphi = \frac{1}{2} \left(\frac{d\varphi}{dt} \right)^2 + V(\varphi), \quad (\text{D.2a})$$

$$P_\varphi = \frac{1}{2} \left(\frac{d\varphi}{dt} \right)^2 - V(\varphi). \quad (\text{D.2b})$$

Notice that Newton's gravitational constant G has been restored in (D.1b).

A self-consistent system that satisfies (D.1) is as follows

$$a(t) = \sqrt[3]{\frac{t^2}{t_0^2}}, \quad (\text{D.3a})$$

$$\rho_\varphi(t) = \frac{1}{6\pi G} \frac{1}{t^2}, \quad (\text{D.3b})$$

$$P_\varphi(t) = 0, \quad (\text{D.3c})$$

$$V(\varphi) = \frac{1}{12\pi G} e^{\mp 2\sqrt{6\pi G}\varphi}, \quad (\text{D.3d})$$

$$\varphi(t) = \pm \frac{1}{\sqrt{6\pi G}} \ln |t|, \quad (\text{D.3e})$$

with

$$t \in (-\infty, b] \cup [b, +\infty) \quad (\text{D.4})$$

and where $a(t)$ is normalized to unity at $t_0 > 0$.

As $\rho_\varphi \propto a^{-3}$ and $P_\varphi = 0$ from (D.3), the scalar field φ behaves like nonrelativistic matter.

In terms of the T coordinate, (D.3) can be written as

$$a(T) = \sqrt[3]{\frac{T^2 + b^2}{T_0^2 + b^2}}, \quad (\text{D.5a})$$

$$\rho_\varphi(t) = \frac{1}{6\pi G} \frac{1}{T^2 + b^2}, \quad (\text{D.5b})$$

$$P_\varphi(t) = 0, \quad (\text{D.5c})$$

$$V(\varphi) = \frac{1}{12\pi G} e^{\mp 2\sqrt{6\pi G}\varphi}, \quad (\text{D.5d})$$

$$\varphi(t) = \pm \frac{1}{2\sqrt{6\pi G}} \ln(T^2 + b^2), \quad (\text{D.5e})$$

with

$$T \in \mathbb{R} \quad (\text{D.6})$$

and where $a(T)$ is normalized to unity at $T_0 > 0$.

Notice that the cosmic scale factor evolution for a universe filled by a scalar field (given by (D.5a)) is exactly the same as it for a hydrodynamic matter-dominated nonsingular bouncing universe (given by (4.7)). However, these two systems are not equivalent to each other, especially when we consider cosmological perturbations. For example, the speed of sound for the scalar field φ is unity, but it vanishes for nonrelativistic matter.

Primordial anisotropies and initial conditions

In this appendix, we will review the primordial anisotropies in the CMB spectrum and show how the observed CMB spectrum implies a scale-invariant power spectrum of gravitational potential. Our discussion follows Chapter 9 of Ref. [63].

E.1. Boltzmann equation

The collisionless Boltzmann equation reads [63, 74]

$$0 = \frac{df(x^i(\eta), p_i(\eta), \eta)}{d\eta} \equiv \frac{\partial f}{\partial \eta} + \frac{dx^i}{d\eta} \frac{\partial f}{\partial x^i} + \frac{dp_i}{d\eta} \frac{\partial f}{\partial p_i}, \quad (\text{E.1})$$

where f is the distribution function which gives the number density in one-particle phase space. Equation (E.1) says that the number of particles in a given phase volume does not change with time. Recall that the physical distance is given by $\Omega(\eta)|\mathbf{x}|$.

Consider a photon which is characterized by a 4-momentum p_μ . The spatial direction of the photon is given by [17]

$$l^i \equiv \frac{p_i}{p}, \quad (\text{E.2})$$

where

$$p \equiv \sqrt{\sum_i p_i p_i}. \quad (\text{E.3})$$

The frequency measured by an observer with 4-velocity u^μ is equal to

$$\omega = -p_\mu u^\mu. \quad (\text{E.4})$$

Then, the distribution function for a photon is given by [63, 74]

$$f = \frac{2}{\exp\left[\frac{\omega}{\mathcal{T}(x^i, l^i, \eta)}\right] - 1}, \quad (\text{E.5})$$

where \mathcal{T} is the effective temperature from the blackbody radiation. The factor 2 in the numerator of (E.5) accounts for the two possible polarizations of the photon. The temperature

\mathcal{T} depends on x^i and l^i , which implies we are considering an inhomogeneous and anisotropic universe.

Note that in the rest frame of an observer, we have

$$u^i = 0, \quad (\text{E.6})$$

and

$$u^0 = \frac{1}{\sqrt{-g_{00}}}. \quad (\text{E.7})$$

For scalar metric perturbations

$$g_{00} = -\Omega^2(1 + 2\tilde{\Phi}), \quad (\text{E.8})$$

$$g_{ij} = \Omega^2(1 - 2\tilde{\Phi})\delta_{ij}, \quad (\text{E.9})$$

we have

$$\omega = -p_0 u^0 = -\frac{p_0}{\sqrt{-g_{00}}}. \quad (\text{E.10})$$

Notice that, for massless particles, we have

$$0 = g_{\mu\nu} p^\mu p^\nu \quad (\text{E.11a})$$

$$= -\Omega^2(1 + 2\tilde{\Phi})p^0 p^0 + \frac{1}{\Omega^2(1 - 2\tilde{\Phi})} \sum_i p_i p_i$$

$$= -\Omega^2(1 + 2\tilde{\Phi})p^0 p^0 + \frac{(1 + 2\tilde{\Phi})}{\Omega^2} p^2,$$

where in the last line, we have neglected a term proportional to the second-order metric perturbations ($\tilde{\Phi}^2$).

From (E.11), we can express p^0 and p_0 in terms of p

$$p^0 = \frac{p}{\Omega^2}, \quad (\text{E.12a})$$

$$p_0 = -(1 + 2\tilde{\Phi})p. \quad (\text{E.12b})$$

For a nearly homogeneous and isotropic universe, the temperature can be written as [63, 74]

$$\mathcal{T}(x^i, l^i, \eta) = \mathcal{T}_0(\eta) + \delta\mathcal{T}(x^i, l^i, \eta), \quad (\text{E.13})$$

with $\mathcal{T}_0 \gg \delta\mathcal{T}$.

Now we will decompose the distribution function into two parts [74]

$$f = \bar{f} + \delta f, \quad (\text{E.14})$$

where \bar{f} and δf are the zero-order and first-order distribution function, respectively.

Notice that

$$\begin{aligned} \frac{\omega}{\mathcal{T}} &= -\frac{p_0}{\mathcal{T}\sqrt{-g_{00}}} \\ &= \frac{-(1 + 2\tilde{\Phi})p}{\mathcal{T}\Omega\sqrt{1 + 2\tilde{\Phi}}} \\ &= \frac{p}{\Omega\mathcal{T}_0} \cdot \frac{\sqrt{1 + 2\tilde{\Phi}}}{1 + \delta\mathcal{T}/\mathcal{T}_0}. \end{aligned} \quad (\text{E.15})$$

For $\tilde{\Phi} \ll 1$ and $\delta\mathcal{T}/\mathcal{T}_0 \ll 1$, we have

$$\sqrt{1 + 2\tilde{\Phi}} \simeq 1 + \tilde{\Phi}, \quad (\text{E.16a})$$

$$\frac{1}{1 + \delta\mathcal{T}/\mathcal{T}_0} \simeq 1 - \frac{\delta\mathcal{T}}{\mathcal{T}_0}, \quad (\text{E.16b})$$

from which we get

$$\frac{\sqrt{1 + 2\tilde{\Phi}}}{1 + \delta\mathcal{T}/\mathcal{T}_0} \simeq 1 + \tilde{\Phi} - \delta\mathcal{T}/\mathcal{T}_0. \quad (\text{E.17})$$

Considering (E.17), (E.15) can be written as

$$\frac{\omega}{\mathcal{T}} = -\frac{p}{\Omega\mathcal{T}_0}(1 + \tilde{\Phi} - \delta\mathcal{T}/\mathcal{T}_0). \quad (\text{E.18})$$

By taking $\tilde{\Phi} = 0$ and $\delta\mathcal{T} = 0$, we have the following zero-order distribution function

$$\bar{f} = \frac{2}{\exp\left[\frac{p}{\Omega\mathcal{T}_0}\right] - 1}. \quad (\text{E.19})$$

The first-order distribution function is given by

$$\delta f = \left. \frac{df}{d(\tilde{\Phi} - \delta\mathcal{T}/\mathcal{T}_0)} \right|_{\tilde{\Phi} - \delta\mathcal{T}/\mathcal{T}_0 = 0} (\tilde{\Phi} - \delta\mathcal{T}/\mathcal{T}_0). \quad (\text{E.20})$$

From (E.5) and (E.18), we have

$$\delta f = \frac{A e^A}{2f} (\tilde{\Phi} - \delta\mathcal{T}/\mathcal{T}_0), \quad (\text{E.21})$$

in which $A \equiv \frac{p}{\Omega\mathcal{T}_0}$.

Considering the geodesic of a photon with affine parameter λ , we have

$$\begin{aligned} \frac{dx^i}{d\eta} &= \frac{dx^i/d\lambda}{d\eta/d\lambda} \\ &= \frac{dp^i}{dp^0} \\ &= \frac{p_i/[\Omega^2(1 - 2\tilde{\Phi})]}{p/\Omega^2} \\ &= l^i(1 + 2\tilde{\Phi}), \end{aligned} \quad (\text{E.22})$$

where (E.3) and (E.12a) have been used.

From geodesic equations

$$\frac{dp_\alpha}{d\lambda} - \frac{1}{2} \frac{\partial g_{\mu\nu}}{\partial x^\alpha} p^\mu p^\nu = 0, \quad (\text{E.23})$$

we have

$$\begin{aligned}
\frac{dp_\alpha}{d\eta} &= \frac{dp_\alpha/d\lambda}{d\eta/d\lambda} \\
&= \frac{1}{2} \frac{\partial g_{\mu\nu}}{\partial x^\alpha} p^\mu p^\nu \frac{1}{p^0} \\
&= \frac{1}{2p^0} \left(\frac{\partial g_{00}}{\partial x^\alpha} p^0 p^0 + \frac{\partial g_{ij}}{\partial x^\alpha} p^i p^j \right) \\
&= -2p \frac{\partial \tilde{\Phi}}{\partial x^\alpha},
\end{aligned} \tag{E.24}$$

where second-order perturbations have been neglected.

With (E.22) and (E.24), we can write (E.1) as¹⁴

$$\frac{\partial f}{\partial \eta} + l^i (1 + 2\tilde{\Phi}) \frac{\partial f}{\partial x^i} - 2p \frac{\partial \tilde{\Phi}}{\partial x^i} \frac{\partial f}{\partial p_i} = 0. \tag{E.25}$$

The zero-order terms in (E.25) give

$$\frac{\partial \bar{f}}{\partial \eta} = 0, \tag{E.26}$$

from which we can get

$$\frac{\partial(\Omega \mathcal{T})}{\partial \eta} = 0. \tag{E.27}$$

Note that $\Omega(\eta) = a(t)$ for a given $\eta = \eta(t)$. So, (E.27) tell us that, for a homogeneous and isotropic universe, the temperature of the background radiation is inversely proportional to the cosmic scale factor.

The first-order terms in (E.25) gives

$$\begin{aligned}
0 &= \frac{\partial \delta f}{\partial \eta} + l^i \frac{\partial \delta f}{\partial x^i} - 2p \frac{\partial \tilde{\Phi}}{\partial x^i} \frac{\partial \bar{f}}{\partial p_i} \\
&= \left(\frac{\partial}{\partial \eta} + l^i \frac{\partial}{\partial x^i} \right) \left(\frac{\delta \mathcal{T}}{\mathcal{T}_0} + \tilde{\Phi} \right) - 2 \frac{\partial \tilde{\Phi}}{\partial \eta},
\end{aligned} \tag{E.28}$$

where (E.19) and (E.21) have been used.

Keep in mind that in deriving the zero-order and first-order equations, x^i and p_i are independent variables in the distribution function.

E.2. Sachs–Wolfe effect

After recombination, photons start to travel freely through space and the universe is mainly dominated by nonrelativistic matter. As we have discussed in Sec. 4.3, the main mode of the gravitational potential $\tilde{\Phi}$ is time independent (see (4.46)) for the matter-dominated universe. Taking this into account, (E.28) reduces to

$$\left(\frac{\partial}{\partial \eta} + l^i \frac{\partial}{\partial x^i} \right) \left(\frac{\delta \mathcal{T}}{\mathcal{T}_0} + \tilde{\Phi} \right) = 0. \tag{E.29}$$

¹⁴The Boltzmann equation in terms of cosmic time coordinates t can be found in Sec.4.2 of Ref. [74], where a physical interpretation can be easily observed.

Note that

$$l^i = \frac{1}{1 + 2\tilde{\Phi}} \frac{dx^i}{d\eta}. \quad (\text{E.30})$$

So, up to first-order metric perturbations, the operator on the left-hand side of (E.29) is equivalent to a total derivative in time. Then, (E.29) reduces to

$$\frac{\delta\mathcal{T}}{\mathcal{T}_0} + \tilde{\Phi} = \text{constant}. \quad (\text{E.31})$$

The temperature fluctuation due to the gravitational potential at last scattering is known as the Sachs–Wolfe effect (SW) [75].

For the real case, the gravitational potential changes slowly between the time of last scattering and the present [63]. The temperature fluctuation due to the time-dependent gravitational potential is known as the integrated Sachs–Wolfe effect (ISW). Compared with SW, ISW has a minor contribution to the temperature fluctuation.

E.3. Temperature fluctuations

Consider our earth as a given observer, with $\frac{\delta\mathcal{T}}{\mathcal{T}_0}(\mathbf{l})$ representing the temperature fluctuations in the direction $\mathbf{l} \equiv (l^1, l^2, l^3)$. The temperature autocorrelation function is defined as [63]:

$$C(\theta) \equiv \left\langle \frac{\delta\mathcal{T}}{\mathcal{T}_0}(\mathbf{l}_1) \frac{\delta\mathcal{T}}{\mathcal{T}_0}(\mathbf{l}_2) \right\rangle, \quad (\text{E.32})$$

with $\langle \rangle$ representing the average over all directions, and where θ satisfies

$$\cos\theta = \mathbf{l}_1 \cdot \mathbf{l}_2. \quad (\text{E.33})$$

With (E.32), we have

$$\begin{aligned} \left\langle \left(\frac{\delta\mathcal{T}}{\mathcal{T}_0}(\theta) \right)^2 \right\rangle &\equiv \left\langle \left(\frac{\mathcal{T}(\mathbf{l}_1) - \mathcal{T}(\mathbf{l}_2)}{\mathcal{T}_0} \right)^2 \right\rangle \\ &= \left\langle \left(\frac{\mathcal{T}(\mathbf{l}_1) - \mathcal{T}_0}{\mathcal{T}_0} - \frac{\mathcal{T}(\mathbf{l}_2) - \mathcal{T}_0}{\mathcal{T}_0} \right)^2 \right\rangle \\ &= \left\langle \left(\frac{\delta\mathcal{T}}{\mathcal{T}_0}(\mathbf{l}_1) \right)^2 \right\rangle + \left\langle \left(\frac{\delta\mathcal{T}}{\mathcal{T}_0}(\mathbf{l}_2) \right)^2 \right\rangle - 2 \left\langle \frac{\delta\mathcal{T}}{\mathcal{T}_0}(\mathbf{l}_1) \frac{\delta\mathcal{T}}{\mathcal{T}_0}(\mathbf{l}_2) \right\rangle \\ &= 2C(0) - 2C(\theta). \end{aligned} \quad (\text{E.34})$$

$C(\theta)$ can be expanded as a sum of multipole moments C_l

$$C(\theta) = \frac{1}{4\pi} \sum_{l=2}^{\infty} (2l+1) C_l P_l(\cos\theta), \quad (\text{E.35})$$

where $P_l(\cos\theta)$ are the Legendre polynomials. Notice that, in (E.35), the component $l=0$ (monopole) and $l=1$ (dipole) are not been taken into account.¹⁵

¹⁵The monopole component gives the background temperature, and the dipole is interpreted to be the result of the solar system motion relative to the nearly isotropic blackbody field [67].

From (E.31), we have, along the geodesic of a photon

$$\frac{\delta\mathcal{T}}{\mathcal{T}}(\eta, x^i(\eta), , l^i) = \frac{\delta\mathcal{T}}{\mathcal{T}}(\eta_r, x^i(\eta_r), , l^i) + \tilde{\Phi}(\eta_r, x^i(\eta_r)) - \tilde{\Phi}(\eta, x^i(\eta)), \quad (\text{E.36})$$

where η_r denotes the conformal time of last scattering (recombination). The temperature fluctuations observed at a given time after recombination are determined by the initial conditions (temperature fluctuations and initial gravitational potential at the time of last scattering) and the gravitational potential at the time of observation.

Now, the key step is determining the temperature fluctuations at η_r . Approximately, we could use the following matching conditions. Before decoupling, the energy-momentum tensor for photon is given by the hydrodynamic one and after decoupling, the energy-momentum tensor is given by the kinetic one. For a plane-wave scalar metric perturbation, the temperature fluctuations at recombination are given by [63]

$$\left(\frac{\delta\mathcal{T}}{\mathcal{T}_0}\right)_{\mathbf{k}}(\mathbf{l}, \eta_r) = \frac{1}{4} \left(\frac{\delta\rho_{\mathbf{k}}}{\bar{\rho}_\gamma} + \frac{3i}{k^2} (k_i l^i) \left(\frac{\delta\rho_{\mathbf{k}}}{\bar{\rho}_\gamma}\right)' \right), \quad (\text{E.37})$$

where $\frac{\delta\rho}{\bar{\rho}_\gamma}$ is the density perturbation for photons.

It can be shown [63] that C_l can be expressed in terms of $\tilde{\Phi}$ and $\frac{\delta\rho}{\bar{\rho}_\gamma}$ as

$$C_l = \frac{2}{\pi} \int \left| \left(\tilde{\Phi}_k(\eta_r) + \frac{\delta\rho_k}{4\bar{\rho}} \right) j_l(k\eta_0) - \frac{3[\delta\rho_k/\bar{\rho}(\eta_r)]'}{4k} \frac{dj_l(k\eta_0)}{d(k\eta_0)} \right|^2 k^2 dk, \quad (\text{E.38})$$

where $j_l(k\eta)$ are the spherical Bessel functions.

The Hubble horizon at the time of last scattering is about 0.87° , so the above discussion is valid for $l \ll 200$. For adiabatic scalar metric perturbations, we have [63]

$$\frac{\delta\rho_k}{\bar{\rho}_\gamma}(\eta_r) \simeq -\frac{8}{3}\tilde{\Phi}_k(\eta_r), \quad (\text{E.39a})$$

$$[\delta\rho_k/\bar{\rho}(\eta_r)]' \simeq 0, \quad (\text{E.39b})$$

which hold in the super-horizon region.

Then, for a scale invariant power spectrum with

$$|\tilde{\Phi}_k(\eta_r)|^2 k^3 = B(\eta_r), \quad (\text{E.40})$$

we have [63]

$$l(l+1)C_l \simeq \frac{9B}{100\pi} = \text{constant}, \quad (\text{E.41})$$

for $l \ll 200$. So, the Sachs-Wolfe effect predicts a flat plateau of $l(l+1)C_l$ for small l if the initial power spectrum is scale invariant. For the real case, the ISW also should be considered, so the spectrum is not completely flat [67]. The temperature power spectrum measured in astronomy [68, 76–79] is presented in Fig. E.1.

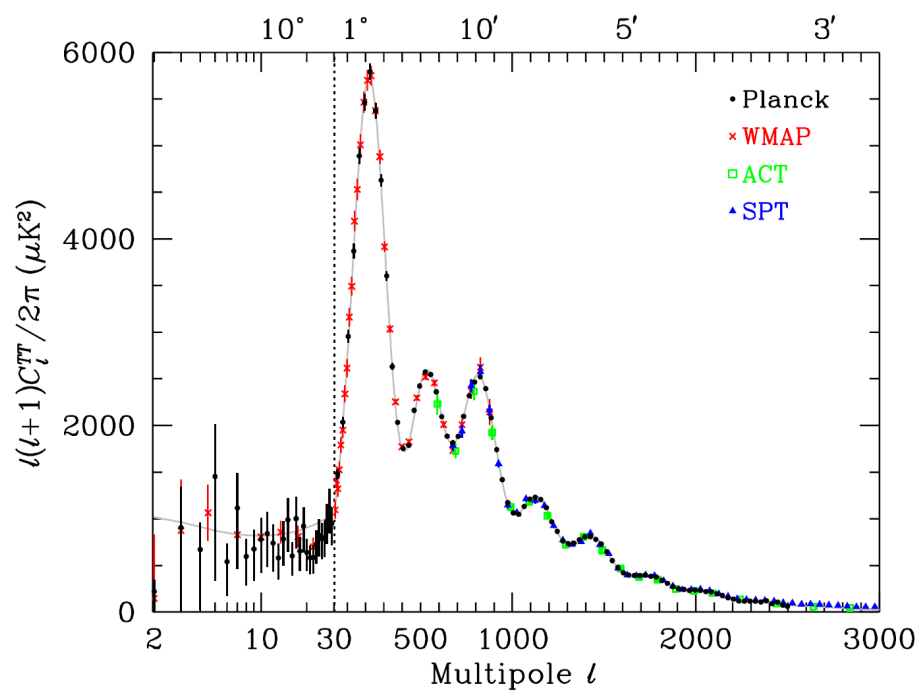


Figure E.1.: CMB temperature anisotropy estimates from the *Planck*, *WMAP*, ACT, and SPT experiments. The curve shows the temperature spectrum for the best-fit *Planck* Λ CDM cosmology. Figure from [80].

Acknowledgements

First of all, I would like to express my gratitude to my supervisor Prof. Dr. Frans R. Klinkhamer, for introducing me to the subject of spacetime defects. In particular, I want to thank him for his support and guidance over the last three years.

I want to express my gratitude to Prof. Dr. Janos Polónyi for being the second referee of my thesis.

I would also like to thank my friends and colleagues for their support, proofreading and many interesting discussions. In particular, I would like to thank Dr. Wenyuan Ai, Dr. Emmanuele Battista, Dr. Slava Emelyanov, Dr. Kumar Ghosh, Max Haubenwallner, Wenjie Hou, Xuewen Liu, Dr. Pascal Nagel, Dr. Jose Queiruga, Dr. Shiyamala Thambyahpillai, and Albert Zhou.

I want to express my special thanks to my fiancée Miao Zhang, for her constant support and understanding over the past few years.

Finally, I want to thank my parents and grandparents for their love and support over the past three decades.

References

- [1] J. A. Wheeler, “On the nature of quantum geometrodynamics,” *Annals Phys.* **2** (1957) 604–614.
- [2] M. Visser, *Lorentzian Wormholes. From Einstein to Hawking*. Springer, New York, USA, 1995.
- [3] S. W. Hawking, “Spacetime foam,” *Nucl. Phys. B* **144** (1978) 349–362.
- [4] S. W. Hawking, D. N. Page, and C. N. Pope, “The propagation of particles in spacetime foam,” *Phys. Lett. B* **86** (1979) 175–178.
- [5] S. W. Hawking, D. N. Page, and C. N. Pope, “Quantum gravitational bubbles,” *Nucl. Phys. B* **170** (1980) 283–306.
- [6] S. Bernadotte and F. R. Klinkhamer, “Bounds on length-scales of classical spacetime foam models,” *Phys. Rev. D* **75** (2007) 024028, [arXiv:hep-ph/0610216](#).
- [7] F. R. Klinkhamer, “A new type of nonsingular black-hole solution in general relativity,” *Mod. Phys. Lett. A* **29** (2014) 1430018, [arXiv:1309.7011](#).
- [8] F. R. Klinkhamer, “Skyrmion spacetime defect,” *Phys. Rev. D* **90** (2014) 024007, [arXiv:1402.7048](#).
- [9] J. M. Queiruga, “Particle propagation on spacetime manifolds with static defects,” *J. Phys. A* **51** (2018) 045401, [arXiv:1703.03606](#).
- [10] F. R. Klinkhamer, “Regularized big bang singularity,” *Phys. Rev. D* **100** (2019) 023536, [arXiv:1903.10450](#).
- [11] F. R. Klinkhamer and Z. L. Wang, “Lensing and imaging by a stealth defect of spacetime,” *Mod. Phys. Lett. A* **34** (2019) 1950026, [arXiv:1808.02465](#).
- [12] F. R. Klinkhamer and Z. L. Wang, “Nonsingular bouncing cosmology from general relativity,” *Phys. Rev. D* **100** (2019) 083534, [arXiv:1904.09961](#).
- [13] F. R. Klinkhamer and Z. L. Wang, “Nonsingular bouncing cosmology from general relativity: Scalar metric perturbations,” *Phys. Rev. D* **101** (2020) 064061, [arXiv:1911.06173](#).
- [14] S. Weinberg, *Gravitation and Cosmology: Principles and Applications of the General Theory of Relativity*. John Wiley and Sons, New York, USA, 1972.
- [15] **LIGO Scientific, Virgo** Collaboration, B. P. Abbott *et al.*, “Observation of gravitational waves from a binary black hole merger,” *Phys. Rev. Lett.* **116** (2016) 061102, [arXiv:1602.03837](#).
- [16] K. Schwarzschild, “Über das gravitationsfeld eines massenpunktes nach der einsteinschen theorie,” *Sitzungsberichte der Deutschen Akademie der Wissenschaften zu Berlin, Klasse für Mathematik, Physik, und Technik* (1916) 189–196.

-
- [17] R. M. Wald, *General Relativity*. Chicago Univ. Press, Chicago, USA, 1984.
- [18] M. D. Kruskal, “Maximal extension of Schwarzschild metric,” *Phys. Rev.* **119** (1960) 1743–1745.
- [19] G. Szekeres, “On the singularities of a Riemannian manifold,” *Publ. Math. Debrecen* **7** (1960) 285–301.
- [20] C. W. Misner, K. S. Thorne, and J. A. Wheeler, *Gravitation*. Princeton Univ. Press, Princeton, USA, 2017.
- [21] A. Friedman, “On the curvature of space,” *Zeitschrift für Physik* **10** (1922) 377–386.
- [22] R. Penrose, “Gravitational collapse and space-time singularities,” *Phys. Rev. Lett.* **14** (1965) 57–59.
- [23] S. W. Hawking, “The occurrence of singularities in cosmology. III. causality and singularities,” *Proc. Roy. Soc. Lond. A* **A300** (1967) 187–201.
- [24] S. W. Hawking and R. Penrose, “The singularities of gravitational collapse and cosmology,” *Proc. Roy. Soc. Lond. A* **A314** (1970) 529–548.
- [25] S. W. Hawking and G. F. R. Ellis, *The Large Scale Structure of Space-time*. Cambridge Monographs on Mathematical Physics. Cambridge Univ. Press, Cambridge, UK, 2011.
- [26] M. Schwarz, *Nontrivial spacetime topology, modified dispersion relations, and an SO(3)-Skyrme model*. Verlag Dr. Hut, Munich, Germany, 2010.
- [27] M. Günther, *Skyrmion spacetime defect, degenerate metric, and negative gravitational mass*. Master thesis, KIT, Karlsruhe, Germany, 2017.
- [28] E. Poisson, *A Relativist’s Toolkit: The Mathematics of Black-hole Mechanics*. Cambridge Univ. Press, Cambridge, UK, 2009.
- [29] S. M. Carroll, *Spacetime and Geometry*. Cambridge Univ. Press, Cambridge, UK, 2019.
- [30] D. Gannon, “Singularities in nonsimply connected space-times,” *J. Math. Phys.* **16** (1975) 2364–2367.
- [31] S. W. Hawking, “Black hole explosions,” *Nature* **248** (1974) 30–31.
- [32] S. W. Hawking, “Particle creation by black holes,” *Commun. Math. Phys.* **43** (1975) 199–220. [Erratum: *Commun. Math. Phys.* **46**, 206 (1976)].
- [33] L. Susskind and J. Lindesay, *An Introduction to Black Holes, Information and the String Theory Revolution: the Holographic Universe*. World Scientific, 2005.
- [34] P. Chen and R. J. Adler, “Black hole remnants and dark matter,” *Nucl. Phys. B Proc. Suppl.* **124** (2003) 103–106, [arXiv:gr-qc/0205106](#).
- [35] R. J. Adler, P. Chen, and D. I. Santiago, “The generalized uncertainty principle and black hole remnants,” *Gen. Rel. Grav.* **33** (2001) 2101–2108, [arXiv:gr-qc/0106080](#).
- [36] S. B. Giddings, “Black holes and massive remnants,” *Phys. Rev. D* **46** (1992) 1347–1352, [arXiv:hep-th/9203059](#).
- [37] J. Preskill, “Do black holes destroy information?,” in *International Symposium on Black holes, Membranes, Wormholes and Superstrings*, pp. 22–39. 1, 1992. [arXiv:hep-th/9209058](#).
- [38] F. R. Klinkhamer and J. M. Queiruga, “Antigravity from a spacetime defect,” *Phys. Rev. D* **97** (2018) 124047, [arXiv:1803.09736](#).

- [39] F. R. Klinkhamer and J. M. Queiruga, “A stealth defect of spacetime,” *Mod. Phys. Lett. A* **33** (2018) 1850127, [arXiv:1805.04091](#).
- [40] F. R. Klinkhamer and F. Sorba, “Comparison of spacetime defects which are homeomorphic but not diffeomorphic,” *J. Math. Phys.* **55** (2014) 112503, [arXiv:1404.2901](#).
- [41] R. P. Feynman, R. B. Leighton, and M. Sands, *The Feynman Lectures on Physics, Vol. I*. Addison–Wesley, Reading MA, USA, 1963.
- [42] P. Mouroulis and J. Macdonald, *Geometrical Optics and Optical Design*. Oxford Univ. Press, New York, USA, 1997.
- [43] A. Einstein, “Lens-like action of a star by the deviation of light in the gravitational field,” *Science* **84** (1936) 506–507.
- [44] K. S. Virbhadra and G. F. R. Ellis, “Schwarzschild black hole lensing,” *Phys. Rev. D* **62** (2000) 084003, [arXiv:astro-ph/9904193](#).
- [45] P. Schneider, J. Ehlers, and E. E. Falco, *Gravitational Lenses*. Springer-Verlag, Berlin, Germany, 1992.
- [46] J. Wambsganss, “Gravitational lensing in astronomy,” *Living Rev. Rel.* **1** (1998) 12, [arXiv:astro-ph/9812021](#).
- [47] S. Dodelson, *Gravitational Lensing*. Cambridge Univ. Press, Cambridge, UK, 2017.
- [48] V. Perlick, “On the exact gravitational lens equation in spherically symmetric and static space-times,” *Phys. Rev. D* **69** (2004) 064017, [arXiv:gr-qc/0307072](#).
- [49] A. Shatskiy, “Einstein-Rosen bridges and the characteristic properties of gravitational lensing by them,” *Astron. Rep.* **48** (2004) 7, [arXiv:astro-ph/0407222](#).
- [50] K. K. Nandi, Y. Z. Zhang, and A. V. Zakharov, “Gravitational lensing by wormholes,” *Phys. Rev. D* **74** (2006) 024020, [arXiv:gr-qc/0602062](#).
- [51] R. Shaikh and S. Kar, “Gravitational lensing by scalar-tensor wormholes and the energy conditions,” *Phys. Rev. D* **96** (2017) 044037, [arXiv:1705.11008](#).
- [52] M. Novello and S. E. P. Bergliaffa, “Bouncing cosmologies,” *Phys. Rept.* **463** (2008) 127–213, [arXiv:0802.1634](#).
- [53] F. Finelli and R. Brandenberger, “On the generation of a scale invariant spectrum of adiabatic fluctuations in cosmological models with a contracting phase,” *Phys. Rev. D* **65** (2002) 103522, [arXiv:hep-th/0112249](#).
- [54] A. Ijjas and P. J. Steinhardt, “Bouncing cosmology made simple,” *Class. Quant. Grav.* **35** (2018) 135004, [arXiv:1803.01961](#).
- [55] F. R. Klinkhamer, “More on the regularized big bang singularity,” *Phys. Rev. D* **101** (2020) 064029, [arXiv:1907.06547](#).
- [56] L. Boyle, K. Finn, and N. Turok, “CPT-symmetric universe,” *Phys. Rev. Lett.* **121** (2018) 251301, [arXiv:1803.08928](#).
- [57] A. Borde, A. H. Guth, and A. Vilenkin, “Inflationary space-times are incomplete in past directions,” *Phys. Rev. Lett.* **90** (2003) 151301, [arXiv:gr-qc/0110012](#).
- [58] A. H. Guth, “The inflationary universe: A possible solution to the horizon and flatness problems,” *Adv. Ser. Astrophys. Cosmol.* **3** (1987) 139–148.

- [59] A. A. Starobinsky, “A new type of isotropic cosmological models without singularity,” *Adv. Ser. Astrophys. Cosmol.* **3** (1987) 130–133.
- [60] A. D. Linde, “A new inflationary universe scenario: A possible solution of the horizon, flatness, homogeneity, isotropy and primordial monopole problems,” *Adv. Ser. Astrophys. Cosmol.* **3** (1987) 149–153.
- [61] A. Barrau, K. Martineau, and F. Moulin, “Seeing through the cosmological bounce: Footprints of the contracting phase and luminosity distance in bouncing models,” *Phys. Rev. D* **96** (2017) 123520, [arXiv:1711.05301](#).
- [62] R. Brandenberger and P. Peter, “Bouncing cosmologies: Progress and problems,” *Found. Phys.* **47** (2017) 797–850, [arXiv:1603.05834](#).
- [63] V. Mukhanov, *Physical Foundations of Cosmology*. Cambridge Univ. Press, Oxford, UK, 2005.
- [64] S. Weinberg, *Cosmology*. Oxford Univ. Press, New York, USA, 2008.
- [65] V. F. Mukhanov, H. Feldman, and R. H. Brandenberger, “Theory of cosmological perturbations,” *Phys. Rept.* **215** (1992) 203–333.
- [66] A. A. Penzias and R. W. Wilson, “A measurement of excess antenna temperature at 4080-Mc/s,” *Astrophys. J.* **142** (1965) 419–421.
- [67] D. Scott and G. F. Smoot, “Cosmic microwave background mini-review,” [arXiv:1005.0555](#).
- [68] **Planck** Collaboration, N. Aghanim *et al.*, “Planck 2018 results. V. CMB power spectra and likelihoods,” [arXiv:1907.12875](#).
- [69] R. Brandenberger and F. Finelli, “On the spectrum of fluctuations in an effective field theory of the Ekpyrotic universe,” *JHEP* **11** (2001) 056, [arXiv:hep-th/0109004](#).
- [70] A. Ijjas, J. L. Lehners, and P. J. Steinhardt, “General mechanism for producing scale-invariant perturbations and small non-Gaussianity in ekpyrotic models,” *Phys. Rev. D* **89** (2014) 123520, [arXiv:1404.1265](#).
- [71] C. Rovelli, *Quantum Gravity*. Cambridge Monographs on Mathematical Physics. Cambridge Univ. Press, Cambridge, UK, 2004.
- [72] C. Rovelli and F. Vidotto, *Covariant Loop Quantum Gravity: An Elementary Introduction to Quantum Gravity and Spinfoam Theory*. Cambridge Monographs on Mathematical Physics. Cambridge Univ. Press, Cambridge, UK, 2014.
- [73] F. R. Klinkhamer, “IIB matrix model: Emergent spacetime from the master field,” [arXiv:2007.08485](#).
- [74] S. Dodelson, *Modern Cosmology*. Academic Press, Amsterdam, Netherlands, 2003.
- [75] R. Sachs and A. Wolfe, “Perturbations of a cosmological model and angular variations of the microwave background,” *Astrophys. J.* **147** (1967) 73–90.
- [76] **Planck** Collaboration, P. A. R. Ade *et al.*, “Planck 2013 results. XVI. cosmological parameters,” *Astron. Astrophys.* **571** (2014) A16, [arXiv:1303.5076](#).
- [77] **WMAP** Collaboration, G. Hinshaw *et al.*, “Nine-year Wilkinson Microwave Anisotropy Probe (WMAP) observations: Cosmological parameter results,” *Astrophys. J. Suppl.* **208** (2013) 19, [arXiv:1212.5226](#).

-
- [78] S. Das *et al.*, “The Atacama Cosmology Telescope: Temperature and gravitational lensing power spectrum measurements from three seasons of data,” *JCAP* **04** (2014) 014, [arXiv:1301.1037](#).
- [79] K. Story *et al.*, “A measurement of the cosmic microwave background damping tail from the 2500-square-degree SPT-SZ survey,” *Astrophys. J.* **779** (2013) 86, [arXiv:1210.7231](#).
- [80] **Particle Data Group** Collaboration, C. Patrignani *et al.*, “Review of particle physics,” *Chin. Phys. C* **40** (2016) 100001.